NASP CONTROL OF H3-H4 DYNAMICS IN THE EARLY EMBRYO

By

Reyhaneh Tirgar

Dissertation
Submitted to the Faculty of the
Graduate School of Vanderbilt University
in partial fulfillment of the requirements
for the degree of

DOCTOR IN PHILOSOPHY
In
Biological Sciences

August 9, 2024
Nashville, Tennessee

Approved

Dr. Jared Nordman
Dr. Katherine Friedman
Dr. William Tansey
Dr. David Cortez
Dr. Lars Plate

To my parents

TABLE OF CONTENTS

LIST OF FIGURES

LIST OF ABBREVIATIONS

ABO	Abnormal Oocyte
AEL	After Egg Laying
ASF1	to Anti-Silencing Factor 1
ATAC-seq	Assay for Transposase-Accessible Chromatin with Sequencing
BSA	Bovine Serum Albumin
C/N	Cytoplasm to Nucleus Ratio
CAF1	Chromatin Assembly Factor 1
CDC25	Cell Division Cycle 25
CDK1	Cyclin Dependent Kinase 1
CDK2	Cyclin Dependent Kinase 2
ChIP-MS	Chromatin Immunoprecipitation-Mass Spectrometry
ChIP-Seq	Chromatin Immunoprecipitation Sequencing
CHK1	Checkpoint Kinase 1
CK2	Casein Kinase 2
CldU	5-chloro-2′-deoxyuridine
CPSF100	Cleavage and Polyadenylation Specificty Factor 100
CPSF73	Cleavage and Polyadenylation Specifity Factor 73
CRISPR	Clustered Regularly Interspaced Short Palindromic Repeats
CstF64	Cleavage Stimulating Factor 2
DAPI	4',6-diamidino-2-phenylindole
DGRC	Drosophila Genomics Resource Center
DRSC	Drosophila RNAi Screening Center

DTT	Dithiothreitol
EBR	Ephrussi Beadle Ringers
ECL	Enhanced chemiluminescence
FACT	Facilitates Chromatin Transcription
FBS	Fetal Bovine Serum
FLASH	FLICE-Associated Huge Protein
G2	Gap Phase 2
gRNA	Guide RNA
GSC	Germline Stem Cells
HAT1	Histone Acetyltransferase 1
HCC	Histone Cleavage Complex
HCl	Hydrochloric Acid
HDAC1	Histone Deacetylase 1
HDE	Histone Downstream Element
Hif1p	Hat1p-Interacting Factor 1
HIRA	Histone Regulation Complex
HLB	Histone Locus Body
HNSCC	Head Neck Squamos Cancer Cells
HSC70	Heat Shock Cognate 70
HSP90	Heat Shock Protein 90
IP	Immunoprecipitation
IP	Immunoprecipitation
IP-MS	Immunoprecipitation Mass Spectrometry

IPO4	Importin 4
IPO4	Importin 4
IPO5	Importin 5
IPO5	Importin 5
iPOND	Isolation of Protein on Nascent DNA
Karyβ3	Karyopherin β 3
LB3	Lysis Buffer 3
MBT	Mid-Blastula Transition
miRNA	microRNA
NAP1	Nucleosome Assembly Protein 1
NC	Nuclear Cycles
NCC	Nascent Chromatin Capture
NES	Nuclear Export Signal
NF-kB	Nuclear Factor Kappa B
NLS	Nuclear Localization Signal
NPAT	Nuclear Protein at the Ataxia-Telangiectasia locus
ORF	Open Reading Frame
PBS	Phosphate Buffered Saline
PBX	Phosphate Buffered Saline with Triton-X
PC-3	Prostate Cancer Cells
PCR	Polymerase Chain Reaction
PTM	Post Translational Modifications
PP4	Protein Phosphate 4

PVDF	Polyvinylidene fluoride
qPCR	Quantitative Polymerase Chain Reaction
RBAP46	Retinoblastoma Associated Protein 46
RD	Replication Dependent
RI	Replication Independent
RNAi	RNA Interference
RNAse A	Ribonuclease A
sfGFP	Super Folding Green Flourscent Protein
Sims3	Silencing in the Middle of the Centromere Protein 3
SLBP	Stem Loop Binding Protein
SLIP1	SLBP-Interacting Protein 1
smFISH	single molecule Fluorescence in situ hybridization
sNASP	Somatic Nuclear Autoantignetic Sperm Protein
SNBP	Sperm Specific Nuclear Baisc Proteins
SRCAP	Snf2-Related CREBBP Activato Protein
TAK1	Transforming Growth Factor (TGF)-β Activated Kinase 1
TCEP	Tris (2-carboxyethyl) phosphine
TLR4	Toll-like Receptor 4 Related
TMT	Tandem Mass Tag
tNASP	Testicular Nuclear Autoantignetic Sperm Protein
TPR	tetratricopeptide repeat
TRA-1	Transformer 1
TRA-4	Transformer 4

TRAF6	Tumor Necrosis Factor (TN4) Receptor Associated Factor 6
UBE3	Ubiquitin Protein Ligase E3A
UBR7	Ubiquitin Protein Ligase E3 Component N-Recognin 7

CHAPTER I

I.INTRODUCTION

Histone life cycle: from synthesis to chromatin deposition

Prelude

Nucleosomes are the most basic unit of chromatin packaging. Canonical H3-H4 tetrasomes or two H3-H4 heterodimers are deposited simultaneously to form the core of a nucleosome. Then, H2A-H2B heterodimers are incorporated to form an octamer that is wrapped by 147bp of DNA. This packaging allows for the six feet of DNA that encode the directions for the cell's identity to be stuffed inside a nucleus diameter of 10μm.

Histones are classified into two categories: DNA replication dependent (RD) or canonical and DNA replication independent (RI) or variant histones. RD histones consist of H3, H4, H2A, and H2B whereas RI histones are variants such as H3.3, CENPA, and H2AX. RD histones form the majority of nucleosomes in chromatin packaging, so they are mass produced during S-phase, in which DNA is duplicated. Histone variants, however, can be expressed and incorporated in chromatin at any point in the cell cycle. In the following sections, I will focus on the coordinated expression of RD histones during S-phase, which allows for the coordinated packaging of chromatin.

Histone genomic organization

Histone genes are organized as clusters in a few genomic locations. In mammals, there is one major and two minor clusters of histone genes. HIST1, on chromosome 6, contains

80% of histone genes. HIST2 and HIST3, on chromosome 1, contain 6 and 3 genes, respectively. In humans and mouse, RD histones each have 14-22 copies of their respective genes (Albig et al. 1997; Amatori et al. 2021; Marzluff et al. 2002; Wang, Krasikov, et al. 1996; Wang, Tisovec, et al. 1996). In Drosophila, all RD histones and H1 are clustered on chromosome 2 in 5kb tandem repeats (x100) (Lifton et al. 1978). Other model organisms such as *X. laevis* and *C. elegans*, also maintain clusters of multiple copies of histone genes in their genome (Perry, Thomsen, and Roeder 1985; Pettitt et al. 2002). This infers that histone genes are tightly linked throughout evolution. The selective pressure to maintain this unique organization indicates the importance of clustering for histone synthesis.

Histone transcription and translation

Given the high demand for RD histones (4x10^8 molecules per core histone) during S-phase, the cell cycle phase in which DNA is replicated, histone expression is coupled to the cell cycle (Armstrong and Spencer 2021; Duronio and Marzluff 2017). In S-phase, Cyclin E in complex with Cyclin-Dependent Kinase 2 (CDK2) phosphorylates Nuclear Protein at the Ataxia-Telangiectasia locus (NPAT) (Ma et al. 2000; Zhao et al. 1998, 2000). Through an unidentified mechanism, NPAT is specifically recruited to histone gene clusters along with FLICE-Associated Huge Protein (FLASH) to form the Histone Locus Body (HLB) (Armstrong et al. 2023; Barcaroli et al. 2006; White et al. 2011). The HLB resembles a phase separated condensate that concentrates the proteins necessary for histone gene transcription and pre-mRNA processing (Duronio and Marzluff 2017).

Briefly, phosphorylation of NPAT allows NPAT to be maintained in the HLB and to recruit RNA polymerase II to induce transcription of histones genes. RD histone mRNAs lack introns and form a stem loop at their 3' end. Cleavage downstream to the stem loop is required for histone mRNAs to be released and exported into the cytoplasm (Moss et al. 1977). Stem Loop Binding Protein (SLBP) binds close to the stem loop and LSM1 and LSM11 of the U7 snRNP complex bind to the Histone Downstream Element (HDE) 15 nucleotides downstream of the cleavage site to stabilize and recruit the Histone Cleavage Complex (HCC). HCC consists of Cleavage Stimulating Factor 2 (CstF64), Cleavage and Polyadenylation Specificity Factor 100 (CPSF100), and Cleavage and Polyadenylation Specificity Factor 73 (CPSF73) which will cleave the mRNA between the stem loop and HDE (Dominski, Yang, and Marzluff 2005; Mandel et al. 2006; Mandel, Bai, and Tong 2008; Romeo, Griesbach, and Schümperli 2014; Ryan, Calvo, and Manley 2004; Strub, Birnstiel, and Birnstiel 1986; Yang et al. 2013). Once histone mRNA is cleaved, it is exported with SLBP by antigen peptide transporters into the cytoplasm (Erkmann et al. 2005; Huang et al. 2003; Huang and Steitz 2001) (Figure 1-1 A and B).

Translation of RD histone mRNA is induced by the interaction of SLBP with SLBP-Interacting Protein 1 (SLIP1) that mediates binding to Eukaryotic Initiation Factor 4G (EIF4G) (Cakmakci et al. 2008; Gallie, Lewis, and Marzluff 1996; Gorgoni et al. 2005; Von Moeller et al. 2013; Sànchez and Marzluff 2002; Whitfield et al. 2004). This circularizes the mRNA leading to the efficient translation of histone mRNA (Wells et al. 1998) (Figure 1-1 C). Once translated, histone proteins are imported into the nucleus, oligomerized, then deposited into chromatin, which I will discuss in more detail under 'histone oligomerization, import, and chromatin deposition.'

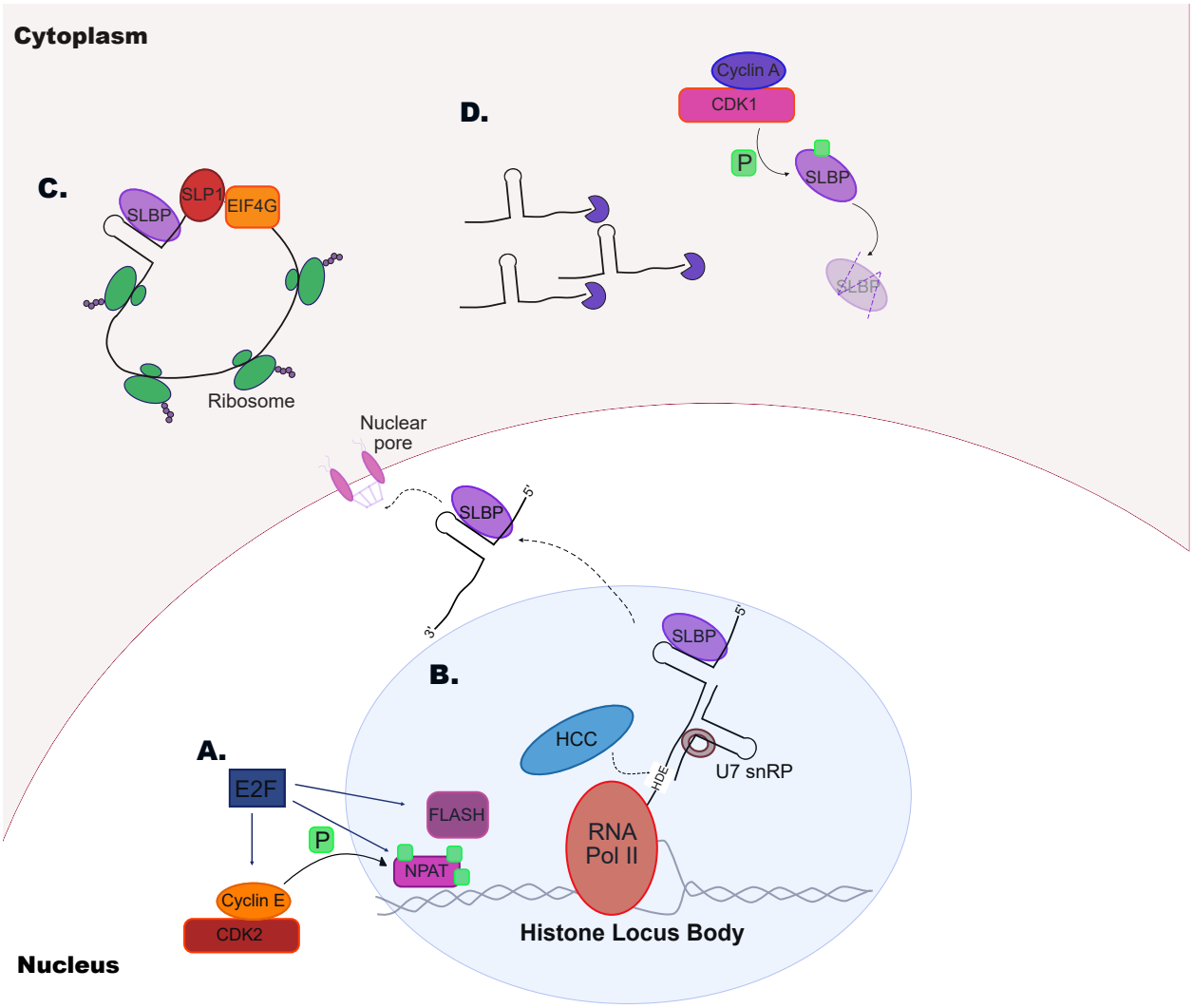

Figure 1-1.Schematic of canonical histone biosynthesis

(A) Transcription factor E2F induces cell cycle dependent transcription of Cyclin E, NPAT, and FLASH at the cusp of G1 to S-phase of the cell cycle. (B) Cyclin E/CDK1 complex phosphorylates NPAT which along with FLASH forms the histone locus body at the histone clusters in the genome. This recruits RNA polymerase II and mRNA processing proteins that will induce transcription and allow for the cleavage of the mRNA so that it can be released. (C) Once SLBP transports histone mRNA into the cytoplasm, it will circularize with the aid of SLP1 and EIF4G to be translated efficiently. (D) At the end of S-phase, when histone proteins are no longer needed at high demand, SLBP will be phosphorylated by G2 Cyclin A/CDK1 complex which causes its degradation. Once SLBP is depleted, histone mRNA synthesis will be terminated in the nucleus and the remaining mRNA in the cytoplasm will be degraded by exonucleases.

At the end of S-phase, when the demand for histones is decreased, histone production must come to an end. The end of S-phase is correlated with the depletion of Cyclin E. Thus, NPAT phosphorylation will lessen, and transcription of RD histones will decrease. Phosphorylation of SLBP by the G2 specific Cyclin A/CDK1 results in SLBP degradation (Koseoglu, Graves, and Marzluff 2008; Zheng et al. 2003). In the absence of SLBP, the already transcribed mRNA will be degraded, and mRNA processing will cease (Figure 1-1 D).

In contrast to RD histones, RI (or variant histones), are expressed throughout the cell cycle (eg. H3.3) or during a specific stage of the cell cycle (eg. CID during G2). Unlike RD histones, RI histones have introns, are polyadenylated, and are processed like all other mRNA in the cell.

Histone oligomerization, import, and chromatin deposition

Once translated, histone proteins are always bound by chaperones to maintain their stability and prevent their aggregation. This class of proteins termed histone chaperones, work in a network to shuttle histones from the cytoplasm into the nucleus to deposit them onto chromatin whilst they dimerize and become post translationally modified. Histone chaperones are categorized based on their specificity to H3-H4 or H2A-H2B. In the below section, I will briefly outline the current models of histone chaperone networks that function to prepare and deliver histones H3-H4 and H2A-H2B to their chromatin destination.

H3-H4

Most work in understanding histone trafficking and chromatin deposition has been done on histone H3-H4. I will describe two models: Dimer and Monomer models.

Dimer model

This model emerged from immunoprecipitation-mass spectrometry (IP-MS) of pre-deposited H3. In one major article, Campos *et al.* fractionated cells to identify the earliest chaperone complexes to bind H3-H4 once they are translated in the cytoplasm. According to this model, once H3 is translated, it is bound by heat shock cognate 70 (HSC70) to assist in folding. Then H3 and H4 are transferred to heat shock protein (Hsp90) which in complex with Testicular Nuclear Autoantigenic Sperm Protein (tNASP) aids in dimerization. Somatic Nuclear Autoantigenic Sperm Protein (sNASP) binds to the H3-H4 heterodimer and binds in such manner that allows H4 binding to Retinoblastoma Associated Protein 46 (RBAP46) that then recruits Histone Acetyltransferase 1 (HAT1) to acetylate the H4 histone tail. The H3-H4 complex is transferred to Anti-Silencing Factor 1 (ASF1) that associates with Importin 4 (IPO4) to allow histones to be transported into the nucleus. ASF1 is the central histone chaperone for H3-H4 as it mediates import and transfer of H3-H4 to Chromatin Assembly Factor 1 (CAF1) complex (p150, p60, p48) for RD deposition into chromatin. ASF1 can also bind to the H3.3-H4 variant and transfer H3.3-H4 to the Histone Regulation Complex (HIRA) (HIRA, UBN1, CABIN1) for

replication-independent deposition (Campos et al. 2010, 2015; Tagami Hideaki et al. 2004) (Figure 1-2 A).

Monomer model

This model arose, from Adam Bowman's lab, due to the following points. The histone chaperone NASP described in the 'dimer' model was localized in the cytoplasm in biochemical experiments but has now been shown to be in the nucleus via immunofluorescence or fluorescent tagging of NASP (Apta-Smith, Hernandez-Fernaud, and Bowman 2018). This observation and the limitations of fractionation studies which can lead to nuclear proteins leaking from the nucleus during cell disruption led researchers to believe that NASP may function solely in the nucleus. Further, artificially tethered cytoplasmic histones do not bind to histone chaperones and only bind importins (Apta-Smith et al. 2018). Lastly, immunoprecipitations (IP) of NASP led to a two-fold enrichment of H3 over H4. Whereas ASF1 binds to equimolar ratios of H3:H4 (Apta-Smith, Hernandez-Fernaud, and Bowman 2018). Thus, in this model, it is postulated that NASP binds monomers of histones (Apta-Smith et al. 2018; Maksimov et al. 2016; Pardal and Bowman 2022). Altogether, the major difference in this model is that NASP binds H3 monomers in the nucleus, not in the cytoplasm. H3 and H4 remain as monomers in the cytoplasm after translation and are imported by Importin 4 (IPO4) or Importin 5 (IPO5) into the nucleus and are received by NASP (H3) or RBAP46-HAT1(H4) once in the nucleus. H4 will be acetylated in the nucleus then a NASP-RBAP46-HAT1 complex will form and dimerize H3-H4. Only then will H3-H4 or H3.3-H4 heterodimers bind to ASF1

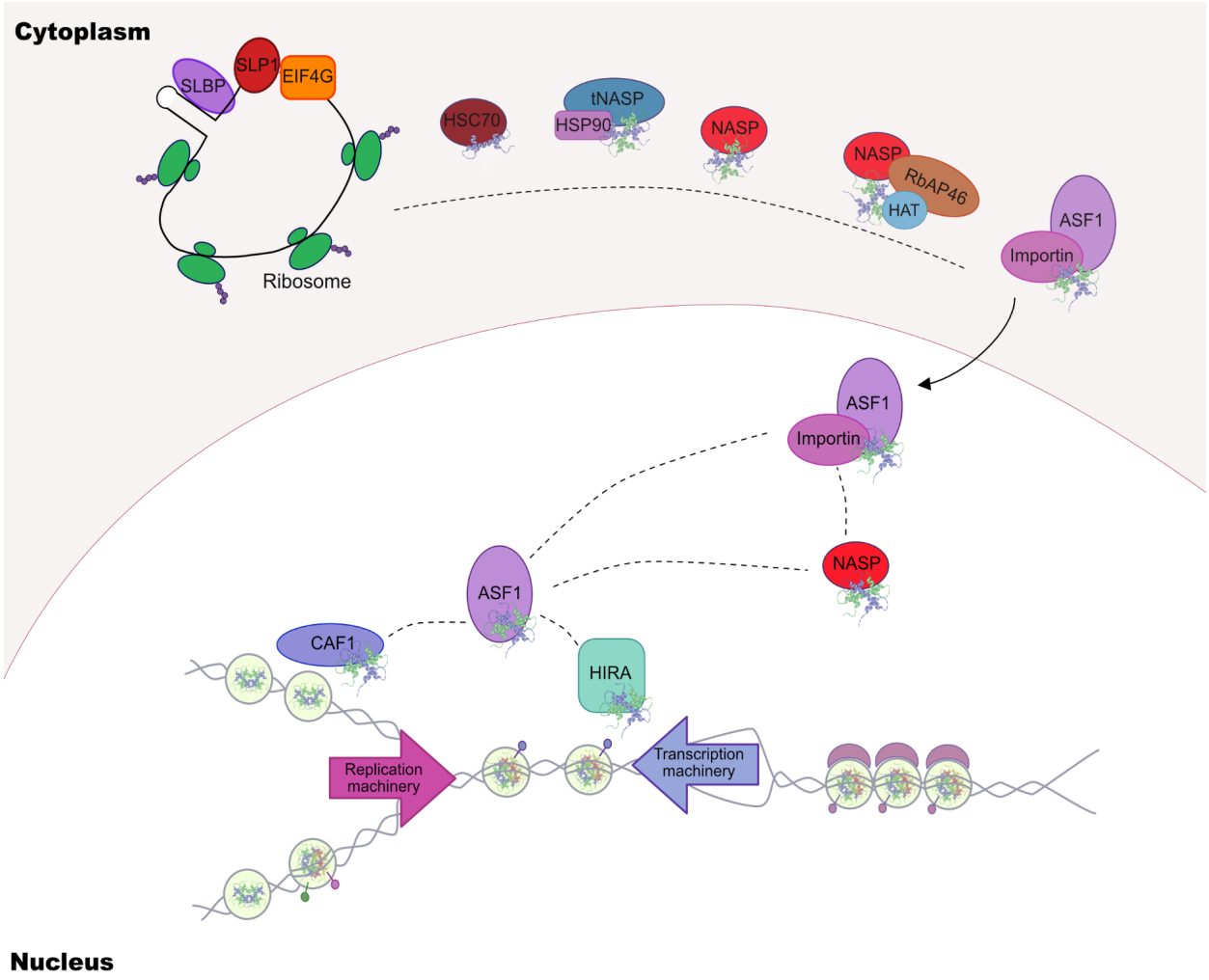

Figure 1-2. Outline of the dimer model of H3-H4 dimerization, import, and chromatin deposition.

The dimer model is exclusively extracted from fractionation studies in which histone chaperones bind to H3-H4 to aid in their dimerization, acetylation, and import into the nucleus.

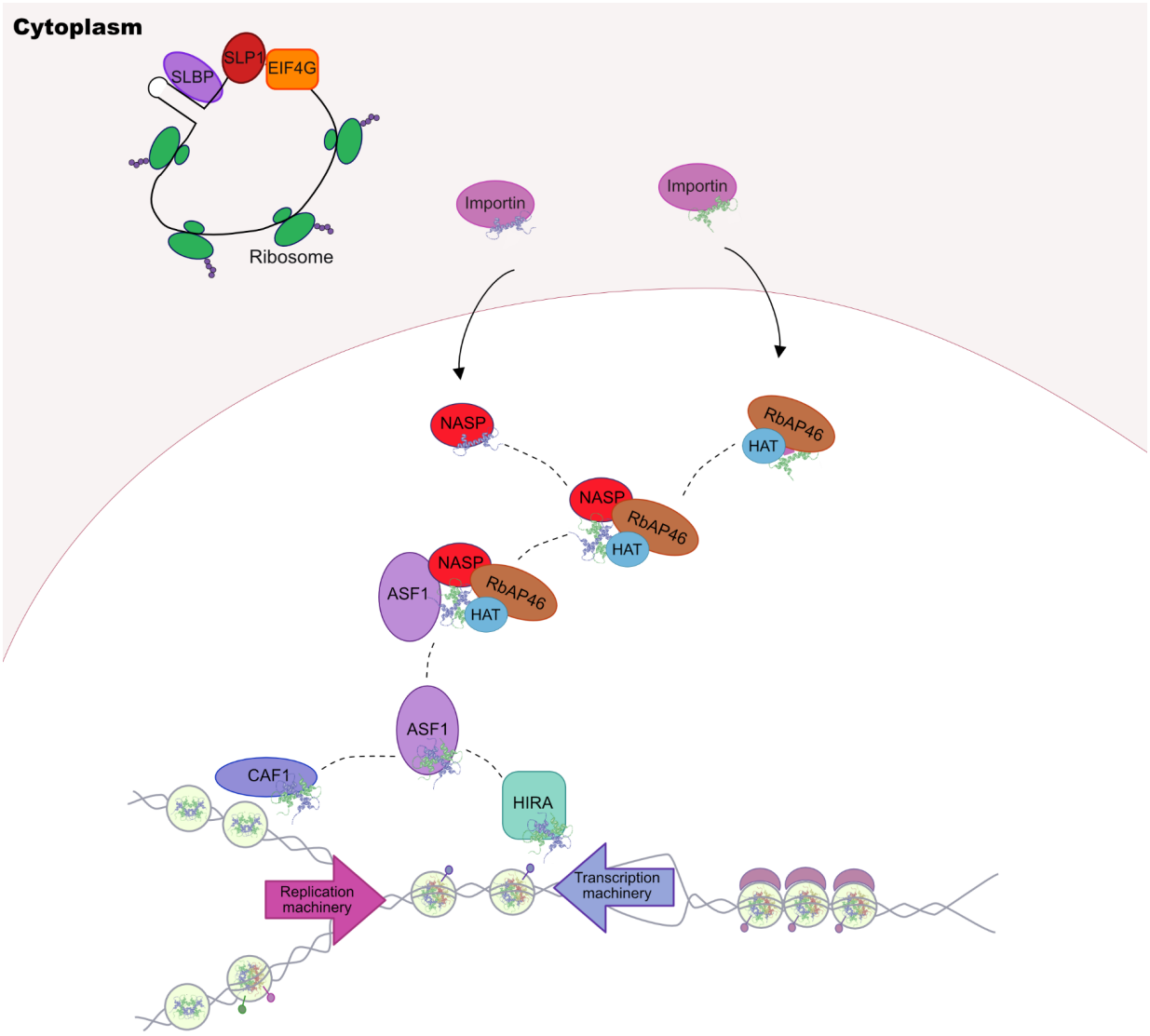

Figure 1-3. Outline of the monomer model of H3-H4 dimerization, import, and chromatin deposition.

H3-H4 histone chaperones, like NASP, are exclusively in the nucleus. Further, histones are imported as monomers, are dimerized, and acetylated once they are in the nucleus.

which can mediate transfer to CAF1 or HIRA for replication-dependent or independent chromatin deposition, respectively (Figure 1-2 B).

H2A-H2B

Once a tetramer of H3-H4 has been incorporated into chromatin, H2A-H2B heterodimers will be added to form the nucleosome. There is less known about H2A-H2B travel and deposition, but the current model is that once H2A-H2B are translated, they are dimerized then transferred to Nucleosome Assembly Protein 1 (NAP1). Importin 9 (IPO9) will import the dimer into the nucleus (Aguilar-Gurrieri et al. 2016; Andrews et al. 2010; Ito et al. 1996; Namboodiri et al. 2003; Rodriguez et al. 1997; Straube, Blackwell, and Pemberton 2010; Zlatanova, Seebart, and Tomschik 2007). While H2A-H2B stay intact with NAP1, H2AZ-H2B are handed off to the protein YL1 (YL1) subunit of Snf2-related CREBBP activator protein (SRCAP) complex (Latrick et al. 2016; Liang et al. 2016; Luk et al. 2007). Then, Facilitates Chromatin Transcription (FACT) can incorporate dimers in a replication-dependent or replication-independent manner onto chromatin (Belotserkovskaya et al. 2003). In this case, there is a major overlap of histone chaperone functions. For example, in the absence of NAP1, FACT can facilitate H2AZ-H2B import and incorporation (Luk et al. 2007).

Consequences of aberrant histone levels

From yeast to man, histone surplus or dearth leads to detrimental consequences. As such, deletion of the histone cluster in *D. melanogaster* causes embryonic lethality (Günesdogan, Jäckle, and Herzig 2010). Further, in mammalian cells and *S. cerevisiae*, depletion of histones leads to open chromatin, an increase in transcription, and sensitivity to DNA damage (Celona et al. 2011; O'Sullivan et al. 2010). On the other hand, overexpression of histones in Drosophila oogenesis, in an *abnormal oocyte* (*abo*) mutant, leads to aberrant transcription and is associated with embryonic lethality (Berloco et al. 2001a). In *S. cerevisiae*, overabundance of histones can cause chromosome loss and increase in DNA damage sensitivity (Herrero and Moreno 2011; Singh et al. 2010).

Due to the requirement for stringent control of histone levels, the cell has in place multiple layers of regulation to balance the supply and demand of histones. Histone biosynthesis is carefully coordinated with S-phase and histone proteins are always bound by histone chaperones to prevent aggregation.

Drosophila model organism to study histone storage and dynamics

Prelude

D. melanogaster provides plenty of benefits to utilize in developmental research. It has a short generation time, ease of husbandry and maintenance, and low cost. Further, it has a well-annotated genome, in which 60% of the genome is homologous to humans. Thanks to many predecessors and the current community of Drosophila researchers, Drosophila

has a well-defined development system and well-established genetics, which includes numerous genetic mutants. These consist of balancer stocks that assist in chromosomal mapping of phenotypes and complementation of CRISPR mutants, P-elements that potentially disrupt gene function, and transgenic flies that harbor dsRNA for knockdown of genes or fluorophore tagged proteins for imaging in specific tissues. Significantly, the Drosophila community has a publicly available and well annotated bioinformatics database (flybase) and a repository for transgenic flies (Bloomington).

For this thesis's purposes, I am grateful that Drosophila embryogenesis has been well established. As I will describe in the later sections, it provides the ideal system to study histone chaperone networks. Briefly, current histone chaperone network models are formulated based upon fractionation studies in somatic cells where contents from the nucleus can leak into the cytoplasmic fractions. This is a real concern because somatic cells contain only a small pool of soluble histones (<1% of total). During *D. melanogaster* embryogenesis, there can be >99% soluble histones, which provides an optimal system to study histone chaperone networks for storage, cytoplasmic folding, dimerization, nuclear import, and chromatin deposition (Shindo et al. 2022).

In the following sections, I will outline the Drosophila developmental system and briefly summarize our current understanding of histone chaperone functions in oogenesis and early embryogenesis.

Drosophila oogenesis, fertilization, and embryogenesis

The female fly possesses a pair of ovaries comprised of 15-20 ovarioles. Each ovariole contains egg chambers that increase in maturity from anterior to posterior end. At the most anterior tip remains the germarium while the posterior end consists of larger and most mature egg chambers. At the anterior end, Germline Stem Cells (GSC) divide asymmetrically to give rise to a new stem cell and a cytoblast (Lin and Spradling 1993; Schupbach, Wieschaus, and Nothiger 1978; Wieschaus and Szabad 1979). The cytoblast will undergo four rounds of mitotic divisions with incomplete cytokinesis creating a 16-cell cyst interconnected via ring canals. One of these cells will form the oocyte whereas the 15 others will become nurse cells. In each egg chamber, there is a monolayer of epithelial cells termed the follicle cells that surround a single oocyte and 15 supporting nurse cells (Lin and Spradling 1993). Nurse cells will synthesize histone mRNA and protein throughout oogenesis that will be dumped into the egg chamber starting at stage 10 of oogenesis as the nurse cells degenerate (Quinlan 2016). It is important to note that histone mRNA synthesis increases 4-fold after nurse cell dumping. This increase in gene and protein expression is uncoupled from DNA synthesis and contributes to the maternal pools that supplement rapid embryonic cleavages (Ruddell and Jacobs-Lorenat 1985; Walker and Bownes 1998).

Female flies can store up to ~600 sperm, and eggs are fertilized and activated as the embryo is being laid (Lefevre and Jonsson 1962). Molecularly, the chromosomes of the Drosophila oocyte are arrested in metaphase of the first meiotic division (King 1970). At fertilization, mature spermatozoa will enter an egg in the female's oviduct. The sperm must then decondense, a process during which sperm specific nuclear basic proteins (SNBP) are replaced with histones

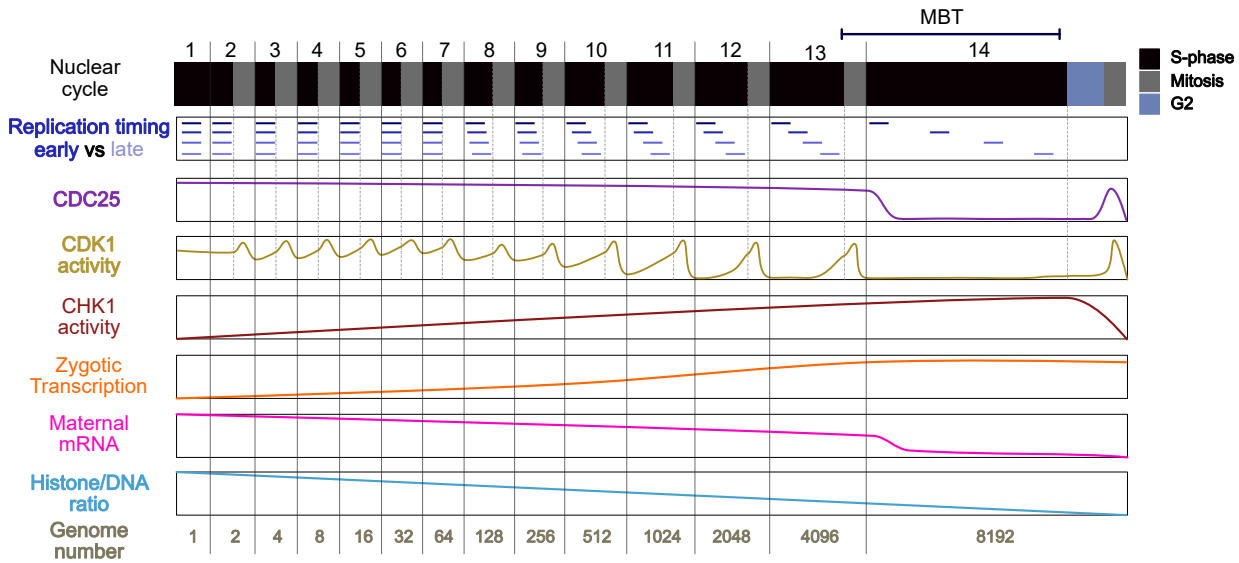

Figure 1-4. Trends of major changes in Drosophila embryogenesis.

As nuclear cycles proceed through embryogenesis, interphase is lengthened with the longest interphase taking place in NC 14 in which G2 is introduced to the cell cycle profile. Below the NC, the major changes that occur in NC14 during MBT are graphed. Replication timing becomes active (blue). CDC25 protein levels (purple) and CDK1 activity (gold) is decreased until entry into Mitosis opposite to the trend seen in CHK1 activity (brown). The embryo is no longer dependent on maternal deposited materials as maternal mRNA (pink) is degraded and zygotic transcription (orange) becomes active. Lastly, the Histone/DNA ratio (light blue) is decreased as soluble histones decrease from >99% to less than 1%.

(Perreault, Wolff, and Zirkin 1934; Sutovsky and Schatten 1997). This is done with maternally deposited histone chaperone HIRA, which facilitates the replacement of SNBPs with H3.3 histones to form the male pronucleus (Loppin et al. 2000; Loppin, Berger, and Couble 2001). Once egg activation occurs, female meiosis is resumed, and the innermost meiosis product becomes the female pronucleus which then migrates towards the male pronucleus and combines to form a diploid rosette (Horner and Wolfner 2008). At this point, the diploid rosette initiates metaphase of the first mitosis which contains half of each parental chromosome (Loppin, Dubruille, and Horard 2015).

The early embryo experiences rapid synchronous nuclei division utilizing the maternally deposited materials, including histone mRNA and protein. Nuclear cleavage occurs in one syncytium as fast as every ~8 minutes compared to 8-24 hours in somatic cells (Brown, Wensink, and Jordan 1971; Shermoen, McCleland, and O'Farrell 2010). In the early embryo, the nuclei alternate between S-phase (~3 minutes) and mitosis (~5 minutes) in the absence of gap phases (Blumenthal, Kriegstein, and Hogness 1974). As DNA is replicated in a span of ~3 minutes, histones are required to package the chromatin quickly. Unlike somatic cells, the early embryo contains >99% soluble histones to drive rapid chromatinization during nuclear cycles (NC) 1-13. As the embryo proceeds through embryogenesis, interphase is elongated (Foe and Alberts 1983; Rabinowitz 1941). The lengthening of interphase is correlated with Cyclin Dependent Kinase 1 (CDK1) inactivity as CDK1 triggers entry into mitosis (Farrell and O'Farrell 2014). In early NCs, CDK1 activity is high, and all DNA is replicated at once (Edgar et al. 1994). As NCs proceed, interphase elongates, and CDK1 activity is hindered until the end of interphase. It is during the lengthened interphase of NCs 8 and 9 that nuclei begin to migrate outwards to form

a shell around the embryo called the blastoderm (Foe and Alberts 1983; Rabinowitz 1941). In NC 14, CDK1 activity is kept inactive the longest, leading to the longest interphase yet (~70 minutes) and the beginning of cellularization. This transition also introduces Gap phase 2 (G2) in which gastrulation occurs (Edgar and D 1989; Edgar and G 1990). This phenomenon is called the Mid-Blastula Transition (MBT). Multiple overlapping yet independently regulated events occur during the MBT which contribute to the change in cell cycle profile: (1) maternal mRNA is degraded and zygotic transcription is activated (Edgar and Schubigert 1986; Zalokar 1976) (2) replication timing is established (McCleland, Shermoen, and O'Farrell 2009; Shermoen et al. 2010; Yuan, Shermoen, and O'Farrell 2014) (3) activation of DNA damage checkpoints become active (Farrell and O'Farrell 2014) (Figure 1-3).

What triggers this major change in cell cycle profile during embryogenesis? The 'titration' model depicts that there may be a sensor for the nuclear to cytoplasmic ratio that relays the cascade of overlapping events at the MBT (Chen et al. 2019; Edgar, Kiehle, and Schubigert 1966; Kane and Kimmel 1993; Newport and Kirschner 1982b, 1982a). Given that histone concentration decreases from >99% from NCs 1 to 14, histones have been postulated to be this titrating biosensor (Almouzni and Wolffe 1993, 1995; Amodeo et al. 2015; Chari et al. 2019; Joseph et al. 2017; Prioleau et al. 1994; Shindo and Amodeo 2021). Specifically, histones can modulate CHK1 activity to regulate CDK1 activity. Briefly, CDK1 activity is regulated by kinases and phosphatases; it can be inactivated by WEE1 kinases via inhibitory phosphorylation or activated by the removal of the inhibitory phosphorylation by Cell Division Cycle 25 (CDC25)

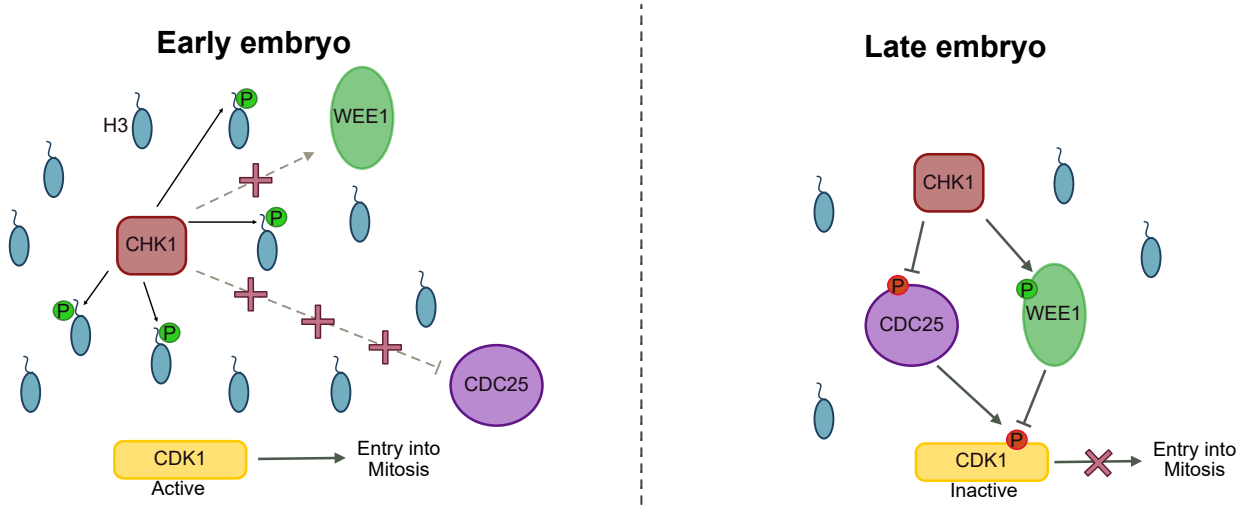

Figure 1-5. Titration model for slowing of cell cycle in Drosophila embryogenesis; H3 may be the biosensor for the nuclear to cytoplasmic ratio.

In the early embryo, there are large pools of soluble histone which outcompete CHK1 phosphorylation targets (like CDC25 and WEE1). Instead, CHK1 will phosphorylate H3 histone tail. This allows for elevated levels of CDK1 activity and the swift entry into Mitosis throughout NCs. As embryogenesis proceeds, soluble H3 will be depleted (Figure 1-3) which allows for phosphorylation of CHK1 target substrates CHK1. This includes kinases that regulate CHK1 activity. Phosphorylated CDC25 is inactive while phosphorylated WEE1 is active; CDK1 will gain inhibitory phosphorylation by WEE1 which cannot be removed by inactive CDC25. Since CDK1 is kept inactive, entry to Mitosis is stalled which leads to the lengthening of interphase and a longer cell cycle.

(Dunphy and Kumagai 1991; Edgar et al. 1994; Edgar and D 1989; Edgar and G 1990; Gould and Nurse 1989; Russell and Nurse 1966). Checkpoint Kinase 1 (CHK1), which is active in nuclear cycle 14, can inhibit CDC25 and activate WEE1 by phosphorylation which leads to CDK1 inactivity (Fogarty et al. 1997; Sibon, Stevenson, and Theurkauf 1997) (Figure 1-4). In Drosophila, *CHK1* mutants (*grapes*) have shorter interphase and incur a premature mitotic entry before DNA replication is complete in NC13 (Fogarty et al. 1997; Sibon et al. 1997; Sullivan, Fogarty, and Theurkauf 1993; Yuan, Farrell, and O'Farrell 2012). Interestingly, depletion of histone levels (*SLBP* mutant) leads to premature CHK1 activation and overexpression of N-terminal tail of H3 delays CHK1 activation (Chari et al. 2019; Shindo and Amodeo 2021). Altogether, this indicates that histones, specifically H3, modulate CHK1 activity. The current model is that soluble pools of H3 have a non-chromatin function by outcompeting CHK1 substrates in the early NCs. As soluble histone levels decrease, CHK1 can phosphorylate its targets, such as CDC25 and WEE1 which leads to CDK1 inactivity and thus the lengthening of interphase (Figure 1-4). Not only has this model suggested an upstream regulatory event in MBT but also identified an off-chromatin function for soluble histones.

Significantly, this presents *D. melanogaster* embryogenesis as a powerful model organism to study soluble histone storage and histone chaperone networks. The early embryo is supplemented with >99% soluble histones that require storage, dimerization, shuttling into the nucleus, and chromatin deposition, all of which is performed by histone chaperones.

Below, I highlight our current understanding of histone chaperone function in early development.

Histone chaperones in early development

HIRA

H3-H4 specific chaperone HIRA incorporates H3.3 during oogenesis for transcriptional regulation in *M. musculus* and *X. laevis* (Nashun et al. 2015; Ray-Gallet et al. 2002). It also is essential for replacing protamine with H3.3 to decondense sperm to allow for male pronucleus formation in *H. sapiens, M. musculus*, and *D. melanogaster*. Thus, it is embryonic lethal in *M. musculus* and *D. melanogaster* (Bonnefoy et al. 2007; Van Der Heijden et al. 2005; Lin et al. 2014a, 2014b; Smith et al. 2021).

CAF1

CAF1 is a major histone chaperone that directly deposits H3-H4 onto chromatin in a replication dependent or DNA damage repair dependent manner. Human H3-H4 chaperone CAF1 consists of subunits p150, p60, and p48. Abolition of *X. laevis* p150 leads to cell cycle arrest during early embryo development and impaired nuclear organization (Quivy, Grandi, and Almouzni 2001). Further, deletion of the *D. melanogaster* p150 is hemizygous lethal in *D. melanogaster* which suggests its importance in H3-H4 chromatin deposition in the early embryo (Song et al. 2007).

ASF1

In somatic cells, ASF1 is the H3-H4 central chaperone in delivering histones to be deposited in a replication-dependent and -independent manner. Thus far, it has been shown that ASF1 functions similarly in mediating the transfer of H3.3 to HIRA to allow for male pronucleus formation (Horard et al. 2018). ASF1 is essential in somatic cells and maternal effect lethal in *D. melanogaster* (Moshkin et al. 2002, Sanematsu et al. 2006).

Nucleoplasmin

Nucleoplasmin has been characterized to exchange sperm-specific basic proteins in sperm for H2A-H2B in *X. laevis* fertilization and store H2A-H2B reservoirs in oocytes (Dilworth, Black, and Laskey 1987; Philpott' and Lenot 1992).

Jabba

H2A-H2B specific chaperone Jabba sequesters H2A-H2B to lipid droplets in the cytoplasm of the early *D. melanogaster* embryos. This allows for the maintenance of the large pools of H2A-H2B and prevents their degradation. Homozygous *Jabba* mutants are viable in Drosophila (Li et al. 2012).

NASP

Previously identified as a H1 linker chaperone important for sperm maturation, NASP was observed in complex with large pools of H3-H4 and was presumed to function as a storage for H3-H4 in *X. laevis* oocytes (Kleinschmidt et al. 1984; Kleinschmidt and Franke 1982; Kleinschmidt and Seiter 1988; Richardson et al. 2000). NASP function is thoroughly outlined in the section below. However, the work outlined in chapter III will forge NASP as the H3-H4 chaperone in the early embryo whose function is important for development.

H3-H4 chaperone NASP: structure and function

Historical context of NASP function

In the late 1980s, *X. laevis* N1 polypeptide was discovered in a complex with large pools of non-nucleosome histone H3-H4 in oocytes. Researchers inferred that N1 provides a mechanism for storage of histones H3-H4 analogous to Nucleoplasmin storage of H2A-H2B in oocytes (Kleinschmidt et al. 1986; Kleinschmidt and Franke 1982; Kleinschmidt and Seiter 1988; Kleinschmidt et al. 1984)

In 1990, N1 rabbit homolog, termed **n**uclear **a**utoantigenic **s**perm **p**rotein (NASP) due to its nuclear localization in rabbit spermatozoa was observed (Welch and O'Rand 1990). NASP exists in two alternatively spliced isoforms: somatic NASP (sNASP), expressed ubiquitously, and testicular NASP (tNASP), predominantly expressed in testis, ovaries, and transformed cells (Richardson et al. 2000) (Figure 1-6). From 2000-2008, research from Michael G. O'Rand's lab focused on NASP function as a histone H1 linker chaperone. Specifically, tNASP co-purified with H1 in mouse testis, mouse myeloma 66-

2 cells and HeLa cells (Alekseev et al. 2002, 2004; Richardson et al. 2000). Also, sNASP can incorporate H1 into nucleosome arrays in vitro (Finn et al. 2008).

In 2004, *S cerevisiae.* and *S. pombe* NASP homologs Hat1p-Interacting Factor-1(Hif1p) and Silencing in the Middle of the Centromere Protein 3 (Sim3) were shown to preferentially bind H3-H4 and the H3-H4 and Centromeric Histone 3 variant CENPA, respectively. Neither protein bound to linker H1 (Ai and Parthun 2004; Dunleavy et al. 2007). Further, in HeLa cells, immunoprecipitation of H3.1 or H3.3 led to NASP enrichment, suggesting that NASP is either directly or indirectly bound to H3 and its variants (Tagami Hideaki et al. 2004).

Two contradictory research papers were published in 2008. One indicated sNASP binds H1 linker protein specifically and the other indicated sNASP binding to both H1 and H3-H4 in vitro (Finn et al. 2008; Wang, Walsh, and Parthun 2008). Both articles demonstrated that sNASP can incorporate H3-H4 or H1 onto DNA deeming its binding to either histone as functional. To note, Finn *et al*. employed native gel electrophoresis for in vitro experiments in which sNASP-H3-H4 mixtures could not migrate past the well. They argued that this is because of sNASP's non-specific binding to histones due to its acidic nature and thus sNASP-H1 interaction is unique. On the other hand, Wang *et al.* utilized native gel electrophoresis, affinity chromatography assays, and surface plasmon resonance to test whether sNASP binds specifically H3-H4. In all cases, sNASP is bound to both H3-H4 and H1.

Since then, research has established that NASP binds to H3-H4 both in vivo and in vitro and functions as a H3-H4 chaperone (Bowman et al. 2015, 2016; Campos et al. 2010, 2015; Cook et al. 2011; Le Goff et al. 2020; Kato et al. 2015; Kleiner et al. 2018; Lambert

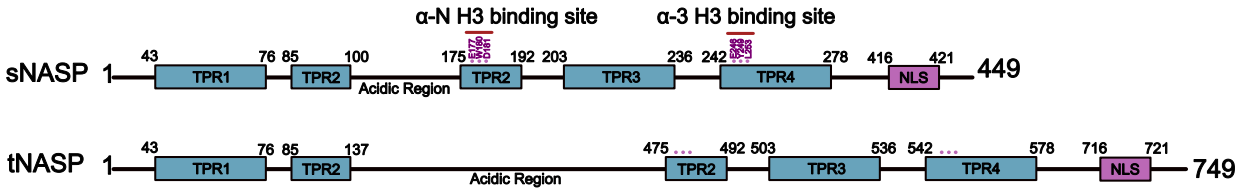

Figure 1-6. Schematics of *H. sapien* sNASP and tNASP.

sNASP and tNASP proteins with 4 TPR domains in which the second TPR domain interrupted by a long acidic region. tNASP has a longer acidic region. NLS is located at the end of both NASP isoforms. H3 α-N and α-3 binding sites are marked by red lines. Magenta dots represent specific amino acids important for H3 binding.

et al. 2015; Liu et al. 2021; Maksimov et al. 2016). In contrast, the *S. cerevisiae* NASP homolog, Hif1p, has also been shown to bind H2A-H2B dimers and H3-H4 tetramers in vitro, under low ionic sensitivity conditions (Zhang et al. 2016).

NASP major domains and structure

All NASP homologs and isoforms (tNASP and sNASP) have 4 tetratricopeptide repeats (TPR) in which the second TPR motif is interrupted by a large acidic region. tNASP has a larger acidic region of unknown function. The TPR motifs are 34 amino acid amphipathic helices that form helix-turn-helix arrangement with the 4^{th} TPR, specifically the alpha-89 region, forming hydrophobic interactions to dimerize. Thus, NASP can be present as a dimer, to bind H3 only, or present as a monomer, to bind to both ASF1 and H3. Lastly, a nuclear localization signal (NLS) is located at the terminal region of the NASP protein (Kleinschmidt et al. 1986; Welch and O'Rand 1990). Though NASP structural domains are similar from yeast to humans, there is functional diversification (Nabeel-Shah et al. 2014).

More recently, two H3 binding motifs in NASP have been discovered; alpha-N and alpha-3 (Bowman et al. 2015). The alpha-3 region becomes available once NASP is bound to ASF1 while the alpha-N is for NASP lone interaction with H3 (Bao et al. 2022).

NASP functions

**unless otherwise specified ‘NASP’ indicates ‘tNASP’ and ‘sNASP’ as it either has not been specifically differentiated or it pertains to both isoforms.

NASP chaperones free soluble histones

Histone synthesis is uncoordinated with DNA synthesis in the early embryo. Instead, an ample supply of 140ng of histones are made in the unfertilized egg to sustain Xenopus development to late blastula stage (20,000 cells) (Woodland and Adamson 1977). This substantial reservoir of histones, critical for early development, is a conserved feature across all animal oocytes with rapid embryonic cleavages (such as Drosophila, Zebrafish, and Xenopus). Given the rapid DNA replication and nuclear division in this developmental context, these histone pools are crucial for chromatin packaging in the early embryo. Previous research has identified that nucleoplasmin binds to H2A-H2B reservoirs in the early embryo (Kleinschmidts et al. 1985). In the 1980s*, X. laevis* NASP homolog, N1 polypeptide, was discovered to be in complex with H3-H4 reservoirs in the oocyte (Kleinschmidt et al. 1984, 1986; Kleinschmidt and Franke 1982; Kleinschmidt and Seiter 1988).

In cultured mammalian U2OS, HeLa and HEK 293 cells, the absence of NASP leads to the depletion of soluble H3.1/H3.2/H3.3-H4 but not centromeric histone 3 variant CENPA (Campos et al. 2010; Cook et al. 2011). Moreover, the overexpression of NASP leads to an increase in H3-H4 levels which means that not only does NASP store H3-H4 but can modulate histone levels. Importantly, NASP modulates both pre- and post-nucleosomal

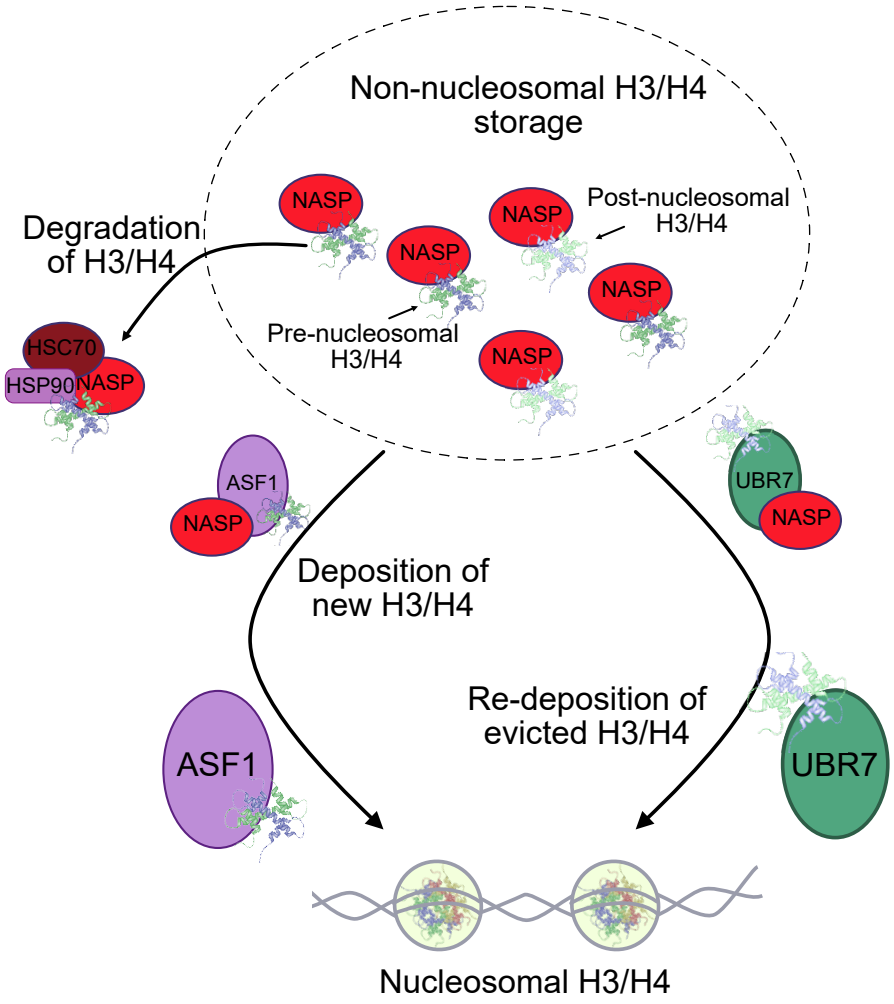

Figure 1-7. NASP mediates histone recycling, chromatin deposition, and degradation.

NASP stores pre- and post-nucleosomal H3-H4 histones. NASP transfers newly synthesized H3-H4 to ASF1 and evicted or post-nucleosome histones to UBR7 for chromatin deposition. Upon stress, NASP will transfer H3/H4 to HSC70 and HSP90 for autophagy directed degradation. This figure was adapted from Cook et al. 2011 and Hogan et al. 2021.

histone levels (Benson et al. 2006; Cook et al. 2011; Hogan et al. 2021; Loyola et al. 2006). Thus, NASP coordinates with the autophagy pathway or Ubiquitin Protein Ligase E3 Component N-Recognin 7 (UBR7) to degrade excess pre- and post-nucleosomal histones or to re-incorporate evicted post- nucleosomal histones in a replication-dependent manner, respectively (Benson et al. 2006; Cook et al. 2011a; Hogan et al. 2021; Loyola et al. 2006) (Figure 1-7)

NASP functions in the cytoplasm and/or the nucleus within histone chaperone networks to deposit histones on to DNA

Clever approaches have been taken to identify the histone chaperone networks that associate with histones from synthesis to the nucleus for chromatin deposition (Alvarez et al. 2011; Campos et al. 2010, 2015; Tagami Hideaki et al. 2004). Specifically, Campos *et al.* fractionated HeLa cells then immunoprecipitated replicative H3.1 from cytosolic and nuclear fractions individually. In doing so, they identified NASP as a predominant factor associated with H3.1 in the cytosolic fraction. tNASP was in complex with HSP90 and H3-H4 while sNASP was featured to be in a complex with H3-H4, HAT1 holoenzyme and sometimes ASF1B. These results suggested that NASP is one of the earliest chaperones to interact with H3-H4 once they are translated . Also, NASP assists in H3-H4 dimerization and H4 acetylation before H3-H4 is passed on to ASF1B and Importins to be imported in to the nucleus (Campos et al. 2010) (Figure 1-2). It is important to note, however, that

sNASP was also an enriched interacting partner of H3.1 in the nucleus (Campos et al. 2015).

Unlike somatic cells, *S. cerevisiae* NASP homolog, Hif1p, has been implicated to bind H3-H4 once they are imported with acetyltransferases in the nucleus. This is evidenced by the fact that immunoprecipitation of acetyltransferases from nuclear extracts were enriched for Hif1p and Hif1p co-localizes with acetyltransferases only in the nucleus (Ai and Parthun 2004).

NASP may directly incorporate histones onto chromatin

Many bodies of work have established NASP to perform chromatin assembly in vitro. Human NASP can promote nucleosome assembly with all H3 variants (H3.1, H3.2, H3.3, and CENPA) and incorporate H1 in arrays depleted of H1 linker histones (Finn et al. 2008; Kato et al. 2015; Osakabe et al. 2010).

In vivo, there is only correlative evidence that NASP functions to directly assemble chromatin. In *S. pombe* and *A. thaliana,* the absence of NASP leads to the depletion of CENPA or CENH3 at specific loci, respectively (Dunleavy et al. 2007; Le Goff et al. 2020). Yet, NASP was not immunoprecipitated as a factor of H3.1 or CENPA nucleosome complexes (Foltz et al. 2006). Further, chromatin immunoprecipitation-mass spectrometry (ChIP-MS) of both active and repressive histone marks did not enrich NASP (Ji et al. 2015). Thus, the absence of NASP may indirectly affect H3 variant levels on DNA.

Other indirect evidence that NASP may function to incorporate histones on to chromatin in vivo may be its enrichment at replication forks. Quantitative proteomic studies such as isolation of protein on nascent DNA (iPOND) and nascent chromatin capture (NCC) coupled to mass spectrometry in human somatic cells, *D. melanogaster* S2 cultured cells, and *D. melanogaster* embryos have all revealed NASP to be enriched on nascent DNA (Alabert et al. 2014; Alvarez et al. 2023; Munden et al. 2022; Wessel et al. 2019). This infers that NASP may be incorporating H3-H4 in a replication-dependent manner or that it was captured due to its presence in complexes with other histone chaperones more directly involved in replication-dependent chromatin assembly.

Overall, though there is ample evidence that NASP can assemble chromatin in vitro, with the addition of cytosolic factors, there is little support for direct chromatin assembly in vivo.

NASP may impact transcription

Transformer 1 (TRA-1) is required to promote female development in *C. elegans* hermaphrodites. Mechanistically, this occurs by NASP bridging Transformer 4 (TRA-4) to Histone Deacetylase 1 (HDAC-1) while being recruited to TRA-1 binding regions, which includes male specific genes. The recruitment of the TRA-4-NASP-HDAC-1 complex represses transcription at the loci, perhaps by deacetylation of histone marks (Grote and Conradt 2006). Though it is not fully understood whether NASP functions beyond a

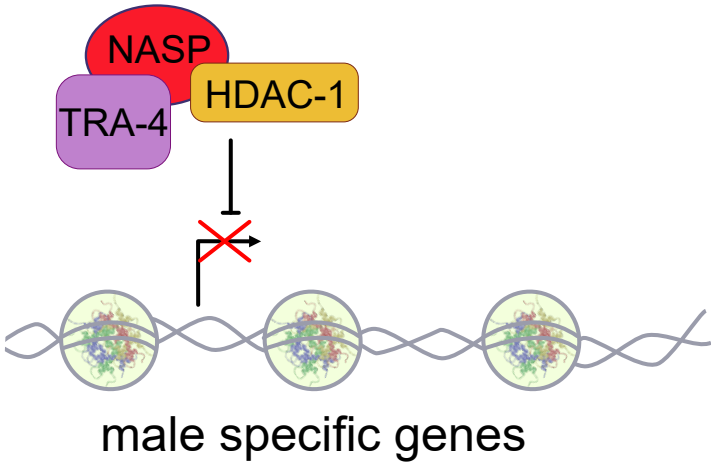

Figure 1-8. NASP promotes female development in *C. elegans.*

NASP acts as a scaffolding protein to bridge TRA-4 and HDAC-1 to allow for the recruitment of HDAC-1 to male specific genomic regions. This will inhibit transcription and inhibit male development thereby promoting female development in *C. elegans.*

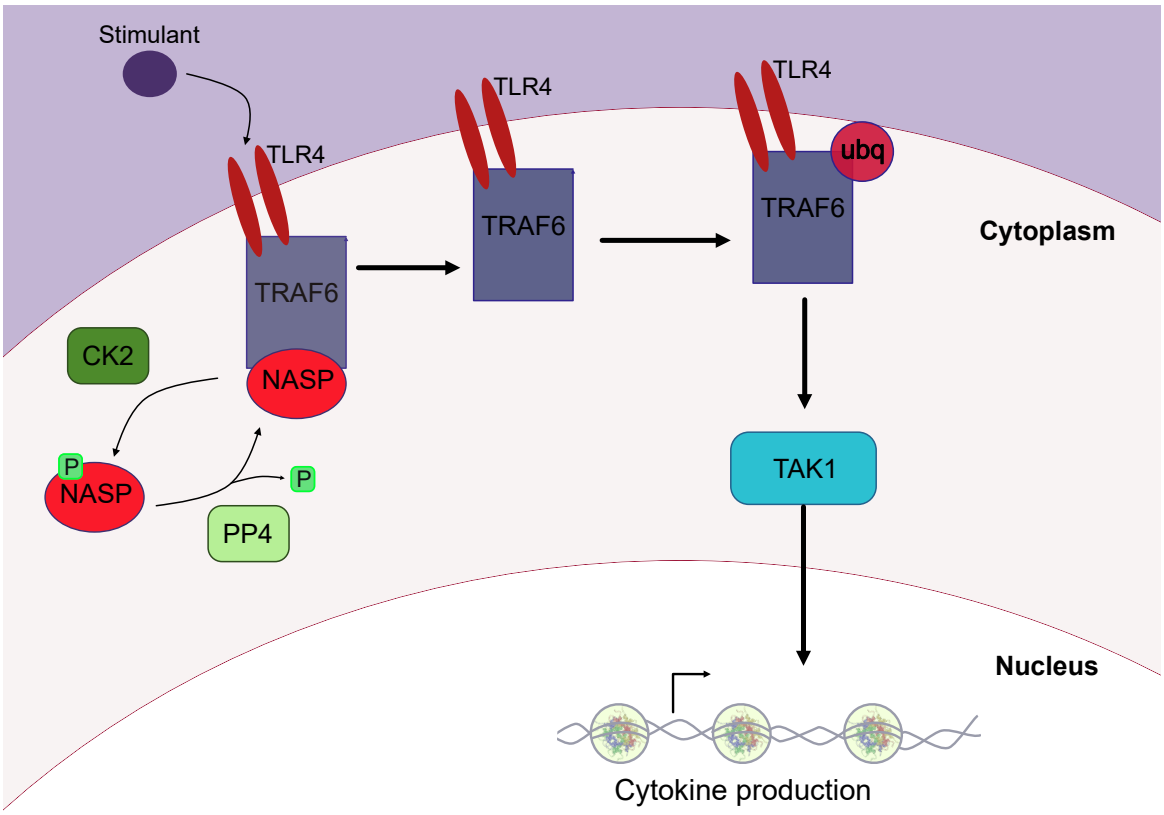

Figure 1-9. NASP phosphorylation promotes immune signaling.

TLR4 based stimulus activation leads to the phosphorylation of NASP by CK2 which can be antagonized by PP4. Once NASP is phosphorylated, it will disassociate from TRAF6, which will be auto-ubiquitinated. Ubiquitinated TRAF6 can activate TAK1 which will lead to cytokine transcription and thus production of an immune response.

scaffold protein between TRA-4 and HDAC-1, this finding has expanded the known roles of NASP to include transcriptional regulation (Figure 1-8).

NASP is major player in immune signaling

Unlike its previous role as related to histone and chromatin, sNASP has been implicated as a scaffold protein in the immune response signaling for sepsis and asthma in macrophages, epithelial, THP1, HEK293 cells, and mice (Chen et al. 2022; Wu et al. 2022; Yang et al. 2018, 2021). Upon immunologic stimulation, sNASP is phosphorylated by Casein Kinase 2 (CK2) which can be counteracted by Protein Phosphatase 4 (PP4) to inhibit signaling (Yang et al. 2021). Once sNASP is phosphorylated, it disassociates from Tumor Necrosis Factor (TN4) Receptor Associated Factor 6 (TRAF6) which is then auto ubiquitinated. This activates TRAF6 to then allow its ubiquitin activity on substrates such as Transforming Growth Factor (TGF)-β Activated Kinase 1(TAK1) to generate cytokine production via transcription (Yang et al. 2018) (Figure 1-9).

Major ideas have sprouted from these findings. sNASP NLS mutants retained the ability to inhibit immune signaling even in the presence of external immunologic stimulants, providing evidence that sNASP is located and functional in the cytoplasm. Also, this work has provided functional regulation of sNASP phosphorylation. The same phosphorylation sites could potentially affect NASP in its role as an H3-H4 chaperone. In *D. melanogaster,* NASP is phospho-regulated during egg activation which could overlap with its potential function as H3-H4 storage in the early embryo (Zhang et al. 2018). Lastly, they have

pinpointed the small region of sNASP (PEP-sNASP peptide) required to inhibit immune signaling which can now be used therapeutically to modulate Toll-like Receptor 4 Related (TLR4) inflammation (Wu et al. 2022).

NASP in disease

NASP role in cancer

NASP has been suggested to be a prognostic marker for renal, liver, melanoma, lung, ovarian, and prostate cancer (Alekseev et al. 2011; Ali-Fehmi et al. 2009; Kang et al. 2018; Maślikowski et al. 2010, The Human Protein Atlas). NASP is highly expressed in all these different cancer cell lines and tissues and thus is nonspecific. Though it has been shown that inhibiting tNASP in prostate cancer cells (PC-3) will inhibit cell proliferation, no specific mechanism has been identified for its role in cancer (Alekseev et al. 2011).

Perhaps, elevated levels of NASP are required to chaperone histones since cancer cells divide in a pluripotent manner as do embryonic cells.

tNASP role in neuronal related diseases

tNASP which includes a larger acidic region than sNASP, has been implicated in neuronal disorders such as autism. tNASP mutations have been observed in three patients diagnosed with autism spectrum disorder. Upon further research in HEK293 cells, the

absence of tNASP alters chromatin accessibility and transcription in neural and immune signaling pathways leading to their dysregulation (Zhang et al. 2024).

Thesis Summary

Histones are essential for the structure and function of chromatin, serving as the basic units of chromatin packaging, thus exerting major influence over DNA organization and gene expression regulation. Additionally, histones contribute to the maintenance of genomic stability and DNA repair. Given the significant role of histones in all chromatin-related biology, it is crucial that histone levels are tightly regulated. Imbalances in histone levels can lead to defects in chromatin packaging, gene expression, and susceptibility to DNA damage.

In somatic cells, histones are stringently regulated. Canonical histones are predominantly synthesized in S-phase to ensure proper packaging of the newly replicated DNA (Duronio and Marzluff 2017). Additionally, 99% of histones are bound by chromatin and the 1% of soluble histones are always bound by histone chaperones (Loyola et al. 2006). This prevents toxicity of overexpressed histones. Interestingly, in the rapidly dividing embryo, there is an abundance of maternally deposited histone proteins (Woodland and Adamson 1977). Presumably the large pools of histones are required to supplement rapid DNA replication. However, the H3-H4 chaperone that maintains these large pools of H3-H4 in the early embryo is unknown. In somatic cells, H3-H4 chaperone NASP functions to store <1% of soluble histone pools (Cook et al. 2011).

Does NASP modulate large reservoirs of H3-H4 in the early embryo?

While there is sufficient evidence to support NASP's role in storing the 1% of soluble H3-H4 levels in somatic cells, the question remains whether it can modulate histone pools (>99%) present in the early embryo. Given that NASP is embryonic lethal and is highly expressed in human and mouse embryonic stem cells, there is suitable rationale that it may function as a H3-H4 chaperone in the early embryo as well (Nagatomo et al. 2016; Richardson et al. 2006; Sun et al. 2008; Torner et al. 2008; Yocum et al. 2008).

In this thesis, I establish that the Drosophila NASP homolog maintains the large pools of H3-H4 in the early embryo. Briefly, I observed that *NASP* null mutant is viable but is a maternal effect gene. Embryos laid by *NASP* mutant mothers have a reduced rate of hatching and show defects in early embryogenesis. Critically, soluble H3-H4 pools are depleted in embryos laid by NASP mutant mothers. This body of work provides evidence for NASP function as a storage for H3-H4 in the early embryo.

*CHAPTER II

II. MATERIALS AND METHODS

Strain list

Wild type–Oregon R (OrR)

NASP null mutant (*NASP*^{2})- *w[1118]; Df(3R)Exel6150, P{w[+mC] = XP-U} Exel6150/TM6B, Tb [1]/NASP*^{2} *or w [1118]; Df(3R) BSC478/TM6C, Sb [1] c u[1]/NASP*^{2}

NASP control mutant (*NASP*^{1})- *w [1118]; Df(3R) Exel6150, P{w[+mC] = XP-U} Exel6150/TM6B, Tb [1]/NASP*^{1} *or w [1118]; Df(3R) BSC478/TM6C, Sb [1] cu [1]/NASP*^{1}

NASP-GFP: +/+; *NASP-GFP/NASP-GFP*

NASP H3 binding control mutant (*NASP*^{CDS}): +/+; NASP*, NASP*^{CDS}*-GFP/ NASP, NASP*^{CDS}*-GFP*

NASP H3 binding mutant (*NASP*^{EWD3A}): +/+; *NASP*, *NASP*^{EWD3}*-GFP/ NASP, NASP*^{CDS}*-GFP*

CRISPR mutagenesis and transgenes

To generate a null allele of NASP, a single gRNA targeting exon 2 of the CG8223 was cloned into pU6-BbsI plasmid as described (Gratz et al. 2015). The guide RNA (gRNA) was identified using the Drosophila RNAi Screening Center (DRSC) Find CRISPRs tool (http://www.flyrnai.org/crispr2/index.html). The gRNA-expressing plasmid was injected

*This section was adapted from Tirgar et. al. 2023

into a nos-Cas9 expression stock (Best Gene Inc.). Surviving adults were individually crossed to TM3/TM6 balancer stock and progeny were screened by Sanger sequencing. The *NASP*^{1} allele contains a 6bp insertion resulting in a two amino acid insertion at amino acid 203. *NASP*^{2} allele contains a 4bp deletion that results in a frameshift starting at amino acid 203 and a premature truncation of NASP.

To generate NASP tagged with Super Folding Green Fluorescent Protein (sfGFP), a single gRNA targeting upstream of NASP C-terminus was cloned into pU6-BbsI plasmid. The gRNA-expressing plasmid was injected into a nos-Cas9 expression stock along with a donor plasmid that contained 2kb homology arms with NASP C-terminus bearing sfGFP (Best Gene Inc.). Donor plasmid was cloned via the PIG method (Han, Churcher, and Nordman 2023). Surviving adults were crossed to TM3/TM6 balancer stock and progeny were scored based on mini white phenotype. Homozygous fly stocks were confirmed via Polymerase Chain Reaction (PCR) with the following primers (P1: gccctctaagaaggtaccgaccggcgtg, P2: ggcggcggcagtcgagagtctaagg) and western blotting for NASP tagged GFP.

For NASP H3 binding mutants, previous reports have pinpointed the amino acids in *H. sapiens* NASP required for H3 binding (E177, W180, D181) (Bao et al. 2022). These same amino acids are conserved in *D. melanogaster* (E259, W262, D263) thus they were targeted for substitution to Alanine. NASP CDS-NASP H3 binding mutants were constructed by synthesizing NASP CDS and NASP EWD3A tagged with sfGFP (Twist biosciences). They were then cloned into pnos-PE2-attB so that they can be expressed during oogenesis and early embryogenesis (Bosch, Birchak, and Perrimon 2021). NASP-

CDS-GFP and NASP-EWD3A-GFP transgenic flies were generated by phiC31 integration of attB-containing plasmids into attP2 by injection in *y*^{1} *w*^{67c23}*; P{CaryP}attP2* (BSDC # 8622) Progeny were scored based on vermillion ocelli then crossed with TM3/TM6 balancer stocks (Best Gene Inc.). Balanced fly stocks were then verified via PCR-sequencing with the following primers (P1: gcgcgtagctttaccacaaa, P2: taaaatcgaacgcgccaggc) and western blotting for NASP-GFP.

Antibodies and antibody production

The NASP Open Reading Frame (ORF) was cloned into the 6His-MBP-containing expression vector pLM302 (Vanderbilt Center for Structural Biology). 6His-MBP- tagged NASP was expressed in *E. coli* Rossetta DE3 cells (Millipore Sigma, Cat# 71400–3) and purified using MBP Agarose beads (Qiagen). The purified protein was used for injection (Cocalico Biologicals Inc.). NASP antiserum was produced in rabbits. Rabbit anti-NASP antibody was used for western blot (1:2000) and immunoprecipitation.

Protein alignment and structural prediction

Protein sequence alignments were performed with MAFFT (default settings) and visualized on Jalview. Sequence identities and similarities were generated on SIAS (http://imed.med.ucm.es/Tools/sias.html) with default settings.

The structure of human NASP was previously solved by X-ray crystallography (Bao et al. 2022). The structure of Drosophila NASP was predicted using the AlphaFold Protein

Structure Database (Q9I7K6). The α-89 was manually removed from the PDB files using PDBTOOLS (Honorato et al. 2021; Jiménez-García et al. 2021; Rodrigues et al. 2018). Superimposition and RSD values of Human NASP core crystal structure (aa 38–140 210–280) and Drosophila NASP predicted structure (aa 1–388) were generated with USCF Chimera. Superimposition was performed on Matchmaker with default settings.

Viability, sterility, and fecundity assays

For viability assays, *NASP*^{1} or *NASP*^{2} virgin females were crossed with male *Df(3R)* flies. The genotype of adult progeny was identified using visible markers. The percentage of viability was calculated as (#observed/# expected) *100. For sterility assays, *NASP*^{1}*/ Df(3R) or NASP*^{2}*/Df(3R)* females or males were incubated with *OrR* males or *OrR* virgin females, respectively. After three days, adult flies were removed, and the number of pupae was scored on day ten. As a control, *OrR* females were crossed to *OrR* males. For Fecundity assays, seventy *NASP*^{2}*/Df(3R) or OrR* female flies were incubated with *OrR* male flies in a bottle capped by a grape juice agar plate with wet yeast for embryo collection. Collection plates were changed twice in one-hour increments prior to collections. 0–2-hour (AEL) embryos were collected and scored.

Embryo hatching assay

Embryos laid by *NASP^{1}/ Df(3R) or NASP^{2}/Df(3R)* mothers were collected on grape juice agar plates with wet yeast. One hundred 0–24-hour after egg laying (AEL) unhatched embryos were transferred to a fresh grape juice plate and incubated at 25°C overnight. Unhatched embryos were scored after 24 hours of incubation. Four hundred embryos were scored for each genotype.

Copy number profiling

Ovaries were dissected from *NASP^{1}/ Df(3R)*, *NASP^{2}/Df(3R)* or *OrR* females fattened for two days on wet yeast in Ephrussi Beadle Ringers (EBR). Stage 12 egg chambers were isolated, re-suspended in Lysis Buffer 3 (LB3) (MacAlpine et al. 2010) and sonicated using a Bioruptor 300 (Diagenode) for five cycles of 30s on and 30s off at maximal power. Lysates were treated with RNase and Proteinase K and genomic DNA was isolated via phenol-chloroform extraction. Quantitative PCR (qPCR) was performed using primers previously described (Claycomb et al. 2002).

Cytology and microscopy

NASP^{2}/Df(3R) or OrR female flies were incubated with *OrR* male flies in a bottle capped by a grape juice agar plate with wet yeast for embryo collection. Collection plates were changed twice in one-hour increments prior to collections. For staging experiments, 0–4 hour (AEL) embryos were collected. For aging experiments, 0–2-hour (AEL) embryos

were collected then aged for two hours. Both samples were dechorionated with 50% bleach for two minutes. Embryos were thoroughly washed with water then dried for 30s. Embryos were transferred to a scintillation vial containing 1mL of heptane. An equal volume of methanol was added, and the vial was vigorously shaken by hand for two minutes. Embryos were allowed to settle; the heptane layer was removed, and embryos were quickly rinsed with methanol thrice. Embryos were kept in methanol at 4°C until staining. Once ready for staining, embryos were gradually rehydrated in increasing concentration of Phosphate Buffered Saline (PBS) (18.6mM NaH_2PO_4, 84.1mM Na_2HPO_4, 1.75M NaCl, pH 7.4). Embryos were then rinsed in Phosphate Buffered Saline with Triton X (PBX) (18.6mM NaH_2PO_4, 84.1mM Na_2HPO_4, 1.75M NaCl, 0.1% Triton X-100, pH 7.4) for five minutes on a nutator. Then, embryos were treated with 0.8mg/mL Ribonuclease A (RNase A) (Macherey-Nagel, 740505) for one hour at 37°C. After incubation, embryos were washed with PBX for 30 minutes then stained with Propidium Iodide (0.1µg/mL) in PBS for 15 minutes at room temperature. After staining, embryos were washed with PBX for one hour and mounted with VECTASHIELD mounting medium (Vector Laboratories, H-1200). Images were taken at 40X on a Nikon Ti-E inverted microscope with a Zyla sCMOS digital camera. Embryos were manually staged (Kotadia et al. 2010) (Figure 3-11) and scored for chromatin bridging. Representative images were rendered with maximum projection intensity.

S2 cells were obtained from the Drosophila Genomics Resource Center (DGRC) and were confirmed negative for mycoplasma contamination via MycoStrip (Invivogen, rep-mys-10). Cells were grown in Schneider's Drosophila Medium (Thermo Fisher Scientific, 21720001) supplemented with 10% heat-inactivated Fetal Bovine Serum (FBS) (Gemini

Bio Products, 900–108) and 100 U/mL of Penicillin/Streptomycin (Thermo Fisher Scientific, 15070063) at 25°C.

For NASP localization in cultured cells, cells were washed with PBS then attached to Concanvan A-coated slides for two hours. Once attached, cells were fixed for 15 minutes in 4% paraformaldehyde and permeabilized with PBX for 15 minutes. Cells were blocked with blocking buffer (PBX supplemented with 1% Bovine Serum Albumin (BSA) and 2% goat serum) for one hour then incubated with the NASP primary antibody at a 1:1000 dilution overnight at 4°C. After overnight incubation, cells were washed with PBX thrice five minutes each followed with an extensive two-hour incubation with the secondary antibody (Life technologies, A11011) at a 1:500 dilution. Cells were then washed with PBX thrice for five minutes. Cells were stained with 4',6-diamidino-2-phenylindole (DAPI) (1µg/mL) in PBS for 15 minutes at room temperature then washed with PBS for 10 minutes before being mounted with VECTASHIELD mounting medium (Vector Laboratories, H-1200). Images were taken at 40X on a Nikon Ti-E inverted microscope with a Zyla sCMOS digital camera. Profile intensities were generated on the NIS Elements AR 3.2 software.

For NASP localization in Drosophila embryos, 0–2-hour (AEL) NASP-GFP embryos were collected on a grape juice agar plate. Embryos were dechorionated with 50% bleach, washed with deionized water, then mounted on a glass-bottom microwell dish. Fluorescent images were acquired via LSM880 with a 20x/0.80 Plan-Apochromat, WD=0.55mm.

For S phase analysis, S2 cells were pulsed with 20 µM of 5-chloro-2′-deoxyuridine (CldU) nucleoside (Sigma-Aldrich, C6891) for 20 minutes. Cells were washed with PBS then

attached to Concanvan A-coated slides for two hours. Once attached, cells were fixed for 15 minutes in 4% paraformaldehyde and permeabilized with PBX for 15 minutes. Cells were acid treated with 2N Hydrochloric Acid (HCl) for 30 minutes then neutralized for two minutes in 0.1M Sodium Borate. Cells were washed with PBX three times for 10 minutes each then blocked with blocking buffer (PBX supplemented with 5% goat serum (Sigma-Aldrich, G9023-10ML)) for 30 minutes at room temperature. After blocking, cells were incubated with the primary antibodies (NASP 1:1000, CldU 1:25 Abcam ab6326) in blocking buffer overnight at 4°C. After overnight incubation, cells were washed with PBX three times for five minutes each. They were once again blocked for 30 minutes at room temperature then probed with secondary antibodies for two hours at room temperature. For NASP, secondary antibodies Alexa flour 488 Goat anti-Rabbit (Life technologies, A11034) was used at 1:500. For CldU, Goat anti-Rat 594 (Abcam, ab15160) was used at 1:350. Cells were rinsed three times with PBX then washed four times for five minutes each. Cells were stained with DAPI (1µg/mL) in PBS for 15 minutes at room temperature then washed with PBS for 10 minutes before being mounted with VECTASHIELD mounting medium (Vector Laboratories, H-1200). Images were taken at 40X on a Nikon Ti-E inverted microscope with a Zyla sCMOS digital camera. Profile intensities were generated on the NIS Elements AR 3.2 software.

For live imaging of embryos, flies were incubated in a bottle capped by a grape juice agar plate with wet yeast for embryo collection. 0-1hour (AEL) embryos were dechorionated with 50% bleach, washed with deionized water, then mounted on a glass-bottom microwell dish. Fluorescent images were acquired by a Andor DU-897 EMCCD on a Nikon Spinning Disk Confocal with a Plan Fluor (oil) 40x 1.30 NA WD 0.20mm. Images

were taken at room temperature at time resolution of 30 second intervals. For import rate analysis, nuclear regions were first segmented by ilastik in which nuclear intensities were quantified from nuclear envelope formation to nuclear envelop breakdown. The slope of a linear regression of the first five points of nuclear intensity was generated which indicated the import rate of NASP-GFP or H3-Dendra2.

For single molecule FISH in Drosophila embryos, female flies were incubated with OrR male flies in a bottle capped by a grape juice agar plate with wet yeast for embryo collection. 0-6 hour (AEL) embryos were collected then fixed and stained with Kruppel and cyclin smFISH as previously described (Trcek et al.,2017). Images were taken at 40X on an LSM880 confocal microscopy. Analysis was performed on ZEN by quantifying the average intensity of three background regions of interest and subtracting from the average intensity three regions of interest of Kruppel staining.

Tissue collection and western blotting

NASP^{1}/ Df(3R), NASP^{2}/Df(3R), or *OrR* female flies were fattened on wet yeast for 3–4 days, ovaries were dissected in EBR, and stage 14 egg chambers were isolated. For embryo isolation, 0–2-hour (AEL) embryos were collected from *NASP^{1}/ Df(3R), NASP^{2}/Df(3R),* or *OrR* mothers as described above. For total protein preparation, embryos and egg chambers were homogenized with a pestle in 2x Lammeli buffer (Bio-Rad, 1610737) supplemented with 50mM Dithiothreitol (DTT), boiled for five minutes and loaded onto a Mini-PROTEAN TGX Stain-Free Gel (Bio-Rad). For soluble protein preparations, embryos and egg chambers were flash frozen, and stored at –80°C until

use. Samples were thawed on ice and 50 µL of NP40 lysis buffer was added. Samples were then homogenized five times with a B-type pestle, transferred into a 1.5mL Eppendorf tube and centrifuged for 30s at 10,000RCF at 4°C. 50 µL of supernatant was transferred to a new 1.5mL Eppendorf tube for protein precipitation. Samples were precipitated using methanol:chloroform:water (3:1:3) and washed three times with methanol. Each wash was followed by a five-minute spin at 10,000xg at room temperature. Protein pellets were air dried and resuspended in 10µL of 1% Rapigest SF then denatured with an equal volume of Lammeli buffer supplemented with 50mM DTT. Samples were boiled for five minutes and loaded onto a Mini-PROTEAN TGX Stain-Free Gel.

For staged single embryo western blots, 0–4-hour (AEL) embryos were collected from *NASP*^{2}*/Df(3R),* or *OrR* mothers as described above. Embryos were fixed as described under 'Cytology and Microscopy', stained with DAPI, then placed in glass-bottom microwell dish with a drop of water. Embryos were staged based on their nuclear cycle stage under a Nikon Ti-E inverted microscope at 20X. They were then placed in 1x PBX until collections were complete. PBX was then aspirated, and embryos were homogenized with a pestle in 2x Laemmli sample buffer supplemented with 50mM DTT. Samples were boiled for five minutes then loaded onto a Mini-PROTEAN TGX Stain-Free Gel.

For the fractionation assay, egg chambers were flash frozen, and stored at –80°C until use. Samples were thawed on ice and 50 µL of NP40 lysis buffer was added. Samples were then homogenized five times with a B-type pestle, transferred into a 1.5mL Eppendorf tube. Input was aliquoted then samples were centrifuged for 30s at 10,000RCF

at 4°C. Supernatant was aliquoted into a new 1.5mL Eppendorf tube then the pellet was re-suspended with equal volume NP40 as supernatant. An equal volume of 2x Lammeli buffer (Bio-Rad, 1610737) supplemented with 50mM DTT was added to the input, pellet, and supernatant samples. Samples were boiled for five minutes and loaded onto a Mini-PROTEAN TGX Stain-Free Gel (Bio-Rad). After electrophoresis, the gel was activated and imaged using a BioRad ChemiDoc MP Imaging System following manufacturer recommendations. Protein was transferred to a low fluorescence Polyvinylidene fluoride (PVDF) membrane using a Trans-Blot Turbo Transfer System (Bio-Rad). Membranes were blocked with 5% milk in TBS-T (140mM NaCl, 2.5mM KCl, 50 mM Tris HCl pH 7.4, 0.1% Tween-20) for 10 minutes. Blots were incubated with the primary antibody (anti-NASP-1:2000, anti-H3-1:000, anti-H2B-1:1000) for one hour at room temperature. Blots were washed three times with TBS-T then incubated with the secondary antibody (HRP anti-mouse-1:20,000, HRP anti-Rabbit-1:25,000) for 30 minutes at room temperature. After hybridization, blots were washed three times with TBS-T then incubated with Clarity Enhanced chemiluminescence (ECL) solution (Bio-Rad) before imaging. All blots were imaged on the BioRad ChemiDoc MP Imaging System.

Immunoprecipitation and western blotting

Embryos from *OrR* flies were collected from a population cage. Plates were cleared for one hour, then 0–2-hour embryos (AEL) (pre-MBT) were collected, dechorionated in 50% bleach and flash frozen in nitrogen. Embryo staging was confirmed by DAPI staining. For H3 binding mutants, 0–24-hour embryos (AEL) were collected. Embryos were disrupted

by grinding them with a mortar and pestle in liquid nitrogen. The powdered embryos were thawed and resuspended on ice in NP40 lysis buffer (50mM Tris-Cl pH 7.4, 150mM NaCl, 1% NP40, 1mM EDTA, 1mM EGTA) supplemented with 2X cOmplete Protease Inhibitor Cocktail EDTA-free (Millipore Sigma). Once thawed, the extract was treated with benzonase at a final concentration of 30 U/ml (EMD Millipore, 70664-10KUN) for 30 minutes on ice. After benzonase treatment, the extract was centrifuged at 4000xg for five minutes. Supernatant was used as the starting material for immunoprecipitation. Rabbit IgG (negative control) or NASP serum were added to lysates and incubated at 4°C for two hours. For H3 binding mutants, GFP nanobody (ChromoTek, gtd-20) was used. After antibody incubation, prewashed Protein A Dynabeads (Thermo Fisher Scientific, 10001D) were added to the extract and incubated for one hour at 4°C on a nutator. After incubation, beads were isolated and washed once with NP40 lysis buffer, twice with NP40 lysis high salt wash buffer (50mM Tris-Cl pH 7.4, 500mM NaCl, 1% NP40, 1mM EDTA, 1mM EGTA), and once again with NP40 lysis buffer. Beads were then resuspended in 2x Laemmli sample buffer (Bio-Rad, 1610737) supplemented with 50mM DTT and boiled for five minutes to elute protein. For GFP nanobody IP, after 2 hours of incubation, beads were washed as described then re-suspended with 2x Laemmli sample buffer (Bio-Rad, 1610737) supplemented with 50mM DTT and boiled for five minutes to elute protein. Western blot analysis was performed as described previously (Tissue collection and western blotting).

Mass spectrometry sample preparation

For NASP-immunoprecipitation (IP), samples were prepared as described previously (Immunoprecipitation and Western blotting). For soluble protein levels in stage 14 egg chambers and embryos, 20 embryos or stage 14 egg chambers were collected for each replicate, flash frozen, and stored at –80°C until use. Once all samples for four biological replicates were collected, samples were thawed on ice and a 100 µL of NP40 lysis buffer was added. Samples were then homogenized ten times with a B-type pestle, transferred into a 1.5mL Eppendorf tube and centrifuged for 30s at 10,000RCF at 4°C. 100 µL of supernatant was transferred to a new 1.5mL Eppendorf tube for protein precipitation.

Both lysate and IP samples were precipitated using mass spectrometry grade methanol:chloroform:water (3:1:3) and washed three times with methanol. Each wash was followed by a five-minute spin at 10,000xg at room temperature. Protein pellets were air dried and resuspended in 5µL of 1% Rapigest SF. Resuspended proteins were diluted with 32.5 µL mass spectrometry grade water and 10 µL 0.5 M HEPES (pH 8.0), then reduced with 0.5 µL of 0.5 M Tris (2-carboxyethyl) phosphine (TCEP) (freshly made) for 30 minutes at room temperature. Free sulfhydryl groups were acetylated with 1 µL of fresh 0.5 M Iodoacetamide for 30 minutes at room temperature in the dark and digested with 0.5 µg trypsin/Lys-C (Thermo Fisher) overnight at 37°C shaking. Digested peptides were diluted to 60 µL with water and labeled for 1 hour at room temperature using 16plex TMTpro (Thermo Scientific) or 10plex TMT (Thermo Scientific) for lysate and IP samples, respectively. Labeling was quenched with the addition of fresh ammonium bicarbonate (0.4% v/v final) for one hour at room temperature. Samples were pooled, acidified to pH < 2.0 using formic acid, concentrated to 1/6th original volume via Speed-vac, and diluted back to the original volume with buffer A (95% water, 5% acetonitrile, 0.1% formic acid).

Cleaved Rapigest products were removed by centrifugation at 17,000xg for 30 minutes and supernatant transferred to fresh tubes for storage at -80°C until mass spectrometry analysis.

MudPIT liquid chromatography-tandem mass spectrometry

Triphasic MudPIT columns were prepared as previously described using alternating layers of 1.5cm C18 resin, 1.5cm SCX resin, and 1.5cm C18 resin (Fonslow et al. 2012). Pooled TMT samples (roughly one-third of pooled IP samples and roughly 20 µg of peptide from lysate samples) were loaded onto the microcapillaries using a high-pressure chamber, followed by a 30-minute wash in buffer A (95% water, 5% acetonitrile, 0.1% formic acid). Peptides were fractionated online by liquid chromatography using an Ultimate 3000 nanoLC system and subsequently analyzed using an Exploris480 mass spectrometer (Thermo Fisher). The MudPIT columns were installed on the LC column switching valve and followed by a 20cm fused silica microcapillary column filled with Aqua C18, 3µm, C18 resin (Phenomenex) ending in a laser-pulled tip. Prior to use, columns were washed in the same way as the MudPIT capillaries. MudPIT runs were carried out by 10µL sequential injections of 0, 10, 20, 40, 60, 80, 100% buffer C (500mM ammonium acetate, 94.9% water, 5% acetonitrile, 0.1% formic acid) for IP samples and 0, 10, 20, 30, 40, 50, 60, 70, 80, 90, 100% buffer C for global lysate samples, followed by a final injection of 90% C, 10% buffer B (99.9% acetonitrile, 0.1% formic acid v/v). Each injection was followed by a 130 min gradient using a flow rate of 500nL/min (0–6 min: 2% buffer B, 8 min: 5% B, 100 min: 35% B, 105min: 65% B, 106–113 min: 85% B, 113–130 min: 2% B).

ESI was performed directly from the tip of the microcapillary column using a spray voltage of 2.2 kV, an ion transfer tube temperature of 275°C and an RF Lens of 40%. MS1 spectra were collected using a scan range of 400–1600 m/z, 120k resolution, AGC target of 300%, and automatic injection times. Data-dependent MS2 spectra were obtained using a monoisotopic peak selection mode: peptide, including charge state 2–7, TopSpeed method (3s cycle time), isolation window 0.4 m/z, HCD fragmentation using a normalized collision energy of 36% (TMTpro) or 32% (TMT 10plex), resolution 45k, AGC target of 200%, automatic (lysate) or 150 ms (IP) maximum injection times, and a dynamic exclusion (20 ppm window) set to 60s.

Peptide identification and quantification

Identification and quantification of peptides were performed in Proteome Discoverer 2.4 (Thermo Fisher) using a UniProt *Drosophila melanogaster* proteome database (downloaded February 6th, 2019) containing 21,114 protein entries. The database was adjusted to remove splice-isoforms and redundant proteins and supplemented with common MS contaminants. Searches were conducted with Sequest HT using the following parameters: trypsin cleavage (maximum 2 missed cleavages), minimum peptide length 6 AAs, precursor mass tolerance 20ppm, fragment mass tolerance 0.02 Da, dynamic modifications of Met oxidation (+15.995 Da), protein N-terminal Met loss (-131.040 Da), and protein N-terminal acetylation (+42.011 Da), static modifications of TMTpro (+304.207 Da) or TMT 10plex (+229.163 Da) at Lys and N-termini and Cys carbamidomethylation (+57.021 Da). Peptide IDs were filtered using Percolator with an

FDR target of 0.01. Proteins were filtered based on a 0.01 False Discovery Rate (FDR), and protein groups were created according to a strict parsimony principle. TMT reporter ions were quantified considering unique and razor peptides, excluding peptides with co-isolation interference greater than 25%. Peptide abundances were normalized based on total peptide amounts in each channel, assuming similar levels of background in the IPs. Protein quantification used all quantified peptides. Post-search filtering was done to include only proteins with two identified peptides. Unique peptides for each canonical and variant histone were manually identified, summed, and statistically analyzed on Graphpad Prism. For IP samples, multiple t-test was performed ($p<0.05$). For lysate samples, multiple t-test with Holm-Sidak correction was performed ($p<0.05$).

*CHAPTER III

III. THE HISTONE CHAPERONE NASP MAINTAINS H3-H4 RESERVOIRS IN THE EARLY DROSOPHILA EMBRYO

Introduction

Histones are small, highly conserved, and positively charged proteins essential for packaging the eukaryotic genome. The core of chromatin is 147bp of DNA wrapped around an octamer of histones H2A, H2B, H3, and H4 (Arents and Moudrianakis 1993; Kornberg 1974; Luger et al. 1997; Noll and Kornberg 1977). Histone occupancy affects nearly every aspect of chromatin metabolism including transcription, DNA replication, DNA repair and DNA packaging (Bannister and Kouzarides 2011; Khorasanizadeh 2004; Kornberg and Lorch 2020; Talbert and Henikoff 2017). Thus, it is crucial that histone expression levels are delicately balanced as histone reduction or overexpression is detrimental to the cell (Celona et al. 2011; Gunjan and Verreault 2003; Herrero and Moreno 2011; Meeks-Wagner and Hartwell 1966; Singh et al. 2010). Exemplifying the importance of histone balance, the production of histones is tightly coordinated with cell cycle progression; histone expression peaks at S phase when the demand for histones is highest (Bonner et al., 1988; Oliver et al., 1974; Osley, 1991; J. Zhao et al., 2000). Furthermore, the soluble pools of histones are less than 1% of the total histone levels in cells, and mechanisms exist to degrade and prevent the overabundance of soluble

*This section was adapted from Tirgar et. al. 2023

histones (Bonner et al. 1988; Gunjan, Paik, and Verreault 2006; Marzluff, Wagner, and Duronio 2008; Oliver et al. 1974).

Early embryogenesis of many organisms, including Drosophila, presents a challenge to the histone supply and demand paradigm. The early Drosophila embryo develops extremely rapidly in the first few hours of development (Vastenhouw, Cao, and Lipshitz 2019; Yuan et al. 2016). The first 14 nuclear divisions are fast, synchronous, and occur in the absence of zygotic transcription as they alternate between S phase and mitosis in a shared cytoplasm (Yuan et al. 2016). Therefore, early embryogenesis must be driven from maternally supplied stockpiles of RNA and protein, including histones (Ambrosio and Schedl 1985; Horard and Loppin 2015; Song et al. 2017; Walker and Bownes 1998). As blastoderm nuclei enter cycle 10, the cell cycle elongates until nuclear cycle 14, in which the embryo undergoes mid blastula transition (MBT). At this point, maternally deposited RNA is degraded, and zygotic transcription ensues (Yuan et al. 2016). Importantly, soluble histones decrease from 55% in nuclear cycle 11 to less than 1% post-MBT (Shindo and Amodeo 2019). Thus, there must be mechanisms present in the early embryo to suppress the toxicity associated with excess histones in somatic cells.

From their molecular birth to their eventual deposition into chromatin, histones are continuously bound by a network of proteins known as histone chaperones (Pardal, Fernandes-Duarte, and Bowman 2019). Histone chaperones are key for histone stability and affect all aspects of histone metabolism including histone folding, storage, transport, post translational modifications, and histone turnover (Hammond et al. 2017). Importantly, histone chaperones directly or indirectly affect chromatin structure and function by delivery and handoff of histones to other histone chaperones or chromatin-associated

factors within a given network (Gurard-Levin, Quivy, and Almouzni 2014). While a few chaperones can bind all histones, most histone chaperones bind specifically to H3-H4 or H2A-H2B (Elsässer et al. 2012; Hammond et al. 2017; Natsume et al. 2007; Ramos et al. 2010). In Drosophila embryos, the histone chaperone Jabba sequesters histones H2A-H2B to lipid droplets and protects H2A and H2B from degradation (Li et al., 2012). It is still unknown, however, what histone chaperone protects soluble H3 and H4 pools in the early embryo. While there are multiple H3-H4-specific histone chaperones, nuclear autoantigenic sperm protein (NASP) is an alluring candidate to chaperone H3-H4 in Drosophila embryos as NASP is known to maintain a soluble reservoir of histone H3-H4 in mammalian cells (Cook et al. 2011; Horard and Loppin 2015) Furthermore, the Xenopus NASP homolog N1/N2 associates with soluble pools of H3 and H4 in egg lysates (Kleinschmidts et al. 1985). Lastly, *NASP* is essential for embryonic development in mammals, and maternal knockdown of the putative Drosophila NASP homolog led to an arrest in early embryogenesis (Nagatomo et al., 2016; Richardson et al., 2006; Z. Zhang et al., 2018). Thus, we hypothesized that Drosophila NASP is a histone H3-H4 chaperone in the early embryo.

Here, based on sequence, structure, and function, we identified CG8223 as the Drosophila NASP homolog. We show that CG8223/NASP specifically binds to histones H3-H4 in vivo. We demonstrate that NASP is a maternal effect gene in Drosophila and that embryos laid by *NASP* mutant mothers have impaired development. Finally, we show that in the absence of NASP, soluble H3 and H4 levels decrease in both eggs and embryos. Overall, our findings demonstrate that NASP protects soluble pools of H3-H4 from degradation in Drosophila embryos.

Results

Drosophila melanogaster CG8223 is the histone H3-H4 chaperone NASP

In Drosophila, Jabba serves as the major H2A-H2B-specific chaperone, but the H3-H4-specific chaperone has yet to be identified (Li et al. 2012). NASP, Nuclear Autoantigenic Sperm Protein, is an H3-H4-specific chaperone known to buffer excess H3-H4 supply in mammalian cells and Xenopus (Cook et al., 2011; Kleinschmidts et al., 1985). Previous work has identified CG8223 as a possible NASP homolog based on the conserved Tetratricopeptide (TRP) motifs, which are found in NASP homologs (Nabeel-Shah et al., 2014). To verify that CG8223 is in fact NASP, we searched the Drosophila proteome for a homolog of human NASP and identified CG8223 as the one and only putative NASP homolog. Alignment of CG8223 with human NASP revealed a similar domain structure with 28% identity (Figure 3-1). Critically, the regions of CG8223 with the highest degree of conservation to human NASP are the regions known to bind to H3 directly (Figure 3-2A). Furthermore, a structural prediction of CG8223 (excluding the dimerization domain, α-89) is highly similar to a recent human crystal structure of sNASP, with a 1.074 angstrom RMSD value (Figure 3-2B) (Bao et al., 2022). In human cultured cells, NASP is localized to both the nucleus and the cytoplasm (Alekseev et al. 2003) or exclusively to the nucleus (Apta-Smith et al., 2018).

To understand CG8223 localization in Drosophila, we stained Drosophila S2 cells with a CG8223-specific antibody. We observed the majority of the signal resides around the periphery of the nucleus (Figure 3-3A). Given that NASP delivers H3 and H4 for

replication-dependent histone deposition, we asked if NASP localization is altered in cells in S phase. Consistent with work in human cells (Apta-Smith et al., 2018), NASP localization was not changed in cells in S phase (Figure 3-3B).

To test experimentally whether CG8223 is an H3-H4-specific binding protein in vivo, we immunoprecipitated (IP) CG8223 from embryo extracts (0-2h AEL) using a CG8223-specific antibody (Figure 3-4) Western blot analysis of the IP revealed that CG8223 and Histone H3.2 (hereby referred to as the replicative Drosophila histone H3) but not H2B, are in the same protein complex (Figure 3-2C). To extend this analysis beyond H3 and H2B, we used IP coupled to quantitative mass spectrometry to determine which canonical histones and histone variants complex with CG8223. To this end, precipitated material was labelled with tandem mass tag (TMT) and only peptides that were unique to each histone were quantified (Figure 3-2D). This analysis revealed that CG8223 is associated with H3, H4 and H3.3. We did not identify any H3-like centromeric protein Cid peptides in our IPs. Interestingly, we noticed a higher level of H3 and H3.3 in CG8223 IPs relative to H4, suggesting that CG8223 preferentially binds to H3. This is consistent with recent work showing that human NASP has a preference for monomeric H3 (Pardal and Bowman 2022). CG8223 does not, however, associate with H2A or H2B (Figure 3-2E). Lastly, we identified an association between NASP and the H2A variant, H2Av. Based on the conservation, structural similarity, and in vivo association with H3-H4, we conclude that CG8223 is the sole Drosophila NASP homolog, which we will now refer to as NASP.

NASP *is a maternal effect gene*

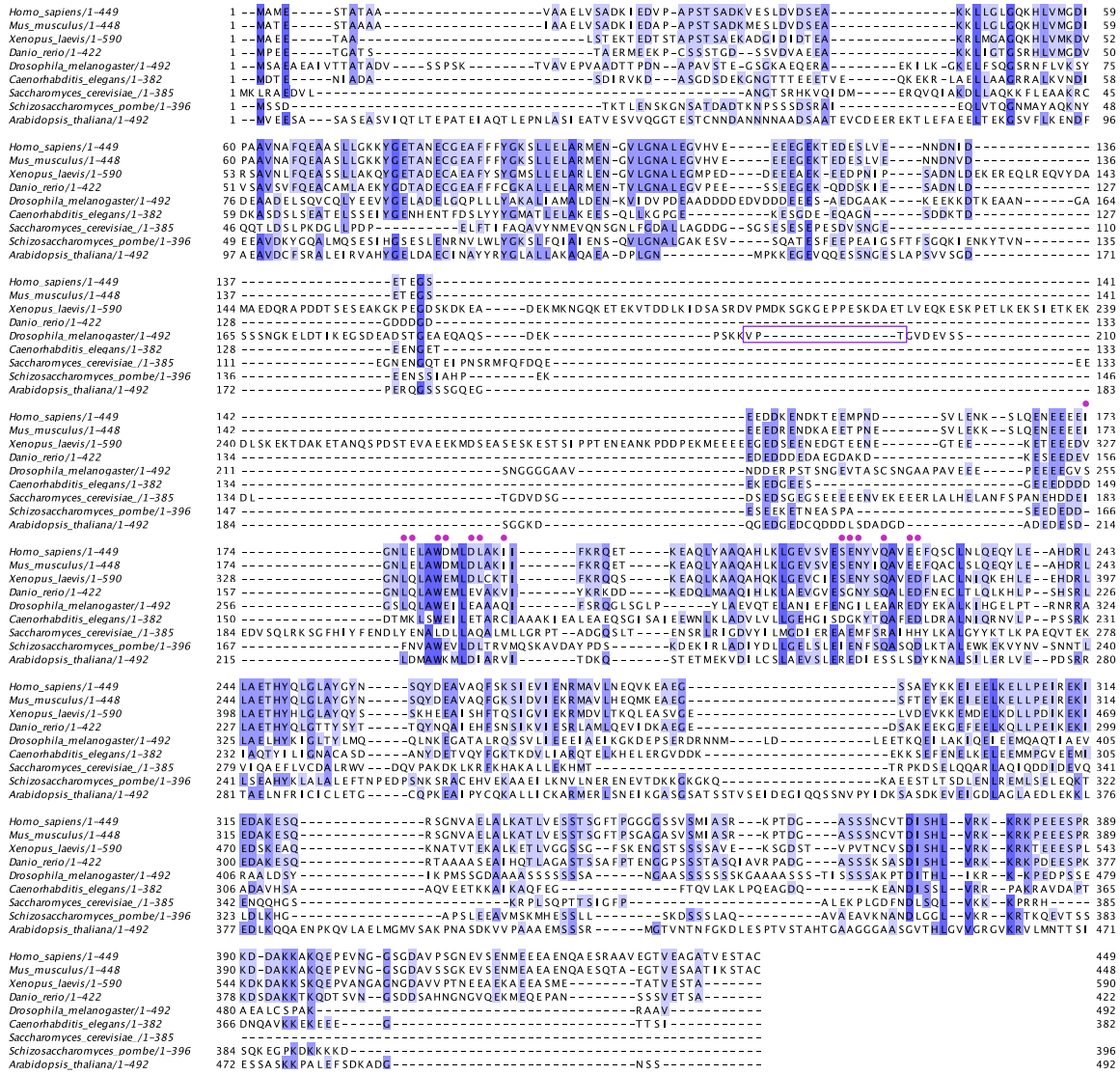

Figure 3-1.Sequence alignment of CG8223 with NASP homologs in other organisms.

Darkening of the color indicates greater conservation. Magenta dots represent the α-N Histone H3 binding region observed in *Homo sapiens* NASP. Boxed region represents the gRNA target sequence for CRISPR-based mutagenesis to generate NASP mutants

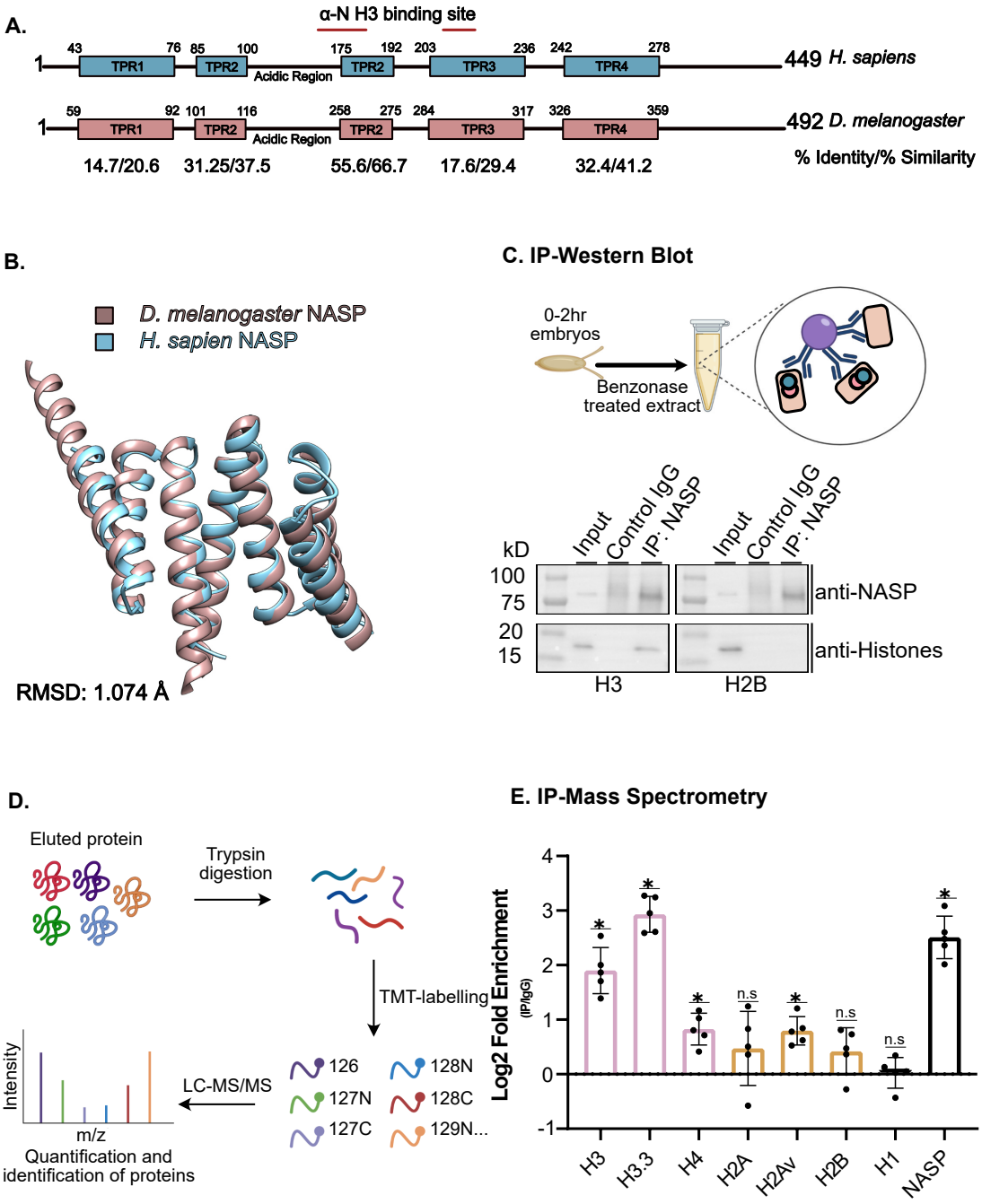

Figure 3-2.Drosophila melanogaster CG8223 is the Histone H3-H4 chaperone NASP.

(A) Schematic of *Homo sapiens* and *Drosophila melanogaster* NASP proteins with TPR domains. Below are the calculated % identity/%similarity for each TPR domain. Red lines indicate the location of residues responsible for binding H3. (B) Superimposition of *Homo sapiens* NASP (as determined by crystallography, aa 38–140 210–280) with *Drosophila melanogaster* NASP (predicted by AlphaFold, aa 1–388). (C) Immunoprecipitation of NASP from 0-2hr AEL embryos. Methodology created with Biorender. (D) Schematic of

IP quantitative mass spectrometry approach to quantify NASP-associated proteins created with Biorender. (E) Average Log2 fold change for five biological replicates of NASP IP-mass spectrometry relative to IgG control in 0-2hr AEL embryos. Multiple t-test was performed to determine significance ($p<0.05$).

Now that we have established NASP as a H3-H4-specific binding protein in Drosophila, we wanted to ask how *NASP* affects Drosophila development. We used Clustered Regylarly Interspaced Short Palindromic Repeats (CRISPR)-based mutagenesis to target exon 2 to generate *NASP* mutants. From this approach, we recovered two mutants; $NASP^{1}$ and $NASP^{2}$ (Figure 3-5A). The $NASP^{1}$ allele contains a 6bp insertion resulting in a two amino acid insertion at amino acid 203. Given this small insertion is in a non-conserved region of the protein, it is not predicted to affect NASP function (Figure 3-1A). In contrast, the $NASP^{2}$ allele contains a 4bp deletion that results in a frameshift starting at amino acid 203 and a truncation of NASP (Figure 3-5A). Western blot analysis of ovary extracts derived from wild type, $NASP^{1}$ or $NASP^{2}$ mutants revealed that there was no detectable $NASP^{2}$ protein, even with 4X the protein loaded. In contrast, however, the $NASP^{1}$ protein was stable (Figure 3-5B). To examine viability of the *NASP* mutants, we counted the number of *NASP* mutant progeny relative to the expected frequency (Figure 3-5C). To account for any CRISPR off target effects, we performed all crosses with two independent deficiency lines (see Chapter II) to generate compound heterozygous mutants. Crossing $NASP^{1}$ or $NASP^{2}$ mutants with either deficiency line revealed that both $NASP^{1}$ and $NASP^{2}$ mutants are viable (Figure 3-5C).

Although the $NASP^{2}$ mutant is viable, it had a lower fecundity (Figure 3-6), and we were unable to maintain a stock. Thus, we hypothesized that the $NASP^{2}$ mutant is either male or female sterile. To test this hypothesis, we measured the number of pupae formed 10 days after egg laying (AEL) from *NASP* mutant parents. $NASP^{2}$ mutant mothers

produced a significantly lower number of pupae compared to both wild type and the *NASP*^{1} mutant mothers (Figure 3-5D). There was no significant difference in the number of progeny produced when wild type females were crossed to male *NASP*^{2} mutants, indicating that loss of NASP function results in female sterility (Figure 3-5D). Results were consistent for both compound heterozygotes from two independent deficiency lines (Figure 3-5D).

Previous proteomic studies revealed NASP to be at replication forks in Drosophila cultured S2 cells, Drosophila embryos, and human cells (Munden et al., 2022; Wessel et al., 2019). Therefore, it is possible that NASP may function during chorion gene amplification in follicle cells, which is critical to produce eggshell protein in a short developmental window (Spradling and Mahowald 1980). To test this, we measured DNA copy number at the highest amplified region, *DAFC-66D*, in stage 12 egg chambers. The *NASP*^{2} mutant did not show a significant difference in amplification (Figure 3-7A). Therefore, we conclude that the female sterility associated with the *NASP*^{2} mutant is independent of gene amplification. Although *NASP*^{2} mutants were viable, embryos laid by *NASP*^{2} mutant mothers showed a significantly lower hatching percentage compared to *NASP*^{1} and wild type (Figure 3-5E).

To ask whether maternally supplied NASP is essential for embryogenesis, we ensured that all progeny have at least one copy of *NASP* by crossing *NASP*^{2} virgin females with wild type males. Interestingly, even when the progeny had a functional *NASP* allele, there was a significantly lower number of progeny compared to crosses with wild type females (Figure 3-8A). Furthermore, embryos laid by *NASP*^{2} mutant mothers crossed with wild

A.

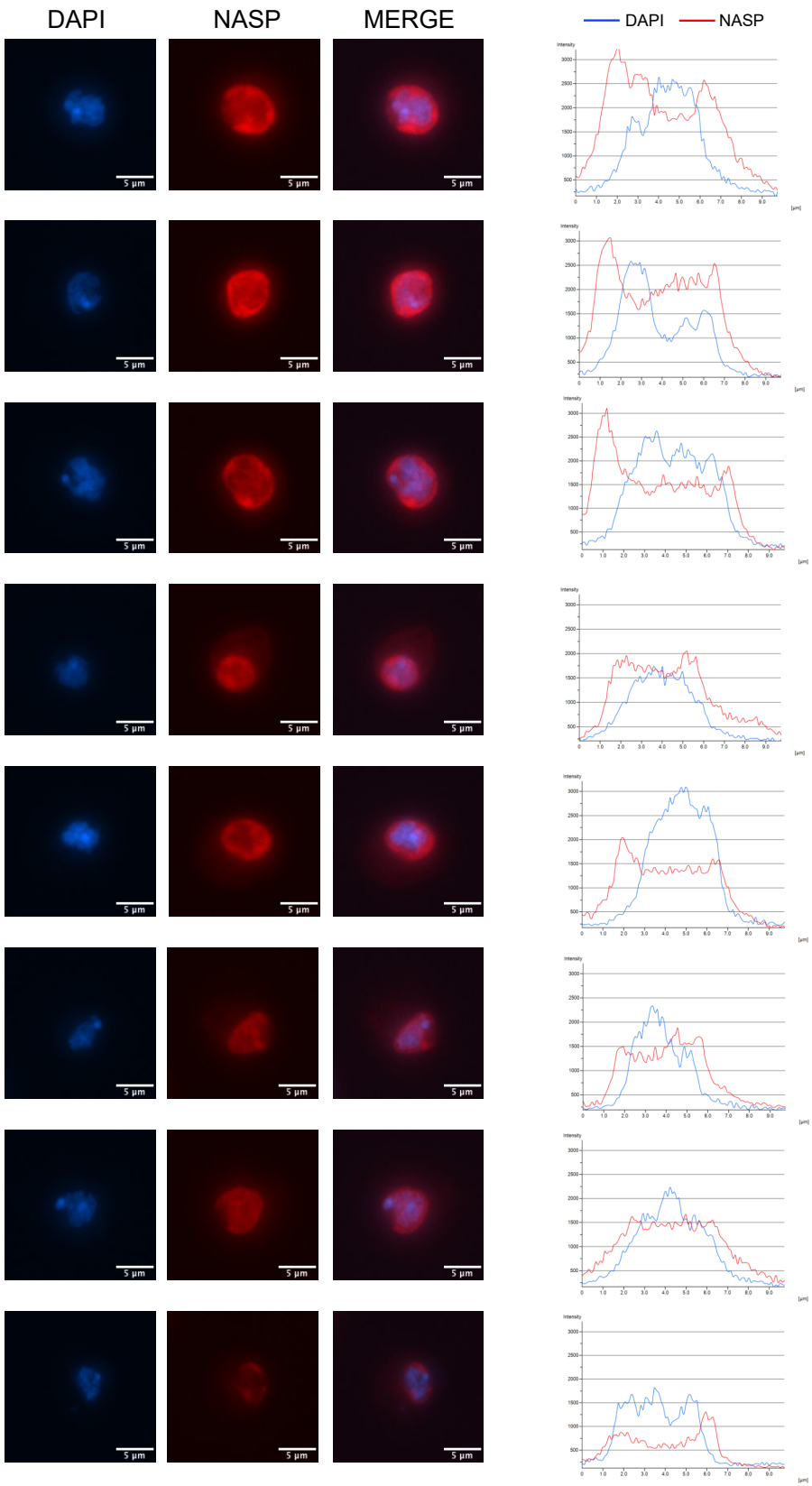

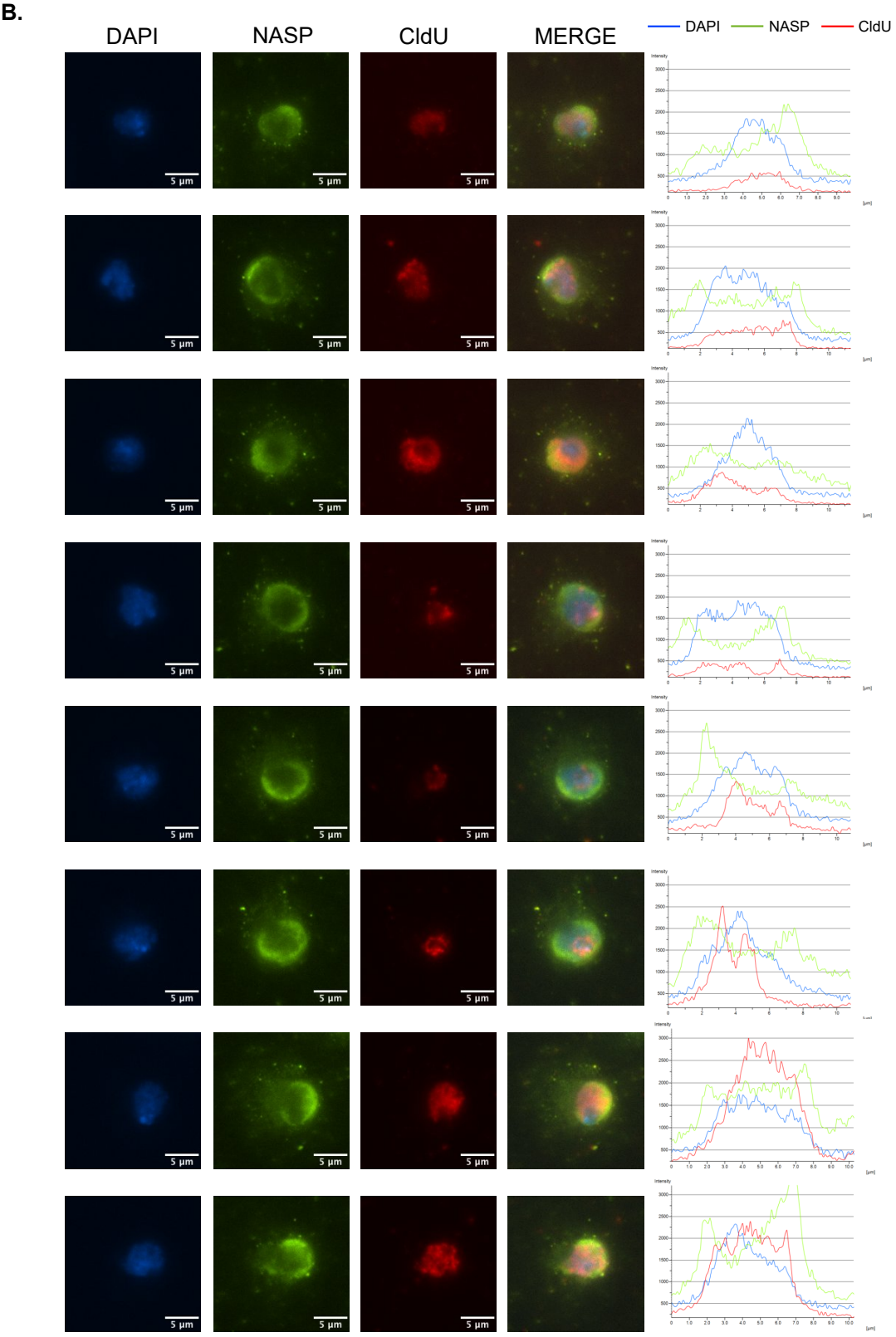

Figure 3-3.NASP localization in S2 Drosophila cultured cells.

(A)Localization of NASP (red) in Drosophila S2 cells. DNA is stained by DAPI (blue). Scale bar, 5 μm. Graph displays intensity profiles of NASP and DAPI through a perpendicular line. (B) Localization of NASP (green) in Drosophila S2 cells. DNA replication is marked by CldU pulsing (red), and DNA is stained by DAPI (blue). Scale bar, 5 μm. Graph displays intensity profiles of NASP, CldU, and DAPI through a perpendicular line.

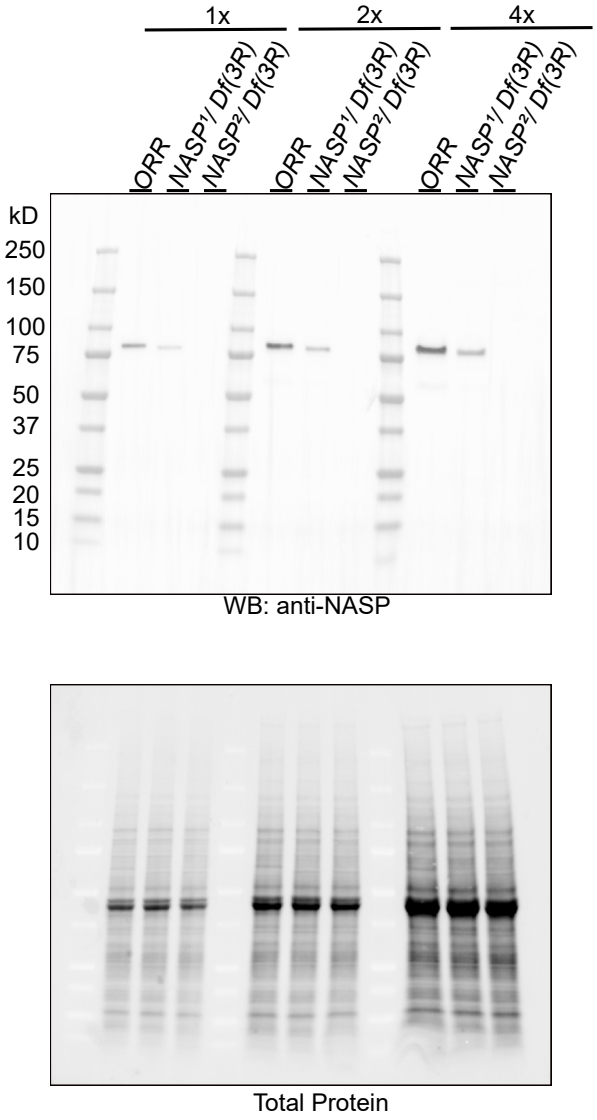

Figure 3-4.NASP antibody is specific.

Western blot analysis of ovary extracts from the indicated genotypes with total protein loading control. Blot is cropped for Figure 3-5B.

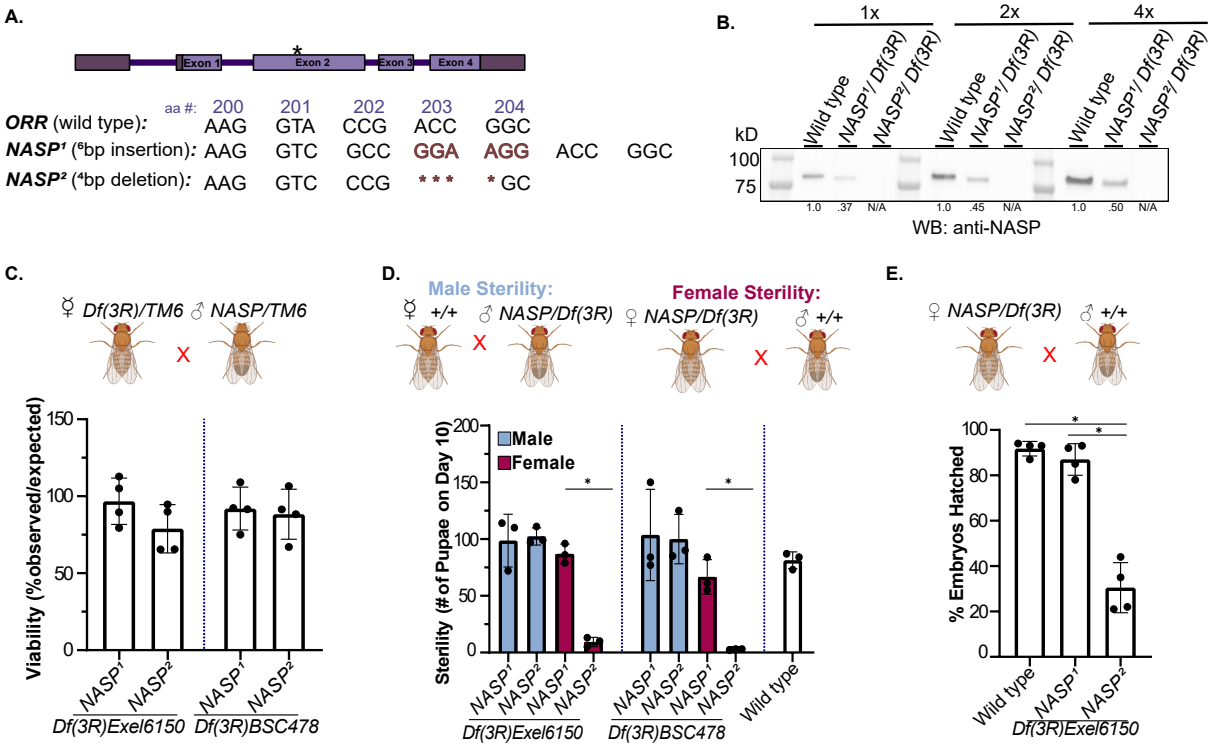

Figure 3-5.NASP is a maternal effect gene.

(A) Schematic of NASP[1] and NASP[2] CRISPR mutants. (B) Western blot analysis of ovary extracts from the indicated genotypes with total protein loading control. *NASP[1]/Df(3R) Exel6150* has less NASP due to a reduction in gene dose. Numbers below lanes represent normalized band quantification relative to wild type. (C) The percentage of progeny observed with the appropriate genotype (as shown on the x-axis) over the expected percentage. Each data point is representative of a biological replicate (n = 4). Unpaired t-test was used to determine significance ($p<0.05$). (D) The number of pupae on day 10 produced from females with the genotypes outlined on the x-axis crossed with wild type males. Each data point is representative of a biological replicate (n = 3). Unpaired t-test was used to determine significance ($p<0.05$). (E) Percentage of embryos hatched laid by wild type, *NASP[1]/Df(3R) Exel6150* or *NASP[2]/Df(3R) Exel6150* mothers. Each data point is representative of a biological replicate (n = 4) and represents the hatch rate of a group of 100 embryos. Dunn's Multiple Comparison post-hoc was performed to determine significance ($p<0.05$). (C-E) Fly crosses created with Biorender.

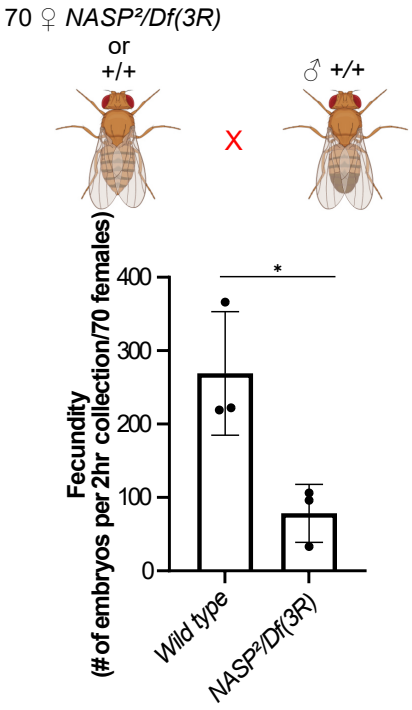

Figure 3-6.NASP mutant mothers have lower fecundity.

Number of embryos laid by wild type or *NASP2/Df(3R) Exel6150* mothers. Each data point is representative of a biological replicate from 70 females (n = 3). Unpaired t-test was used to determine significance ($p<0.05$).

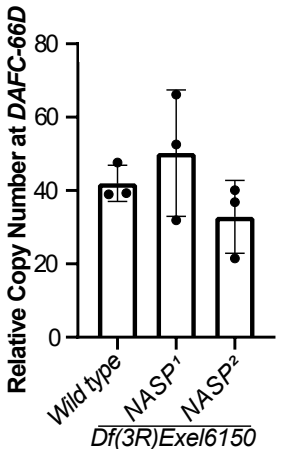

Figure 3-7.NASP mutant oocytes have no defects in gene amplification.

DAFC-66D copy number relative to a non-amplified control locus from stage 12 egg chambers for the genotypes listed on the x-axis. Kruskal-Wallis ANOVA was performed to determine significance ($p<0.05$).

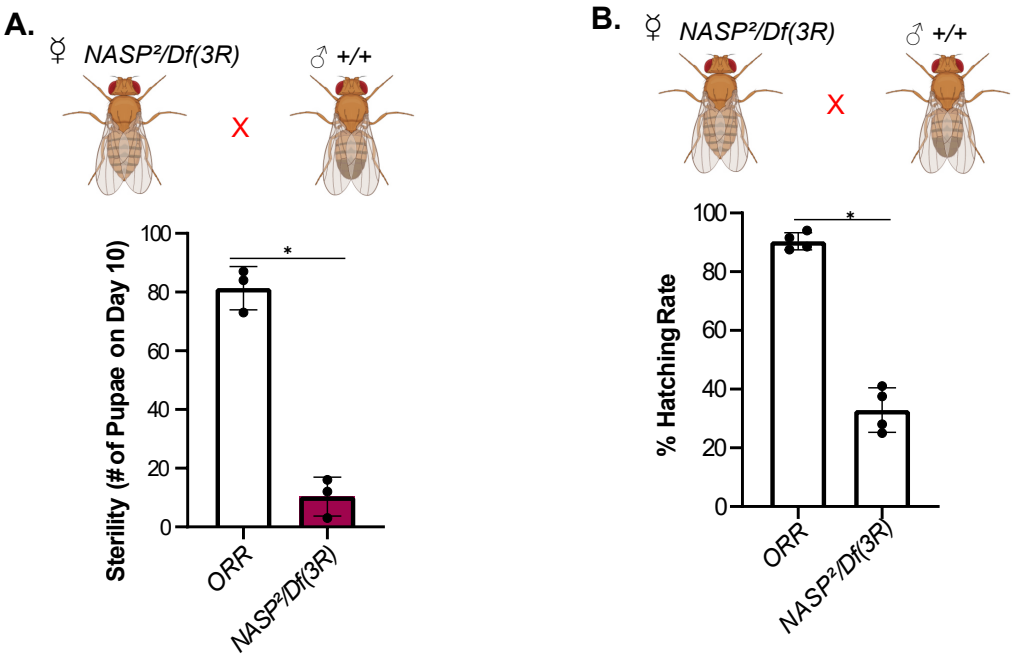

Figure 3-8.NASP is a maternal effect gene as shown by virgin female.

(A) The number of pupae on day 10 produced from virgin females with the genotypes outlined on the x-axis crossed with wild type males. Each data point is representative of a biological replicate (n =3). Unpaired t-test was used to determine significance ($p<0.05$). (B) Percentage of embryos hatched laid by wild type or *NASP²/Df(3R) Exel6150* mothers. Each data point is representative of a biological replicate (n = 4) and represents the hatch rate of a group of 100 embryos. Dunn's Multiple Comparison post-hoc was performed to determine significance ($p<0.05$)

type males had a significant reduction in hatching rate (Figure 3-8B). Therefore, we conclude that *NASP* is a maternal effect gene.

NASP stabilizes H3-H4 reservoirs in the early Drosophila embryo

Since *NASP* is a maternal effect gene, and embryos laid by *NASP* mutant mothers fail to hatch, embryos laid by NASP mutant mothers are likely devoid of a key factor(s) necessary for development. Given that NASP is a H3-H4-specific chaperone, we hypothesized that H3-H4 reservoirs are destabilized in embryos laid by *NASP* mutant mothers. To specifically measure soluble H3 and H2B reservoirs, we performed Western blot analysis on soluble and total protein extracts in embryos collected from $NASP^2$ or wild type mothers (see methods). Qualitatively, embryos laid by $NASP^2$ mothers had lower levels of soluble and total H3, but not H2B, when compared to embryos laid by wild type mothers (Figure 3-9A). To determine when in development H3 pools begin to be degraded in the absence of NASP, we performed Western blot analysis of soluble and total H3 and H2B protein levels in stage 14 egg chambers dissected from $NASP^2$ and wild type mothers. In stage 14 egg chambers, soluble, but not total, H3 levels were decreased.

In contrast, soluble and total H2B protein levels remained the same (Figure 3-9B). This suggests that in the absence of NASP, H3 forms an insoluble aggregate in stage 14 egg chambers. In support of this, a greater fraction of H3 is found in an insoluble fraction in $NASP^2$ mutant egg chambers when compared to wild type egg chambers (Figure 3-10). Therefore, in the absence of NASP, H3 is likely prone to aggregation in stage 14 egg chambers but is then degraded in early embryogenesis. Taken together, we conclude that

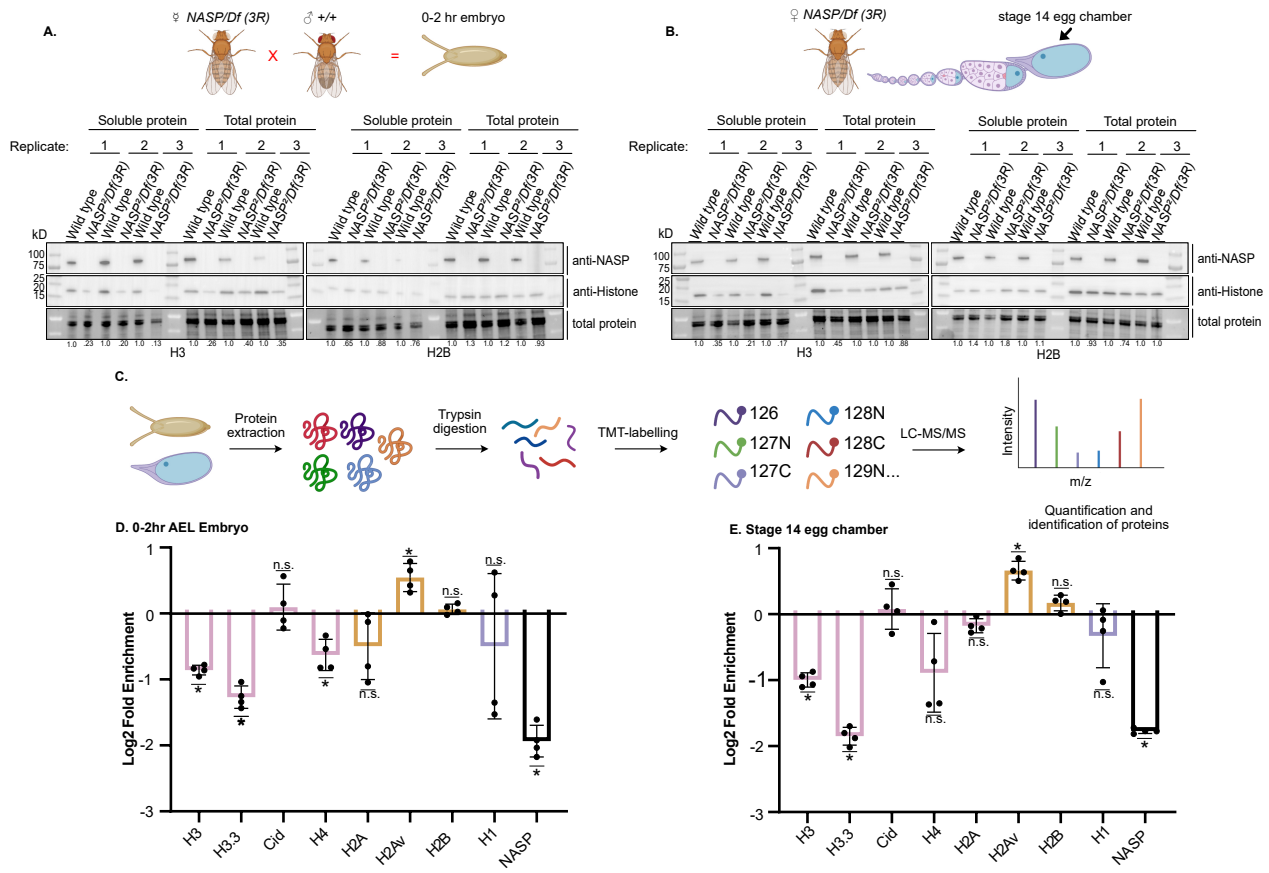

Figure 3-9.NASP stabilizes H3/H4 reservoirs in the early Drosophila embryo.

(A) Western blot analysis of soluble and total protein of 0-2hr AEL embryos laid by wild type or *NASP²/Df(3R) Exel6150* mutant mothers. Fly cross created by Biorender. (B) Western blot analysis of wild type or *NASP²/Df(3R) Exel6150* stage 14 egg chamber soluble or total protein prepped. Fly schematic created by Biorender. (C) Schematic of quantitative mass spectrometry approach to quantify protein abundance created with Biorender. (D) Average Log2 fold change for four biological replicates of unique peptides corresponding to H2A, H2Av, H2B, H3, H3.3, H4, Cid, H1, and NASP in 0-2hr AEL embryos laid by *NASP²/Df(3R) Exel6150* or wild type mothers. Adjusted p-values were calculated by performing multiple t-tests with a Holm-Sidak correction ($p<0.05$). (e) Average Log2 fold change for four biological replicates of unique peptides for H2A, H2Av, H2B, H3, H3.3, H4, Cid, H1, and NASP in *NASP²/Df(3R) Exel6150* or wild type stage 14 egg chambers. Adjusted p-values were calculated by performing multiple t-tests with a Holm-Sidak correction ($p<0.05$).

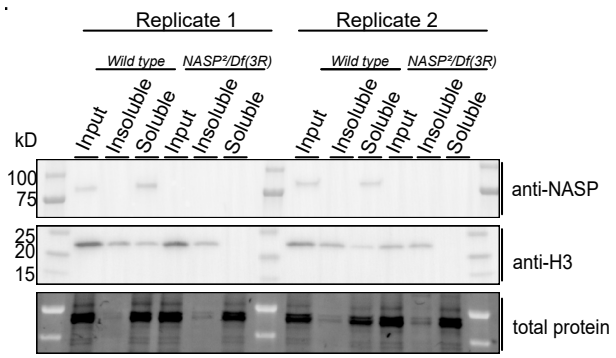

Figure 3-10. Soluble H3 may be aggregating in NASP mutant stage 14 egg chambers.

Western blot analysis of total, insoluble, and soluble protein preps from stage 14 egg chambers dissected from wild type or *NASP²/Df(3R) Exel6150* mutant mothers.

NASP is critical for H3 solubilization and stabilization during both oogenesis and embryogenesis.

To extend this analysis to all canonical and variant histones and gain a quantitative view of histone levels during development, we used quantitative mass spectrometry to measure soluble histone levels in early embryos and stage 14 egg chambers (Figure 3-9C). To this end, we TMT labeled extracts from 0–2-hour (AEL) embryos and stage 14 egg chambers from four biological replicates. This analysis revealed that the soluble levels of histones H3 and H3.3 were significantly reduced in embryos laid by *NASP*^{2} mutant mothers and in *NASP*^{2} mutant stage 14 egg chambers (Figure 3-9 D and E). Soluble H3-like centromeric protein Cid, H4, H1, H2A and H2B levels were stable while H2Av levels increased (Figure 3-9 D and E). Overall, quantitative mass spectrometry reveals that in the absence of NASP, soluble pools of histone H3 are reduced starting in oogenesis whereas histone H4 is destabilized in embryogenesis. H3 and H3.3 are more depleted than H4, which is consistent with recent work showing human NASP has a preference for monomeric H3 (Pardal and Bowman 2022) Thus, we conclude that NASP stabilizes H3 and H4 soluble reservoirs during both oogenesis and embryogenesis with a preference for H3.

Embryos laid by NASP mutant mothers stall or slow in early embryogenesis

60–70% of embryos laid by *NASP* mutant mothers do not hatch. To determine what the underlying defects are in embryogenesis, we propidium iodide stained 0–4-hour AEL embryos and manually scored the number of embryos in each cell cycle (Figure 3-11).

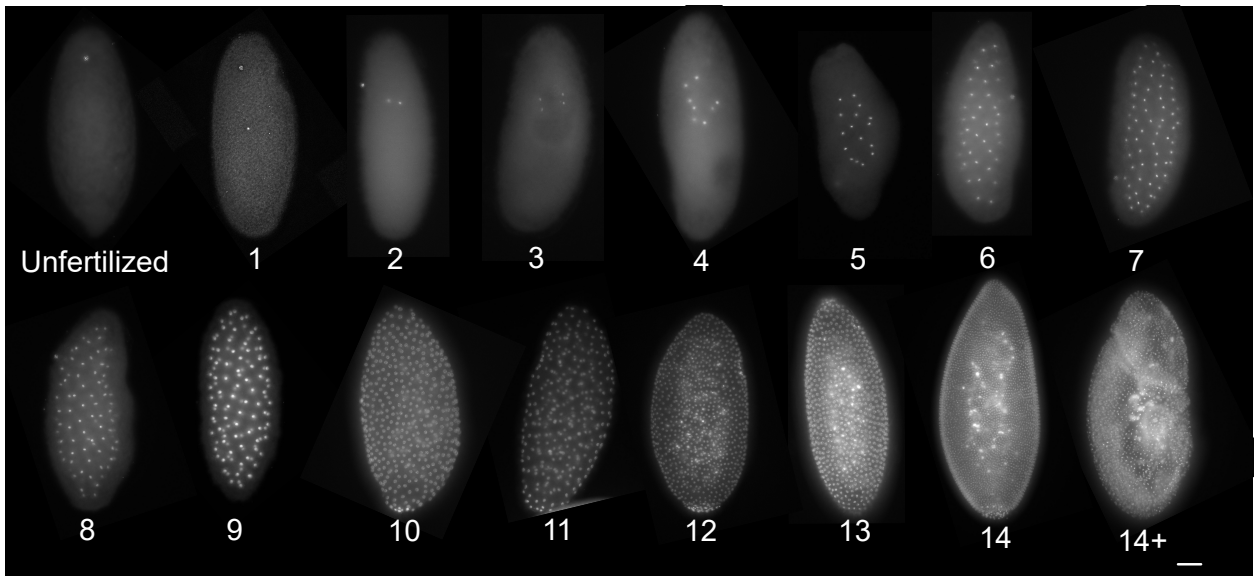

Figure 3-11. Drosophila embryo nuclear cycles.

Representative single embryos cropped from max project images used to define nuclear cycle stages for scoring data presented in Figure 3-12A and 3-12B. Scale bar represents 100μm.

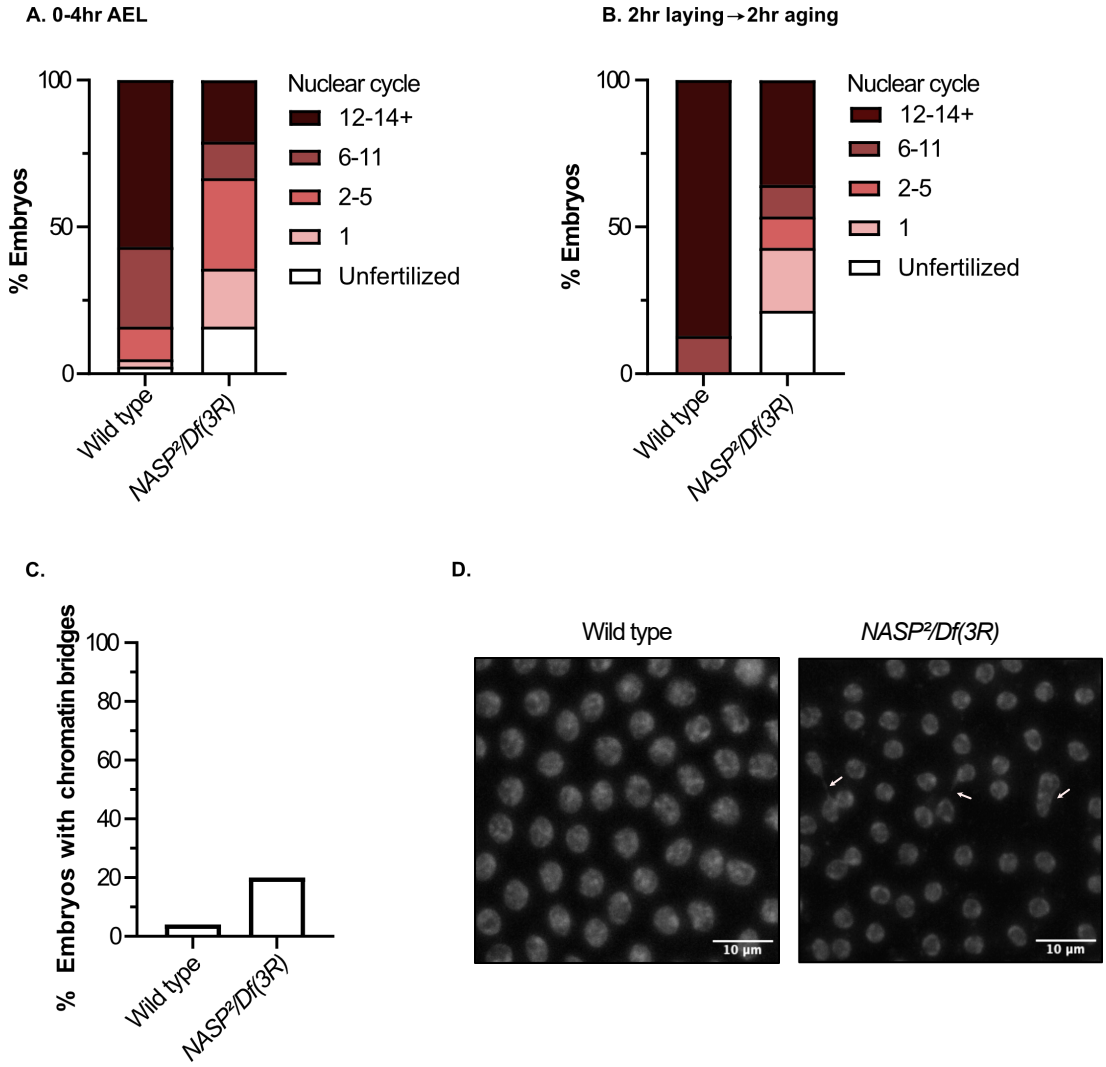

Figure 3-12. Embryos laid by NASP mutant mothers stall or slow in early embryogenesis.

(A) Percentage of 0-4hr AEL embryos laid by wild type or *NASP²/Df(3R) Exel6150* mutant mothers in respective cell cycles (n = 81). (B) Percentage of 0-2hr AEL embryos laid by wild type or *NASP²/Df(3R) Exel6150* mutant mothers in respective cycles after aging for 2 hours (n = 34). (C) Percentage of embryos by wild type or *NASP²/Df(3R) Exel6150* mutant mothers with chromatin bridging (n = 50 pooled from 3 biological replicates). (D)Representative images of propidium iodide-stained embryos laid by wild type or NASP2/Df(3R) Exel6150 mutant mothers. White arrows point to chromatin bridging.

We observed that 16% of embryos laid by *NASP* mutant mothers were unfertilized, 20% were in cell cycle 1, 31% in cell cycle 2–5, 12% in cell cycles 6–11, and 21% in cell cycles 12 or later. Whereas embryos laid by wild type mothers were 3% unfertilized, 3% cell cycle 1, 28% cell cycle 6–11, and 57% in cell cycle 12 or later (Figure 3-12A). This suggests that embryos laid by *NASP* mutant mothers progress more slowly or are stalled in the first embryonic cycles.

To determine if embryos laid by *NASP* mutant mothers are stalled or more slowly progress through the nuclear cell cycles, we collected 0–2-hour AEL embryos and aged them for two hours then scored the embryos for cell cycle stage. The majority of embryos laid by wild type mothers were in cell cycle 12 or later (87%) and only 13% in cell cycles 6–11. In contrast, embryos laid by *NASP* mutant mothers were stalled in an unfertilized stage (20%) or in cell cycle 1 (20%) and only 36% of embryos progressed to cell cycle 12 or later (Figure 3-12B). Our results are consistent with a recent study showing that maternal depletion of CG8223 results in 61% of embryos arresting in cell cycle stage 2 (Z. Zhang et al., 2018). To test if embryos laid by *NASP* mutant mothers are associated with DNA damage that could stall or slow the progression of embryogenesis, we measured chromatin bridging. We observed a five-fold increase in chromatin bridging when comparing embryos laid by *NASP* mutant mothers to embryos laid by wild type mothers (Figure 3-12 C and D). Together, we conclude that embryos laid by *NASP* mutant mothers have cell cycle defects that start in the earliest nuclear cycle of embryogenesis.

Discussion

Early Drosophila embryogenesis provides a unique challenge to histone supply and demand. The early embryo is maternally stockpiled with an overabundance of histones, yet overproduction of histones is detrimental to cells (Berloco et al., 2001; Celona et al., 2011; Gunjan & Verreault, 2003; Herrero & Moreno, 2011). Excess histone supply is likely tolerated through the activity of histone chaperones (Horard & Loppin, 2015; Li et al., 2012). The histone chaperone Jabba stabilizes soluble H2A-H2B pools in the early embryo by sequestering histones to lipid droplets (Li et al., 2012). The histone chaperone that maintains soluble H3-H4 pools in the early Drosophila embryo, however, has yet to be identified. Our work demonstrates that CG8223, the Drosophila homolog of NASP, is a H3-H4 chaperone in the early embryo. This conclusion is supported by several independent lines of evidence. First, NASP associates with H3-H4, but not H2A-H2B in vivo. Second, soluble pools of H3-H4, but not H2A-H2B, are destabilized in the absence of NASP. Interestingly, NASP binds more H3 than H4 and H3 and H3.3 are depleted more than H4 which is consistent with recent work showing that human NASP preferentially binds H3 (Pardal & Bowman, 2022). Third, *NASP* is a maternal effect gene and embryos laid by NASP mutant mothers have defects in embryonic development and embryo hatching. Taken together, we conclude that NASP is the predominant H3-H4 chaperone in the early Drosophila embryo. Now that we have identified NASP as the missing H3-H4-specific chaperone necessary to stabilize soluble H3-H4 pools during Drosophila embryogenesis, we will be able to begin to address fundamental questions about histone storage and stability during oogenesis and embryogenesis.

CHAPTER IV

IV. DISCUSSION AND FUTURE DIRECTIONS

Immediate objectives

NASP functions in the cytoplasm but localizes to the nucleus

Immunoprecipitation of H3.1 from cell fractionated lysates has shown that NASP localizes to the nucleus but is more predominantly located in the cytoplasm. Upon cell lysis, however, the nuclear membrane can rupture causing nuclear components to leak into the cytoplasmic fraction. Most certain evidence that NASP is both located and functions in the cytoplasm has come from its unrelated role in immune signaling (discussed in detail under 'NASP is a major player in immune signaling'). Briefly, NASP binds TRAF6 in the cytoplasm to inhibit TLR4 induced Nuclear Factor Kappa B (NF-kB) activation. Upon an immunologic stimulant, NASP disassociates from TRAF6 allowing for the consequential immune response (Yang et al. 2021). Most importantly, NASP NLS mutants retain their ability to inhibit immune signaling which signifies that NASP localization in the cytoplasm is functional.

In this thesis, I have established that NASP functions to maintain large reservoirs of H3-H4 in the early embryo. Furthermore, Drosophila embryogenesis sets up a suitable experimental model to test whether NASP is located or functions in the nucleus or cytoplasm. This is due to the large reservoirs of histones that are maternally deposited

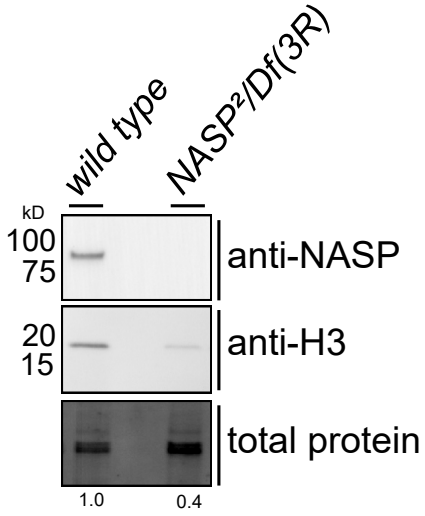

Figure 4-1. H3 levels are depleted as early as NC1 in the absence of NASP

Western blot analysis of NC1 embryos laid by wild type or *NASP²/Df(3R) Exel6150* mutant mothers. Numbers below lanes represent normalized band quantification relative to wild type.

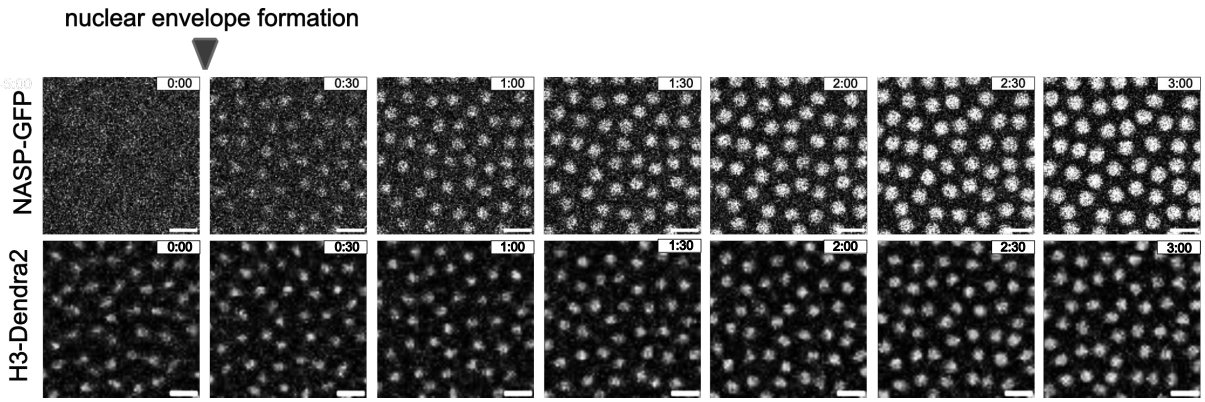

Figure 4-2. NASP is in the nucleus of the Drosophila embryo.

Live embryo imaging of NASP-GFP or H3-Dendra2-expressing embryos imaged at 30 second intervals for the first 3 minutes of nuclear cycle 13. Arrowhead marks nuclear envelope formation. Scale bars = 5μm

into the early embryo in a shared cytoplasm. If NASP functions to store H3-H4 in the cytoplasm, then H3 and H4 should be depleted as early as NC 1, in which there is only one nucleus in the whole embryo. In fact, preliminary western blots from staged NC 1 indicates that H3 levels are decreased in the absence of NASP (Figure 4-1). Additionally, if NASP functions in the cytoplasm then western blotting of unfertilized embryos, in which no nucleus will be formed so all histones are present in the cytoplasm only, should lead to a decrease in H3 levels. To perform this experiment, embryos will be collected from NASP mutant mothers crossed to sterile males. Western blotting of these embryos will further verify that NASP maintains large pools of maternally deposited H3-H4 in the cytoplasm.

Preliminary evidence suggests that NASP maintains large reservoirs of H3-H4 in the cytoplasm. Interestingly, NASP-GFP is localized in the nuclei of dividing Drosophila embryos (Figure 4-2). Previous reports from the Bowman laboratory have also observed that NASP is in the nucleus in mammalian cultured cells via immunofluorescence assays. Further, immunoprecipitation of artificially tethered H3 in the cytoplasm did not enrich NASP. Based on these data, they hypothesize that NASP functions solely in the nucleus to receive H3. To delineate NASP function in the cytoplasm versus in the nucleus, I have generated a $NASP^{NLS}$ mutant so that NASP cannot be imported into the nucleus. If NASP's ability to store H3-H4 is in the cytoplasm only, then embryos laid by $NASP^{NLS}$ mutant mothers should reveal stable H3 and H4 levels as compared to wild type embryos. This will establish $NASP^{NLS}$ as a fantastic separation of function mutant to better understand NASP function in the nucleus versus the cytoplasm.

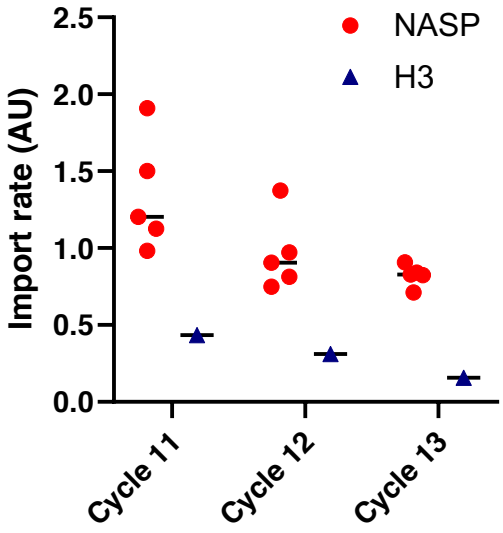

Figure 4-3. NASP import rates are higher than H3 in the early embryo

Rate of NASP-GFP nuclear import (n=5) as measured by initial slopes of nuclear intensities over time. One representative H3-Dendra2 import rate is graphed for comparison.

NASP may store H3-H4 in the cytoplasm and the nucleus. In that case, H3 and H4 levels in NC 1 embryos laid by *NASP^{NLS} and NASP^{2}* null mutant females should be compared. Since there is only nucleus in NC 1, I would expect that there will be a higher decrease in H3 and H4 levels in embryos laid by *NASP^{2}* null mutant females compared to *NASP^{NLS}*, even if NASP functions in both the cytoplasm and nucleus.

NASP affects H3 import dynamics

The Bowman laboratory has postulated that NASP may function to receive H3 in the nucleus. Given that NASP has been visually observed in the nucleus via live imaging of NASP-GFP in embryos, it is possible that NASP acts as a receptor in the nucleus for H3-H4. In this case, then NASP must be imported fasted than H3-H4 so that it may be present in the nucleus to receive histones. NASP import analysis revealed that NASP-GFP import is higher than previously reported H3 import rates (Figure 4-3). If NASP is the H3 receptor in the nucleus, then I would expect H3 import rates to be defected in the absence of NASP. In this case, H3 import rates should be measured in the absence of NASP. H2A import rates will also be measured in the absence of NASP as a control to determine if the reduction in H3 import rates observed are H3- specific. Since import rates are generated from measuring H3 intensity from nuclear envelope formation to nuclear envelope breakdown for each NC, the decrease in lower H3 import rates may be due to higher export rates. It is possible that NASP is required to stabilize H3-H4 in the nucleus, and in its absence, H3-H4 are destabilized and exported to the cytoplasm for degradation. Thus, export rates of H3 should also be measured in the presence and absence of NASP. Nonetheless, higher NASP-GFP import rates infer that NASP may have two distinct functions based on its localization in the nucleus or the cytoplasm.

NASP functional contribution in the nucleus vs the cytoplasm

In the absence of H2A-H2B chaperone Jabba, embryos have no significant defect and can develop properly. It is only in the absence of Jabba and SLBP, which inhibits active translation of histones in the early embryo, that 100% of embryos do not hatch. This implies that active translation of histone mRNA can overcome depletion of H2A-H2B protein levels. Interestingly, in the absence of NASP, which decreases H3-H4 protein levels, 60-70% of embryos do not hatch. Thus, either H3-H4 have a secondary function beyond chromatin (which will be discussed in detail under 'Is CHK1 prematurely activated?') or NASP may have a secondary function essential for embryo development. To test the latter hypothesis, the *NASP*^{NLS} mutant can be utilized. If NASP's function to maintain large pools of H3-H4 is cytoplasm specific, then the *NASP*^{NLS} mutant will be a separation of function mutant. If so, it can be distinguished whether NASP function as a H3 or H3-H4 receptor in the nucleus or its role to maintain H3-H4 soluble pools in the cytoplasm is essential for embryo development. In this case, female sterility and embryo hatching assays will be performed on the *NASP*^{NLS} mutant. If *NASP*^{NLS} mutants are female sterile and embryos cannot hatch, then the depletion of large pools of soluble histones is detrimental to embryo development. If *NASP*^{NLS} mutants are not female sterile and lay embryos that can develop properly, then NASP function as an H3 receptor and consequently the import of H3 into the nucleus is essential for development.

NASP may bind H3 monomers in the nucleus

NASP can bind distinct binding region of H3 at the interface of H3-H4 in vitro. Further, there is a two-fold molar H3 enrichment over H4 in NASP immunoprecipitation experiments, whereas ASF1 immunoprecipitation led to equimolar levels of H3 and H4 enrichment. Thus, it has been hypothesized that NASP may bind H3 monomers in the nucleus (Apta-Smith et al. 2018; Maksimov et al. 2016; Pardal and Bowman 2022). In my own studies of NASP in the early embryo, I have observed that NASP IP leads to higher enrichment of H3 over H4 (Figure 3.2). In the absence of NASP, higher levels of H3 are depleted than H4 in oocyte and embryos (Figure 3.4). Therefore, it is plausible that NASP maintains monomers of H3. To directly test this hypothesis, I have generated a NASP H3 binding mutant (EWD3A) that is expressed during oogenesis and embryogenesis (Figure 4-4A and 4-4B). To confirm that the NASP H3 binding mutant did not interact with H3, I immunoprecipitated GFP from embryo extracts (0-24h AEL) using a GFP nanobody. Western blot analysis of the IP revealed that NASP CDS-GFP control and H3 but not H2B, are in the same protein complex. On the other hand, NASP EWD3A-GFP could not enrich H3 or H2B (Figure 4-4C). If NASP functions to only maintain or act as a receptor in the nucleus for H3 monomers, then only H3 stabilization and import should be impacted by H3 binding mutants. At the same time, H4 import will be measured in NASP EWD3A mutants. If NASP binds and receives H3 monomers only, then H4 import should remain the same. It should be considered that the import of H3 and dimerization of H3-H4 may be important for H4 maintenance in the nucleus, as H4 may be exported to the cytoplasm. Thus, H4 export will also be measured.

Summary

The immediate objectives will address controversy surrounding NASP localization and NASP binding to H3 monomers. If the preliminary evidence stated stands true with the addition of controls and further experimentation, then it will establish NASP dual function in the cytoplasm, to store H3-H4 reservoir, and in the nucleus, to receive imported H3.

Long term objectives

Potential hypothesis for embryo defective development

Embryos laid by *NASP* mutant mothers are stalled in early embryogenesis and display DNA damage. We do not currently know, however, what specific molecular mechanism(s) underlie these defects. Below, I will discuss several non-mutually exclusive mechanisms that could explain the defects we observe in embryogenesis.

Embryos laid by NASP mutant mothers may not be fertilized

Male sperm are required to replace SNBP with H3.3-H4 to de-condense their chromatin to allow for fertilization (as discussed under ‘Drosophila oogenesis, fertilization, and

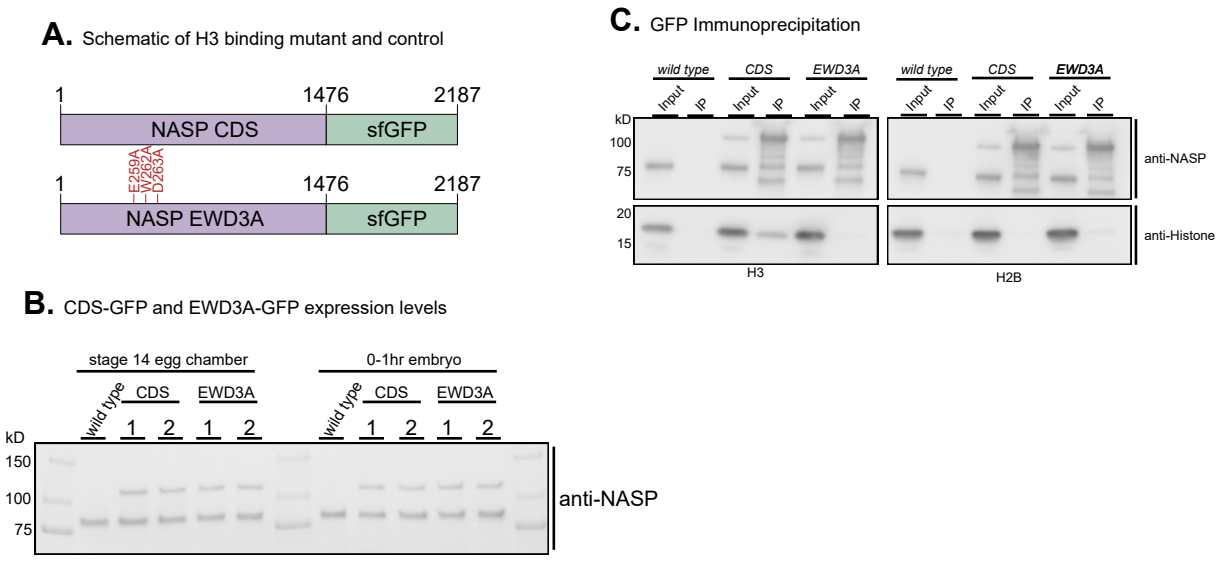

Figure 4-4. Generating a NASP H3 binding mutant

(A) Schematic of *NASP*^{CDS} control and *NASP* ^{EWD3A} transgene H3 binding mutants. (B) Western blot analysis of stage 14 egg chambers and 0-1hr AEL embryos derived from *NASP*^{CDS} /+ and *NASP*^{EWD3A}/+ mothers. The higher band indicates the NASP-GFP while the lower band is the endogenous NASP. (C) Immunoprecipitation of GFP from 0-24hr AEL embryos from wildtype, *NASP*^{CDS} /+ and *NASP*^{EWD3A}/+ .

embryogenesis'). Thus, it is possible that embryos laid by *NASP* mutant mothers are not fertilized due to the depletion of H3 and H3.3 starting in stage 14 egg chambers. Previously, it has been shown that upon maternal depletion of NASP by RNAi, embryos are still fertilized (Zhang et al., 2018). It is important to note, however, that these experiments were carried out with a single RNA interference (RNAi) line, and the absolute level of depletion was not known. Therefore, it is still possible that embryos laid by NASP mutant mothers may not be properly fertilized when NASP is eliminated through mutation. Alternatively, it is possible that, like embryos laid by HIRA mutant mothers, these embryos are fertilized but progress through embryogenesis as haploids (Bonnefoy et al. 2007). To directly test whether embryos laid by NASP mutant females are fertilized, IF can be performed with acetylated H4 antibody in the early embryo to detect male sperm nucleus de-condensation (Bonnefoy et al. 2007). If embryos are fertilized, then acetylated H4 should overlap with the sperm chromatin (marked by DAPI) in the early embryo.

There may not be enough H3-H4 for chromatin packaging

The H3-H4 supply could be insufficient to fuel the demand for chromatin formation in the early embryo. In the early embryo, a single nucleus must rapidly expand to ~8,000 nuclei in two hours (Yuan et al. 2016). To keep up with the demand for chromatin formation, the early embryo is likely dependent on the maternally loaded histones. In the absence of maternally deposited NASP, H3 and H4 pools are substantially reduced. Thus, it is possible that embryos laid by *NASP* mutant mothers simply lack sufficient H3 and H4 supplies for rapid chromatin formation. This hypothesis is less likely because in the

absence of the H2A-H2B-specific chaperone Jabba, active translation can compensate for the destabilization of H2A, H2B, and H2Av. It is only when translation is inhibited in the Jabba mutant that embryos die (Li et al., 2012). However, H3-H4 tetramers set up the foundation of nucleosome arrays in which H2A-H2B dimers are added to, thus it is possible that H3-H4 may be more important in packaging of chromatin than H2A-H2B.

Nonetheless, to test whether chromatin packaging is the underlying mechanism that leads to embryo defects, Assay for Transposase Accessible Chromatin with Sequencing (ATAC-seq) can be performed in carefully staged embryos. Analysis of ATAC-seq in the early embryo is a hard feat since the embryo does not have an established chromatin and has less DNA accessibility than later staged embryos. Chromatin accessibility increases as the embryo reaches MBT to allow for MBT-specific transcripts to be zygotically transcribed (Brennan et al. 2023).Thus, later staged embryos may be more optimal for ATAC-seq experiments. 30-40% of embryos laid by NASP mutant females do hatch, though they die during the larval stage, thus later staged embryos have a higher probability of hatching and may bias the analysis if they do not acquire as large defects as embryos that do not hatch. Therefore, even if large depletion of histones in the absence of NASP may lead to more open chromatin, it may be hard to detect with traditional open chromatin assays.

Instead, the consequence of open chromatin, like transcription, can be measured to determine if chromatin packaging is affected. Thus, RNA-seq can be performed in staged embryos to detect aberrant transcription. Single Molecule Fluorescence in situ hybridization (smFISH) can be performed as a complementary method to RNA-seq. We expected that in the absence of H3-H4, and thus open chromatin, zygotic transcription may increase or occur in earlier NCs. Unexpectedly, preliminary smFISH analysis for a

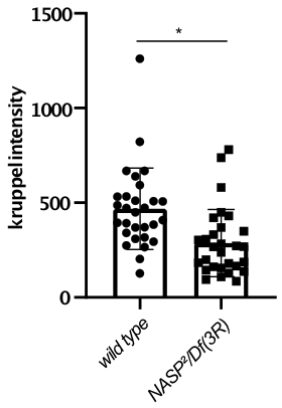

Figure 4-5. Less Kruppel transcripts detected in embryos laid by NASP mutant mothers.

Intensity of kruppel transcripts in stage 14 embryos laid by wild type and *NASP*^{2}*/Df(3R) Exel6150* mothers. Pooled samples of three biological replicates. Unpaired t-test was used to determine significance ($p<0.05$).

single transcript (Kruppel) was observed to be decreased in stage 14 embryos (Figure 4-5A and Figure 4-5B). It is possible that open chromatin may lead to non-specific RNA polymerase II binding and thus an overall increase in transcription, which may take away the transcriptional resources to transcribe developmentally upregulated transcripts. To note, we have only performed smFISH with a single transcript so further experimentation is required. In addition, it would be nice to corroborate this data with RNA polymerase II IF or Chromatin Immunoprecipitation Sequencing (ChIP-seq) data to support an increased RNA polymerase II binding to chromatin.

CHK1 may be prematurely activated

Reduced soluble pools of H3-H4 have the potential to impact cell cycle dynamics in the early embryo. Overexpression of the N-terminal tail of H3 delays CHK1 activation, thereby influencing cell cycle length and the onset of the MBT (Shindo and Amodeo 2021). Therefore, soluble H3 pools could act as a timer to prevent CHK1 activation and promote rapid cell cycles. Decreasing soluble H3 pools during embryogenesis could allow CHK1 to be prematurely activated and cell cycle length to be extended, thereby altering key cell cycle events in the early embryo and the onset of the MBT (Chari et al. 2019). To determine whether CHK1 is prematurely activated in the absence of maternally deposited NASP in the early embryo, a CHK1 target biosensor can be utilized. This biosensor contains a CHK1 phosphorylation site, NLS, Nuclear Export Signal (NES), and GFP. Once phosphorylated by CHK1, the biosensor's NLS will be masked by another protein which prohibits nuclear import during NCs. Thus, the biosensor's cytoplasm to nucleus ratio

(C/N) signal will reflect whether CHK1 is active (Deneke et al. 2016). To determine CHK1 activation, live imaging of the biosensor in embryos laid by wild type and *NASP*^{2} null mutant females should be performed, and the C/N of CHK1 biosensor can be calculated. If depletion of H3-H4 in the absence of NASP in the early embryo leads to premature CHK1 activation, then I would expect a higher C/N, and thus higher CHK1 activation, earlier in embryo NC than in wild type embryos. The results of this experiment would support the model that H3 may be the titrating factor that determines the onset of MBT in vivo.

Equal H2A-H2B to H3-H4 stoichiometry may be required

Proper chromatin packaging requires an equimolar ratio of histones (Camerini-Otero, Sollner-Webb, and Felsenfeld 1976). In *C. elegans*, depletion of embryonic H2B results in animal sterility. Interestingly, this sterility can be suppressed by reducing H3-H4 levels (Zhao et al. 2022). Therefore, proper stoichiometry of histones, rather than absolute histone levels, is critical for embryo viability (Au et al. 2008; Meeks-Wagner and Hartwell 1966). Embryos laid by *NASP*^{2} null mutant mothers have reduced H3 and H4 levels, yet H2A and H2B levels remain unaffected. It is possible that this alteration in histone stoichiometry leads to both female sterility and defects in embryo development. To restore balance for histone stoichiometry, a *NASP Jabba* double null mutant can be generated, in which both the levels of H3-H4 and H2A-H2B should be decreased simultaneously. If the imbalance of H3-H4 to H2A-H2B is responsible for proper embryo development, then I would expect that the double mutant will rescue the defects observed in the *NASP*^{2} null mutant embryos. To note, this hypothesis seems the mostly unlikely, given that Jabba null

mutant embryos, with decreased H2A, H2B, and H2Av levels but stable H3 and H4 levels, can still hatch and develop properly.

Increased H2Av may lead to reduced hatching

Embryos laid by NASP mutant mothers have increased H2Av levels. While it is unclear how NASP would directly or indirectly destabilize H2Av, overexpression of H2Av causes nuclear fallout and reduced hatching rate (Li et al. 2014). Thus, the increased H2Av levels in embryos laid by NASP mutant mothers could contribute to defects in embryo development.

As of now, there have been no studies that link NASP to H2Av. Interestingly, we also observed that NASP is in complex with H2Av, so NASP may influence H2Av degradation. Given how H2Av overexpression is toxic to embryos, NASP may be important for keeping H2Av levels at bay. To better understand the relationship between NASP and H2Av, the regions required for interaction would be essential. Once NASP H2Av binding region or H2Av NASP binding region has been determined, their complex can be better studied. One way to map the regions important for their interaction is by generating truncations of NASP tagged with GFP, transfecting the plasmid into Drosophila S2 cultured cells, and performing GFP IP for H2Av. Once the region required for H2Av binding has been identified, then single amino acid mutations can be generated to determine the amino acids essential for H2Av binding region. Then a NASP H2Av transgene can be generated

to determine whether NASP binding and increase in H2Av levels are the underlying mechanism for embryo lethality observed in the *NASP*^{2} null mutant.

Outstanding Questions

What is the histone degradation pathway in the early Drosophila embryo?

It is still unresolved what mechanism is responsible for histone degradation in embryos laid by *NASP*^{2} null mutant mothers. Our work shows that soluble H3-H4 levels are already reduced in the latest stage of oogenesis, and H3 is likely aggregated in stage 14 egg chambers but not degraded until early embryogenesis. Thus, it will be critical to determine the pathway that degrades unchaperoned H3 and H4 in the early embryo. In mammalian cells, autophagy is responsible for degrading excess H3 and H4 upon NASP depletion (Cook et al., 2011). Therefore, it is possible that, in early Drosophila embryos, autophagy is responsible for H3-H4 degradation in the absence of NASP. In embryos laid by *NASP*^{2} null mutant mothers, we were still able to detect H3 and H4, indicating that H3-H4 pools are not completely degraded in the absence of NASP. This may be because a subset of H3 and possibly H4 are aggregated and not completely degraded. Though it is also possible that another chaperone stabilizes the remaining minor fraction of H3 and H4 in the early embryo (see 'Histone chaperones in early development'). While these chaperones could stabilize a fraction of the total H3-H4 pools, they are not sufficient to drive embryogenesis.

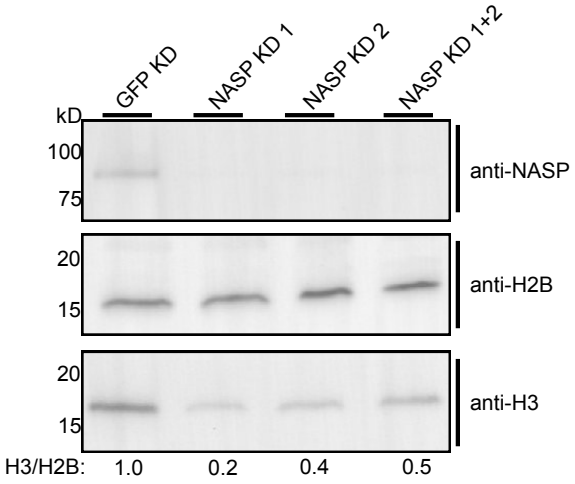

Figure 4-6. Knockdown of NASP in Drosophila S2 cultured cells lead to soluble H3 depletion.

Western blot analysis of Drosophila S2 cultured cells. NASP KD 1 and NASP KD 2 represent two independent RNAi construct. The ratio of H3:H2B for each KD is indicated.

We observed that soluble H3 levels are depleted in the absence of NASP in embryonically derived Drosophila S2 cultured cells (Figure 4-6). This enables an efficient RNAi screen of potential candidates in the autophagy or proteasome pathways. Additionally, proteasome inhibitors can be utilized to test the proteasome degradation pathway. If any genes are involved in degrading H3 or H4, then we expect that simultaneous inhibition of said candidate along with NASP will lead to the rescue of soluble H3 levels in S2 cultured cells. Hits from the S2 cultured cells screen can then be verified in embryos. Null mutant lines of potential candidates may exist in the Drosophila repository fly stock, if not then they would be generated. Western blotting of embryos laid by double null mutant of degradation factor and NASP should show an increased H3 level compared to *NASP*^{2} null mutant. H2A and H2B will be used as control.

It may be possible that the same degradation pathway may be targeting H2A and H2B for degradation. Experiments in both Drosophila S2 cultured cells and embryos should be performed to determine if the potential factor or pathway can rescue H2A/H2B levels in the absence of Jabba. If all histones are targeted by the same protein and degradation pathway, it would be beneficial to determine the region of the protein that dictates their demise. This could be used as a potential tool to deplete maternally deposited proteins. H2A and H2B degradation pathway or factors may differ from H3 and H4. In that case, specific histones can be made to be stable throughout embryogenesis by inhibiting their degradation pathway. This will allow researchers to study the purpose of large reservoirs of soluble histones in the early embryo. For example, soluble H3 function beyond its role for chromatin packaging has been extensively discussed (See' CHK1 may be prematurely activated' or 'Drosophila oogenesis, fertilization, and embryogenesis'). If H3 degradation

pathway is inhibited and H3 remains stable, then I would expect a delay in CHK1 activation and shorter NC 14. Thus, not only will these experiments establish the histones degradation pathway in Drosophila but also enable researchers to test the CHK1 model in vivo.

How is NASP regulated throughout embryogenesis?

Soluble histones are decreased from >99% to ~1% throughout embryogenesis. Thus, NASP function to store H3-H4 reservoirs is a major task in the early embryo that decreases post MBT, as there are fewer soluble histones to store. Further, homozygous NASP null mutants are viable in somatic cells and Drosophila. So how is NASP regulated when its major function as a histone storage is no longer necessary?

Previous research has determined that NASP mRNA can be downregulated by microRNAs (miRNA) (Kong et al. 2020; Ma et al. 2012; Yu et al. 2017; Zhu et al. 2021). In Head Neck Squamous Cancer Cells (HNSCC), miR381-3p targets NASP mRNA (Kong et al. 2020) whereas in gastric cells, hepatoma cancer cells, and rat skin cells, miRNA29-a and miRNA29-c have been shown to specifically target NASP to deplete NASP mRNA levels (Yu et al. 2017; Zhu et al. 2021). Interestingly, miRNA29 levels are low in early development and then increase in post-natal rat skin cells (Ma et al. 2012). Given that NASP has been shown to chaperone large pools of H3-H4 in oocytes which deplete over embryogenesis, miRNAs may be regulating NASP levels in accordance. Though this would be an interesting feat, it is important to note that this inference is from correlative data in different tissues.

At the protein level, NASP has been shown to be phosphorylated and ubiquitinated individually (Lee et al. 2014; Yang et al. 2021). Phosphorylation is functional in immune signaling (details under 'NASP is a major player in immune signaling'). Given that NASP has been shown to be phosphorylated in *D. melanogaster* during the oogenesis to embryogenesis transition, it would be plausible that phosphorylation may impact NASP function as an H3-H4 chaperone. Additionally, it has been shown that NASP can be ubiquitinated by Ubiquitin Protein Ligase E3A (UBE3) in *D. melanogaster* neuronal BG2 cells, though the underlying mechanism or function is not understood.

Firstly, it would be informative to quantify total protein levels of NASP throughout embryogenesis by western blot. This will let researchers know if NASP regulation occurs at the protein level at a specific time point (such as MBT).

Additionally, a two-pronged method can be taken to better understand NASP regulation through embryogenesis. (1) IP-MS can be performed during multiple stages of embryogenesis which will reveal complex partners. This will identify potential factors that may regulate NASP via phosphorylation or ubiquitination at some point in embryogenesis. (2) Since it has previously been established that NASP can be post translationally modified via phosphorylation and ubiquitination, then specific phosphorylation or ubiquitination sites can be targeted for mutation. NASP levels should be inspected throughout embryogenesis to determine whether there is an increase or decrease when PTMs are prohibited. The change in NASP PTMs may lead to a change in its function to store H3-H4, thus H3 levels should also be examined.

Perhaps NASP total levels stay the same throughout embryogenesis. Instead, NASP function is expanded as development proceeds, none of which are essential due to redundancy provided by other H3-H4 chaperones.

REFERENCES

Aguilar-Gurrieri, Carmen, Amédé Larabi, Vinesh Vinayachandran, Nisha A. Patel, Kuangyu Yen, Rohit Reja, Ima-O Ebong, Guy Schoehn, Carol V Robinson, B. Franklin Pugh, and Daniel Panne. 2016. "Structural Evidence for Nap1-dependent H2A–H2B Deposition and Nucleosome Assembly." *The EMBO Journal* 35(13):1465–82. doi: 10.15252/embj.201694105.

Ai, Xi, and Mark R. Parthun. 2004. "The Nuclear Hat1p/Hat2p Complex: A Molecular Link between Type B Histone Acetyltransferases and Chromatin Assembly." *Molecular Cell* 14:195–205. 14(2):195-205. doi: 10.1016/s1097-2765(04)00184-4.

Alabert, Constance, Jimi Carlo Bukowski-Wills, Sung Bau Lee, Georg Kustatscher, Kyosuke Nakamura, Flavia De Lima Alves, Patrice Menard, Jakob Mejlvang, Juri Rappsilber, and Anja Groth. 2014. "Nascent Chromatin Capture Proteomics Determines Chromatin Dynamics during DNA Replication and Identifies Unknown Fork Components." *Nature Cell Biology* 16(3):281–91. doi: 10.1038/ncb2918.

Albig, Werner, Petra Kioschis, Annemarie Poustka, Konstanze Meergans, and Detlef Doenecke. 1997. "Human Histone Gene Organization: Nonregular Arrangement within a Large Cluster." *Im Neuenheimer Feld* 40(2):314-22. doi: 10.1006/geno.1996.4592.

Alekseev, Oleg M., David C. Bencic, Richard T. Richardson, Esther E. Widgren, and Michael G. O'Rand. 2002. "Overexpression of the Linker Histone-Binding Protein tNASP Affects Progression through the Cell Cycle." *Journal of Biological Chemistry* 278(10):8846–52. doi: 10.1074/jbc.M210352200.

Alekseev, Oleg M., Richard T. Richardson, James K. Tsuruta, and Michael G. O'Rand. 2011. "Depletion of the Histone Chaperone tNASP Inhibits Proliferation and Induces Apoptosis in Prostate Cancer PC-3 Cells." *Reproductive Biology and Endocrinology* 9. doi: 10.1186/1477-7827-9-50.

Alekseev, Oleg M., Esther E. Widgren, Richard T. Richardson, and Michael G. O'Rand. 2004. "Association of NASP with HSP90 in Mouse Spermatogenic Cells: Stimulation of ATPase Activity and Transport of Linker Histones into Nuclei." *Journal of Biological Chemistry* 280(4):2904–11. doi: 10.1074/jbc.M410397200.

Ali-Fehmi, Rouba, Madhumita Chatterjee, Alexei Ionan, Nancy K. Levin, Haitham Arabi, Sudeshna Bandyopadhyay, Jay P. Shah, Christopher S. Bryant, Stephen M. Hewitt, Michael G. O'Rand, Oleg M. Alekseev, Robert Morris, Adnan Munkarah, Judith Abrams, and Michael A. Tainsky. 2009. "Analysis of the Expression of Human Tumor Antigens in Ovarian Cancer Tissues." *Cancer Biomarkers* 6(1):33–48. doi: 10.3233/CBM-2009-0117.

Almouzni, Genevieve, and Alan P. Wolffe. 1993. “Replication-Coupled Chromatin Assembly Is Required for the Repression of Basal Transcription in Vivo.” *Genes & Development* 7(10):2033-47. doi: 10.1101/gad.7.10.2033.

Almouzni, Geneviève, and Alan P. Wolffe. 1995. “Constraints on Transcriptional Activator Function Contribute to Transcriptional Quiescence during Early Xenopus Embryogenesis.” *EMBO Journal* 14(8):1752–65. doi: 10.1002/j.1460-2075.1995.tb07164.x.

Alvarez, Francisca, Francisca Muñoz, Pierre Schilcher, Axel Imhof, Geneviève Almouzni, and Alejandra Loyola. 2011. “Sequential Establishment of Marks on Soluble Histones H3 and H4.” *Journal of Biological Chemistry* 286(20):17714–21. doi: 10.1074/jbc.M111.223453.

Alvarez, Vanesa, Susanne Bandau, Hao Jiang, Diana Rios-Szwed, Jens Hukelmann, Elisa Garcia-Wilson, Nicola Wiechens, Eva Griesser, Sara Ten Have, Tom Owen-Hughes, Angus Lamond, and Constance Alabert. 2023. “Proteomic Profiling Reveals Distinct Phases to the Restoration of Chromatin Following DNA Replication.” *Cell Reports* 42(1). doi: 10.1016/j.celrep.2023.111996.

Amatori, Stefano, Simona Tavolaro, Stefano Gambardella, and Mirco Fanelli. 2021. “The Dark Side of Histones: Genomic Organization and Role of Oncohistones in Cancer.” *Clinical Epigenetics* 13(1):71. doi: 10.1186/s13148-021-01057-x.

Ambrosio, Linda, and Paul Schedl. 1985. “Two Discrete Modes of Histone Gene Expression during Oogenesis in *Drosophila Melanogaster*.” *Developmental Biology* 111:220–31. 220-31. doi: 10.1016/0012-1606(85)90447-6.

Amodeo, Amanda A., David Jukam, Aaron F. Straight, and Jan M. Skotheim. 2015. “Histone Titration against the Genome Sets the DNA-to-Cytoplasm Threshold for the Xenopus Midblastula Transition.” *Proceedings of the National Academy of Sciences of the United States of America* 112(10):E1086–95. doi: 10.1073/pnas.1413990112.

Andrews, Andrew J., Xu Chen, Alexander Zevin, Laurie A. Stargell, and Karolin Luger. 2010. “The Histone Chaperone Nap1 Promotes Nucleosome Assembly by Eliminating Nonnucleosomal Histone DNA Interactions.” *Molecular Cell* 37(6):834–42. doi: 10.1016/j.molcel.2010.01.037.

Apta-Smith, Michael James, Juan Ramon Hernandez-Fernaud, and Andrew James Bowman. 2018. “Evidence for the Nuclear Import of Histones H3.1 and H4 as Monomers.” *The EMBO Journal* 37(19). doi: 10.15252/embj.201798714.

Arents, Gina, and Evangelos N. Moudrianakis. 1993. “Topography of the Histone Octamer Surface: Repeating Structural Motifs Utilized in the Docking of Nucleosomal DNA.” *Proc. Natl. Acad. Sci. USA* 90(22):10489-93. doi: 10.1073/pnas.90.22.10489.

Armstrong, Claire, Victor J. Passanisi, Humza M. Ashraf, and Sabrina L. Spencer. 2023. “Cyclin E/CDK2 and Feedback from Soluble Histone Protein Regulate the S Phase Burst of Histone Biosynthesis.” *Cell Reports* 42(7). doi: 10.1016/j.celrep.2023.112768.

Armstrong, Claire, and Sabrina L. Spencer. 2021. “Replication-Dependent Histone Biosynthesis Is Coupled to Cell-Cycle Commitment.” *PNAS* doi: 10.1073/pnas.2100178118.

Au, Wei Chun, Matthew J. Crisp, Steven Z. DeLuca, Oliver J. Rando, and Munira A. Basrai. 2008. “Altered Dosage and Mislocalization of Histone H3 and Cse4p Lead to Chromosome Loss in *Saccharomyces Cerevisiae*.” *Genetics* 179(1):263–75. doi: 10.1534/genetics.108.088518.

Bannister, Andrew J., and Tony Kouzarides. 2011. “Regulation of Chromatin by Histone Modifications.” *Cell Research* 21(3):381-95. doi: 10.1038/cr.2011.22.

Bao, Hongyu, Massimo Carraro, Valentin Flury, Yanhong Liu, Min Luo, Liu Chen, Anja Groth, and Hongda Huang. 2022. “NASP Maintains Histone H3-H4 Homeostasis through Two Distinct H3 Binding Modes.” *Nucleic Acids Research* 50(9):5349–68. doi: 10.1093/nar/gkac303.

Barcaroli, D., L. Bongiorno-Borbone, A. Terrinoni, T. G. Hofmann, M. Rossi, R. A. Knight, A. G. Matera, G. Melino, and V. De Laurenzi. 2006. “FLASH Is Required for Histone Transcription and S-Phase Progression.” *PNAS* 103(40):14808-12 doi: 10.1073/pnas.0604227103.

Belotserkovskaya, Rimma, Sangtaek Oh, Vladimir A. Bondarenko, George Orphanides, Vasily M. Studitsky, and Danny Reinberg. 2003. “FACT Facilitates Transcription-Dependent Nucleosome Alteration.” *Science*. 301(5636):1090-3. doi: 10.1126/science.1085703.

Benson, Laura J., Yongli Gu, Tatyana Yakovleva, Kevin Tong, Courtney Barrows, Christine L. Strack, Richard G. Cook, Craig A. Mizzen, and Anthony T. Annunziato. 2006. “Modifications of H3 and H4 during Chromatin Replication, Nucleosome Assembly, and Histone Exchange.” *Journal of Biological Chemistry* 281(14):9287–96. doi: 10.1074/jbc.M512956200.

Berloco, Maria, Laura Fanti, Achim Breiling, Valerio Orlando, and Sergio Pimpinelli. 2001. “The Maternal Effect Gene, Abnormal Oocyte (Abo), of *Drosophila Melanogaster* Encodes a Specific Negative Regulator of Histones.” *PNAS* 98(21):12126-31. doi: 10.1073/pnas.211428798.

Blumenthal, B. A., J. H. Kriegstein, and S. D. Hogness. 1974. “The Units of DNA Replication in *Drosophila Melanogaster* Chromosomes.” *Cold Spring Harbor* 38:205-23. doi: 10.1101/sqb.1974.038.01.024.

Bonnefoy, Emilie, Guillermo A. Orsi, Pierre Couble, and Benjamin Loppin. 2007a. “The Essential Role of Drosophila HIRA for de Novo Assembly of Paternal Chromatin at Fertilization.” *PLoS Genetics* 3(10):1991–2006. doi: 10.1371/journal.pgen.0030182.

Bonner, W. M., Roy S. Wu, H. T. Panusz, and C. Muneses. 1988. “Kinetics of Accumulation and Depletion of Soluble Newly Synthesized Histone in the Reciprocal Regulation of Histone and DNA Synthesis.” *Biochemistry* 27(17):6542-50. doi: 10.1021/bi00417a052.

Bosch, Justin A., Gabriel Birchak, and Norbert Perrimon. 2021. “Precise Genome Engineering in Drosophila Using Prime Editing.” *PNAS* 118. doi: 10.1073/pnas.2021996118/-/DCSupplemental.

Bowman, Andrew, Akiko Koide, Jay S. Goodman, Meaghan E. Colling, Daria Zinne, Shohei Koide, and Andreas G. Ladurner. 2016. “sNASP and ASF1A Function through Both Competitive and Compatible Modes of Histone Binding.” *Nucleic Acids Research* 45(2):643–56. doi: 10.1093/nar/gkw892.

Bowman, Andrew, Lukas Lercher, Hari R. Singh, Daria Zinne, Gyula Timinszky, Teresa Carlomagno, and Andreas G. Ladurner. 2015. “The Histone Chaperone SNASP Binds a Conserved Peptide Motif within the Globular Core of Histone H3 through Its TPR Repeats.” *Nucleic Acids Research* 44(7):3105–17. doi: 10.1093/nar/gkv1372.

Brennan, Kaelan J., Melanie Weilert, Sabrina Krueger, Anusri Pampari, Hsiao yun Liu, Ally W. H. Yang, Jason A. Morrison, Timothy R. Hughes, Christine A. Rushlow, Anshul Kundaje, and Julia Zeitlinger. 2023. “Chromatin Accessibility in the Drosophila Embryo Is Determined by Transcription Factor Pioneering and Enhancer Activation.” *Developmental Cell* 58(19):1898-1916.e9. doi: 10.1016/j.devcel.2023.07.007.

Brown, Donald D., Pieter C. Wensink, and Eddie Jordan. 1971. “Purification and Some Characteristics of 5S DNA from *Xenopus Laevis*” *PNAS* 68(12):3175-9. doi: 10.1073/pnas.68.12.3175.

Cakmakci, Nihal G., Rachel S. Lerner, Eric J. Wagner, Lianxing Zheng, and William F. Marzluff. 2008. “SLIP1, a Factor Required for Activation of Histone mRNA Translation by the Stem-Loop Binding Protein.” *Molecular and Cellular Biology* 28(3):1182–94. doi: 10.1128/mcb.01500-07.

Camerini-Otero, Rafael D., Barbara Sollner-Webb, and Gary Felsenfeld. 1976. “The Organization of Histones and DNA in Chromatin: Evidence for an Arginine-Rich Histone Kernel.” *Cell* 8:333–47.

Campos, Eric I., Jeffrey Fillingham, Guohong Li, Haiyan Zheng, Philipp Voigt, Wei Hung W. Kuo, Harshika Seepany, Zhonghua Gao, Loren A. Day, Jack F. Greenblatt, and Danny Reinberg. 2010. “The Program for Processing Newly Synthesized Histones

H3.1 and H4." *Nature Structural and Molecular Biology* 17(11):1343–51. doi: 10.1038/nsmb.1911.

Campos, Eric I., Arne H. Smits, Young Hoon Kang, Sébastien Landry, Thelma M. Escobar, Shruti Nayak, Beatrix M. Ueberheide, Daniel Durocher, Michiel Vermeulen, Jerard Hurwitz, and Danny Reinberg. 2015. "Analysis of the Histone H3.1 Interactome: A Suitable Chaperone for the Right Event." *Molecular Cell* 60(4):697–709. doi: 10.1016/j.molcel.2015.08.005.

Celona, Barbara, Assaf Weiner, Francesca Di Felice, Francesco M. Mancuso, Elisa Cesarini, Riccardo L. Rossi, Lorna Gregory, Dilair Baban, Grazisa Rossetti, Paolo Grianti, Massimiliano Pagani, Tiziana Bonaldi, Jiannis Ragoussis, Nir Friedman, Giorgio Camilloni, Marco E. Bianchi, and Alessandra Agresti. 2011. "Substantial Histone Reduction Modulates Genomewide Nucleosomal Occupancy and Global Transcriptional Output." *PLoS Biology* 9(6). doi: 10.1371/journal.pbio.1001086.

Chari, Sudarshan, Henry Wilky, Jayalakshmi Govindan, and Amanda A. Amodeo. 2019. "Histone Concentration Regulates the Cell Cycle and Transcription in Early Development." *Development (Cambridge)* 146(19). doi: 10.1242/dev.177402.

Chen, Hui, Lily C. Einstein, Shawn C. Little, and Matthew C. Good. 2019. "Spatiotemporal Patterning of Zygotic Genome Activation in a Model Vertebrate Embryo." *Developmental Cell* 49(6):852-866.e7. doi: 10.1016/j.devcel.2019.05.036.

Chen, Ming Zhen, Shao An Wang, Shih Chang Hsu, Kleiton Augusto Santos Silva, and Feng Ming Yang. 2022. "Home Dust Mites Promote MUC5AC Hyper-Expression by Modulating the SNASP/TRAF6 Axis in the Airway Epithelium." *International Journal of Molecular Sciences* 23(16). doi: 10.3390/ijms23169405.

Claycomb, Julie M., David M. MacAlpine, James G. Evans, Stephen P. Bell, and Terry L. Orr-Weaver. 2002. "Visualization of Replication Initiation and Elongation in Drosophila." *Journal of Cell Biology* 159(2):225–36. doi: 10.1083/jcb.200207046.

Cook, Adam J. L., Zachary A. Gurard-Levin, Isabelle Vassias, and Geneviève Almouzni. 2011. "A Specific Function for the Histone Chaperone NASP to Fine-Tune a Reservoir of Soluble H3-H4 in the Histone Supply Chain." *Molecular Cell* 44(6):918–27. doi: 10.1016/j.molcel.2011.11.021.

Deneke, Victoria E., Anna Melbinger, Massimo Vergassola, and Stefano Di Talia. 2016. "Waves of Cdk1 Activity in S Phase Synchronize the Cell Cycle in Drosophila Embryos." *Developmental Cell* 38(4):399–412. doi: 10.1016/j.devcel.2016.07.023.

Dilworth, Stephen M., Susan J. Black, and Ronald A. Laskey. 1987. "Two Complexes That Contain Histones Are Required for Nucleosome Assembly In Vitro: Role of Nucleoplasmin and Nl in Xenopus Egg Extracts." *Cell* 51(6):1009-18. doi: 10.1016/0092-8674(87)90587-3.

Dominski, Zbigniew, Xiao Cui Yang, and William F. Marzluff. 2005. “The Polyadenylation Factor CPSF-73 Is Involved in Histone-Pre-mRNA Processing.” *Cell* 123(1):37–48. doi: 10.1016/j.cell.2005.08.002.

Dunleavy, Elaine M., Alison L. Pidoux, Marie Monet, Carolina Bonilla, William Richardson, Georgina L. Hamilton, Karl Ekwall, Paul J. McLaughlin, and Robin C. Allshire. 2007. “A NASP (N1/N2)-Related Protein, Sim3, Binds CENP-A and Is Required for Its Deposition at Fission Yeast Centromeres.” *Molecular Cell* 28(6):1029–44. doi: 10.1016/j.molcel.2007.10.010.

Dunphy, William G., and Akiko Kumagai. 1991. “The Cdc25 Protein Contains an Intrinsic Phosphatase Activity.” *Cell* 67(1):189-96. doi: 10.1016/0092-8674(91)90582-j.

Duronio, Robert J., and William F. Marzluff. 2017. “Coordinating Cell Cycle-Regulated Histone Gene Expression through Assembly and Function of the Histone Locus Body.” *RNA Biology* 14(6):726–38.

Edgar, Bruce A., and Patrick H. D. 1989. “Genetic Control of Cell Division Patterns in the Drosophila Embryo.” *Cell* 57(1):177-87. doi: 10.1016/0092-8674(89)90183-9.

Edgar, Bruce A., and Patrick H. G. 1990. “The Three Postblastoderm Cell Cycles of *Drosophila Embryogenesis* Are Regulated in G2 by String.” *Cell* 62(3):469-80. doi: 10.1016/0092-8674(90)90012-4.

Edgar, Bruce A., Caroline P. Kiehle, and Gerold Schubigert. 1966. “Cell Cycle Control by the Nucleo-Cytoplasmic Ratio in Early Drosophila Development.” *Cell* 44(2):365-72. doi: 10.1016/0092-8674(86)90771-3.

Edgar, Bruce A., and Gerold Schubigert. 1986. “Parameters Controlling Transcriptional Activation during Early Drosophila Development.” *Cell* 44(6):871-7. doi: 10.1016/0092-8674(86)90009-7.

Edgar, Bruce A., Frank Sprenger, Robert J. Duronio, Pierre Leopold, and Patrick H. O. 1994. “Distinct Molecular Mechanisms Regulate Cell Cycle Timing at Successive Stages of *Drosophila Embryogenesis*.” *Genes & Development* 8(4):440-52. doi: 10.1101/gad.8.4.440.

Elsässer, Simon J., Hongda Huang, Peter W. Lewis, Jason W. Chin, C. David Allis, and Dinshaw J. Patel. 2012. “DAXX Envelops a Histone H3.3-H4 Dimer for H3.3-Specific Recognition.” *Nature* 491(7425):560–65. doi: 10.1038/nature11608.

Erkmann, Judith A., Ricardo Sànchez, Nathalie Treichel, William F. Marzluff, and Ulrike Kutay. 2005. “Nuclear Export of Metazoan Replication-Dependent Histone MRNAs Is Dependent on RNA Length and Is Mediated by TAP.” *RNA* 11(1):45–58. doi: 10.1261/rna.7189205.

Farrell, Jeffrey A., and Patrick H. O'Farrell. 2014. "From Egg to Gastrula: How the Cell Cycle Is Remodeled during the Drosophila Mid-Blastula Transition." *Annual Review of Genetics* 48:269–94. doi: 10.1146/annurev-genet-111212-133531.

Finn, Ron M., Kristen Browne, Kim C. Hodgson, and Juan Ausió. 2008. "sNASP, a Histone H1-Specific Eukaryotic Chaperone Dimer That Facilitates Chromatin Assembly." *Biophysical Journal* 95(3):1314–25. doi: 10.1529/biophysj.108.130021.

Foe, Victoria E., and Bruce M. Alberts. 1983. "Studies of nuclear and cytoplasmic behavior during the five mitotic cycles that precede gastrulation in Drosophila Melanogaster" *J. Cell Sci* 61:31-70. doi: 10.1242/jcs.61.1.31.

Fogarty, Patrick, D. Shelagh Campbell, Robin Abu-Shumays, Brigitte de Saint Phalle, R. Kristina Yu, L. Geoffrey Uy, L. Michael Goldberg, and William Sullivan. 1997. "The Drosophila *Grapes* Gene Is Related to Checkpoint Gene Chk1/Rad27 and Is Required for Late Synctial Division Fidelity." *Reseach Paper* 7(6):418–26.

Foltz, Daniel R., Lars E. T. Jansen, Ben E. Black, Aaron O. Bailey, John R. Yates, and Don W. Cleveland. 2006. "The Human CENP-A Centromeric Nucleosome-Associated Complex." *Nature Cell Biology* 8(5):458–69. doi: 10.1038/ncb1397.

Fonslow, Bryan R., Sherry M. Niessen, Meha Singh, Catherine C. L. Wong, Tao Xu, Paulo C. Carvalho, Jeong Choi, Sung Kyu Park, and John R. Yates. 2012. "Single-Step Inline Hydroxyapatite Enrichment Facilitates Identification and Quantitation of Phosphopeptides from Mass-Limited Proteomes with MudPIT." *Journal of Proteome Research* 11(5):2697–2709. doi: 10.1021/pr300200x.

Gallie, Daniel R., Nancy J. Lewis, and William F. Marzluff. 1996. "The Histone 3′-Terminal Stem-Loop Is Necessary for Translation in Chinese Hamster Ovary Cells." *Nucleic Acids Res* 24(10):1954-62. doi: 10.1093/nar/24.10.1954.

Le Goff, Samuel, Burcu Nur Keçeli, Hana Jeřábková, Stefan Heckmann, Twan Rutten, Sylviane Cotterell, Veit Schubert, Elisabeth Roitinger, Karl Mechtler, F. Christopher H. Franklin, Christophe Tatout, Andreas Houben, Danny Geelen, Aline V. Probst, and Inna Lermontova. 2020. "The H3 Histone Chaperone NASP^{SIM3} Escorts CenH3 in Arabidopsis." *Plant Journal* 101(1):71–86. doi: 10.1111/tpj.14518.

Gorgoni, Barbara, Stuart Andrews, André Schaller, Daniel Schümperli, Nicola K. Gray, and Berndt Müller. 2005. "The Stem-Loop Binding Protein Stimulates Histone Translation at an Early Step in the Initiation Pathway." *RNA* 11(7):1030–42. doi: 10.1261/rna.7281305.

Gould, Kathleen L., and Paul Nurse. 1989. "Tyrosine Phosphorylation of the Fission Yeast Cdc2+ Protein Kinase Regulates Entry into Mitosis." *Nature* 342(6245):39-45. doi: 10.1038/342039a0.

Gratz, Scott J., C. Dustin Rubinstein, Melissa M. Harrison, Jill Wildonger, and Kate M. O'Connor-Giles. 2015. "CRISPR-Cas9 Genome Editing in Drosophila." *Current*

Protocols in Molecular Biology 2015:31.2.1-31.2.20. doi: 10.1002/0471142727.mb3102s111.

Grote, Phillip, and Barbara Conradt. 2006. “The PLZF-like Protein TRA-4 Cooperates with the Gli-like Transcription Factor TRA-1 to Promote Female Development in *C. Elegans*.” *Developmental Cell* 11(4):561–73. doi: 10.1016/j.devcel.2006.07.015.

Günesdogan, Ufuk, Herbert Jäckle, and Alf Herzig. 2010. “A Genetic System to Assess in Vivo the Functions of Histones and Histone Modifications in Higher Eukaryotes.” *EMBO Reports* 11(10):772–76. doi: 10.1038/embor.2010.124.

Gunjan, Akash, Johanna Paik, and Alain Verreault. 2006. “The Emergence of Regulated Histone Proteolysis.” *Current Opinion in Genetics and Development* 16(2):112-8. doi: 10.1016/j.gde.2006.02.010.

Gunjan, Akash, and Alain Verreault. 2003. “A Rad53 Kinase-Dependent Surveillance Mechanism That Regulates Histone Protein Levels in *S. Cerevisiae*.” *Cell* 115(5):537-49. doi: 10.1016/s0092-8674(03)00896-1.

Gurard-Levin, Zachary A., Jean Pierre Quivy, and Genevieve Almouzni. 2014. “Histone Chaperones: Assisting Histone Traffic and Nucleosome Dynamics.” *Annual Review of Biochemistry* 83:487-517. doi: 10.1146/annurev-biochem-060713-035536.

Hammond, Colin M., Caroline B. Strømme, Hongda Huang, Dinshaw J. Patel, and Anja Groth. 2017. “Histone Chaperone Networks Shaping Chromatin Function.” *Nature Reviews Molecular Cell Biology* 18(3):141-158. doi: 10.1038/nrm.2016.159.

Han, Dongsheng, Scott Churcher, and Jared T. Nordman. 2023. “PCR Cloning Intermediated Gibson Assembly (PIG) for Constructing DNA Repair Templates in CRISPR-Cas9 Based Gene Editing.” *MicroPublication Biology*. 10.17912/micropub.biology.000916. doi: 10.17912/micropub.biology.000916

Van Der Heijden, Godfried W., Jürgen W. Dieker, Alwin A. H. A. Derijck, Sylviane Muller, Jo H. M. Berden, Didi D. M. Braat, Johan Van Der Vlag, and Peter De Boer. 2005. “Asymmetry in Histone H3 Variants and Lysine Methylation between Paternal and Maternal Chromatin of the Early Mouse Zygote.” *Mechanisms of Development* 122(9):1008–22. doi: 10.1016/j.mod.2005.04.009.

Herrero, Ana B., and Sergio Moreno. 2011a. “Lsm1 Promotes Genomic Stability by Controlling Histone mRNA Decay.” *EMBO Journal* 30(10):2008–18. doi: 10.1038/emboj.2011.117.

Hogan, Ann K., Kizhakke M. Sathyan, Alexander B. Willis, Sakshi Khurana, Shashank Srivastava, Ewelina Zasadzińska, Alexander S. Lee, Aaron O. Bailey, Matthew N. Gaynes, Jiehuan Huang, Justin Bodner, Celeste D. Rosencrance, Kelvin A. Wong, Marc A. Morgan, Kyle P. Eagen, Ali Shilatifard, and Daniel R. Foltz. 2021. “UBR7 Acts as a Histone Chaperone for Post-nucleosomal Histone H3.” *The EMBO Journal* 40(24). doi: 10.15252/embj.2021108307.

Honorato, Rodrigo V., Panagiotis I. Koukos, Brian Jiménez-García, Andrei Tsaregorodtsev, Marco Verlato, Andrea Giachetti, Antonio Rosato, and Alexandre M. J. J. Bonvin. 2021. “Structural Biology in the Clouds: The WeNMR-EOSC Ecosystem.” *Frontiers in Molecular Biosciences* 8. doi: 10.3389/fmolb.2021.729513.

Horard, Béatrice, and Benjamin Loppin. 2015. “Histone Storage and Deposition in the Early Drosophila Embryo.” *Chromosoma* 124(2):163-75. doi: 10.1007/s00412-014-0504-7.

Horard, Béatrice, Laure Sapey-Triomphe, Emilie Bonnefoy, and Benjamin Loppin. 2018. “ASF1 Is Required to Load Histones on the HIRA Complex in Preparation of Paternal Chromatin Assembly at Fertilization.” *Epigenetics and Chromatin* 11(1). doi: 10.1186/s13072-018-0189-x.

Horner, Vanessa L., and Mariana F. Wolfner. 2008. “Transitioning from Egg to Embryo: Triggers and Mechanisms of Egg Activation.” *Developmental Dynamics* 237(3):527-44. doi: 10.1002/dvdy.21454.

Huang, Yingqun, Renata Gattoni, James Sté, and Joan A. Steitz. 2003. “Splicing Factors Serve as Adapter Proteins for TAP-Dependent mRNA Export.” *Molecular Cell* 11(3):837-43. doi: 10.1016/s1097-2765(03)00089-3.

Huang, Yingqun, and Joan A. Steitz. 2001. “Splicing Factors SRp20 and 9G8 Promote the Nucleocytoplasmic Export of mRNA.” *Molecular Cell* 7(4):899-905. doi: 10.1016/s1097-2765(01)00233-7.

Ito, Takashi, Michael Bulger, Ryuji Kobayashi, and James T. Kasonaga. 1996. “Drosophila NAP-1 Is a Core Histone Chaperone That Functions in ATP-Facilitated Assembly of Regularly Spaced Nucleosomal Array.” *Molecular and Cellular Biology* 16(6):3112-24. doi: 10.1128/MCB.16.6.3112.

Ji, Xiong, Daniel B. Dadon, Brian J. Abraham, Tong Ihn Lee, Rudolf Jaenisch, James E. Bradner, and Richard A. Young. 2015. “Chromatin Proteomic Profiling Reveals Novel Proteins Associated with Histone-Marked Genomic Regions.” *Proceedings of the National Academy of Sciences of the United States of America* 112(12):3841–46. doi: 10.1073/pnas.1502971112.

Jiménez-García, Brian, João M. C. Teixeira, Mikael Trellet, João P. G. L. M. Rodrigues, and Alexandre M. J. J. Bonvin. 2021. “PDB-Tools Web: A User-Friendly Interface for the Manipulation of PDB Files.” *Proteins: Structure, Function and Bioinformatics* 89(3):330–35. doi: 10.1002/prot.26018.

Joseph, Shai R., Má té Pá lfy, Lennart Hilbert, Mukesh Kumar, Jens Karschau, Vasily Zaburdaev, Andrej Shevchenko, and Nadine L. Vastenhouw. 2017. “Competition between Histone and Transcription Factor Binding Regulates the Onset of Transcription in Zebrafish Embryos.” *ELife* 6. doi: 10.7554/eLife.23326.001.

Kane, A. Donald, and B. Charles Kimmel. 1993. “The Zebrafish Midblastula Transition.” *Development* 119(2):447-56. doi: 10.1242/dev.119.2.447.

Kang, Xuan, Yun Feng, Zhixue Gan, Shiyang Zeng, Xiaobo Guo, Xirui Chen, Ye Zhang, Chen Wang, Kuinan Liu, Xuelin Chen, Xiaoxue Jiang, Shuting Song, Yabin Li, Su Chen, Feng Sun, Zhiyong Mao, Xiaomei Yang, and Jianfeng Chang. 2018. “NASP Antagonize Chromatin Accessibility through Maintaining Histone H3K9me1 in Hepatocellular Carcinoma.” *Biochimica et Biophysica Acta - Molecular Basis of Disease* 1864(10):3438–48. doi: 10.1016/j.bbadis.2018.07.033.

Kato, Daiki, Akihisa Osakabe, Hiroaki Tachiwana, Hiroki Tanaka, and Hitoshi Kurumizaka. 2015. “Human tNASP Promotes in Vitro Nucleosome Assembly with Histone H3.3.” *Biochemistry* 54(5):1171–79. doi: 10.1021/bi501307g.

Khorasanizadeh, Sepideh. 2004. “The Nucleosome: From Genomic Organization to Genomic Regulation.” *Cell* 116:259–72.

King, Robert C. 1970. “The Meiotic Behavior of the Drosophila Oocyte.” *International Review of Cytology* 28(C):125–68. doi: 10.1016/S0074-7696(08)62542-5.

Kleiner, Ralph E., Lisa E. Hang, Kelly R. Molloy, Brian T. Chait, and Tarun M. Kapoor. 2018. “A Chemical Proteomics Approach to Reveal Direct Protein-Protein Interactions in Living Cells.” *Cell Chemical Biology* 25(1):110-120.e3. doi: 10.1016/j.chembiol.2017.10.001.

Kleinschmidt, J. A., C. Dingwall, G. Maier, and W. W. Franke. 1986. “Molecular Characterization of a Karyophilic, Histone-Binding Protein: CDNA Cloning, Amino Acid Sequence and Expression of Nuclear Protein N1/N2 of *Xenopus Laevis*.” *The EMBO Journal* 5(13):3547–52. doi: 10.1002/j.1460-2075.1986.tb04681.x.

Kleinschmidt, J. A., and A. Seiter. 1988. “Identification of Domains Involved in Nuclear Uptake and Histone Binding of Protein N1 of *Xenopus Laevis*.” *The EMBO Journal* 7(6):1605–14. doi: 10.1002/j.1460-2075.1988.tb02986.x.

Kleinschmidt, Juergen A., Elke Fortkamp, Georg Krohne, Hanswalter Zentgraf, and Werner W. Frankes. 1984. “Co-Existence of Two Different Types of Soluble Histone Complexes in Nuclei of *Xenopus Laevis* Oocytes.” *Journal of Biological Chemistry* 260(2):1166–76.

Kleinschmidt, Juergen A., and Werner W. Franke. 1982. “Soluble Acidic Complexes Containing Histones H3 and H4 in Nuclei of *Xenopus Laevis* Oocytes.” *Cell* 29:799–809 doi: 10.1016/0092-8674(82)90442-1.

Kong, Fanyong, Lianhe Li, Chaoshan Wang, Qiang Zhang, and Shizhi He. 2020. “MiR-381-3p Suppresses Biological Characteristics of Cancer in Head-Neck Squamous Cell Carcinoma Cells by Targeting Nuclear Autoantigenic Sperm Protein (NASP).” *Bioscience, Biotechnology and Biochemistry* 84(4):703–13. doi: 10.1080/09168451.2019.1697195.

Kornberg, Roger D. 1974. “Chromatin Structure: A Repeating Unit of Histones and DNA.” *Science* 184(4139):868–71 doi: 10.1126/science.184.4139.868.

Kornberg, Roger D., and Yahli Lorch. 2020. “Primary Role of the Nucleosome.” *Molecular Cell* 79(3):371–75 doi: 10.1016/j.molcel.2020.07.020.

Koseoglu, M. Murat, Lee M. Graves, and William F. Marzluff. 2008. “Phosphorylation of Threonine 61 by Cyclin A/Cdk1 Triggers Degradation of Stem-Loop Binding Protein at the End of S-Phase.” *Molecular and Cellular Biology* 28(14):4469–79. doi: 10.1128/mcb.01416-07.

Kotadia, Shaila, Justin Crest, Uyen Tram, Blake Riggs, and William Sullivan. 2010. “ Blastoderm Formation and Cellularisation in *Drosophila Melanogaster* .” in *Encyclopedia of Life Sciences*. Wiley.

Lambert, Jean Philippe, Monika Tucholska, Christopher Go, James D. R. Knight, and Anne Claude Gingras. 2015. “Proximity Biotinylation and Affinity Purification Are Complementary Approaches for the Interactome Mapping of Chromatin-Associated Protein Complexes.” *Journal of Proteomics* 118:81–94. doi: 10.1016/j.jprot.2014.09.011.

Latrick, Chrysa M., Martin Marek, Khalid Ouararhni, Christophe Papin, Isabelle Stoll, Maria Ignatyeva, Arnaud Obri, Eric Ennifar, Stefan Dimitrov, Christophe Romier, and Ali Hamiche. 2016. “Molecular Basis and Specificity of H2A.Z-H2B Recognition and Deposition by the Histone Chaperone YL1.” *Nature Structural and Molecular Biology* 23(4):309–16. doi: 10.1038/nsmb.3189.

Lee, So Young, Juanma Ramirez, Maribel Franco, Benoît Lectez, Monika Gonzalez, Rosa Barrio, and Ugo Mayor. 2014. “Ube3a, the E3 Ubiquitin Ligase Causing Angelman Syndrome and Linked to Autism, Regulates Protein Homeostasis through the Proteasomal Shuttle Rpn10.” *Cellular and Molecular Life Sciences* 71(14):2747–58. doi: 10.1007/s00018-013-1526-7.

Lefevre, G., and U. B. Jonsson. 1962. “Sperm Transfer, Storage, Displacement, and Utilization in *Drosophila Melanogaster*” *Genetics* 1719–36 doi: 10.1093/genetics/47.12.1719.

Li, Zhihuan, Matthew R. Johnson, Zhonghe Ke, Lili Chen, and Michael A. Welte. 2014. “Drosophila Lipid Droplets Buffer the H2av Supply to Protect Early Embryonic Development.” *Current Biology* 24(13):1485–91. doi: 10.1016/j.cub.2014.05.022.

Li, Zhihuan, Katharina Thiel, Peter J. Thul, Mathias Beller, Ronald P. Kühnlein, and Michael A. Welte. 2012. “Lipid Droplets Control the Maternal Histone Supply of Drosophila Embryos.” *Current Biology* 22(22):2104–13. doi: 10.1016/j.cub.2012.09.018.

Liang, Xiaoping, Shan Shan, Lu Pan, Jicheng Zhao, Anand Ranjan, Feng Wang, Zhuqiang Zhang, Yingzi Huang, Hanqiao Feng, Debbie Wei, Li Huang, Xuehui Liu,

Qiang Zhong, Jizhong Lou, Guohong Li, Carl Wu, and Zheng Zhou. 2016. “Structural Basis of H2A.Z Recognition by SRCAP Chromatin-Remodeling Subunit YL1.” *Nature Structural and Molecular Biology* 23(4):317–23. doi: 10.1038/nsmb.3190.

Lifton, R. P., M. L. Goldberg, W. R. Karp, and S. D. Hogness. 1978. “The Organization of the Histone Genes in Drosophila Melanogaster: Functional and Evolutionary Implications.” *Cold Spring Harbor* 42:1047–51 doi: 10.1101/sqb.1978.042.01.105.

Lin, Chih Jen, Fong Ming Koh, Priscilla Wong, Marco Conti, and Miguel Ramalho-Santos. 2014. “Hira-Mediated H3.3 Incorporation Is Required for DNA Replication and Ribosomal RNA Transcription in the Mouse Zygote.” *Developmental Cell* 30(3):268–79. doi: 10.1016/j.devcel.2014.06.022.

Lin, Haifan, and Allan C. Spradling. 1993. “Germline Stem Cell Division and Egg Chamber Development in Transplanted Drosophila Germaria.” *Developmental Biology* 140–52 doi: 10.1006/dbio.1993.1228.

Liu, Chao Pei, Wenxing Jin, Jie Hu, Mingzhu Wang, Jingjing Chen, Guohong Li, and Rui Ming Xu. 2021. “Distinct Histone H3-H4 Binding Modes of sNASP Reveal the Basis for Cooperation and Competition of Histone Chaperones.” *Genes and Development* 35(23–24):1610–24. doi: 10.1101/gad.349100.121.

Loppin, Benjamin, Frédéric Berger, and Pierre Couble. 2001. “The Drosophila Maternal Gene *Sésame* Is Required for Sperm Chromatin Remodeling at Fertilization.” *Chromosoma* 110(6):430–40. doi: 10.1007/s004120100161.

Loppin, Benjamin, Mylène Docquier, Francçois Bonneton, and Pierre Couble. 2000. “The Maternal Effect Mutation Sesame Affects the Formation of the Male Pronucleus in *Drosophila Melanogaster.” Developmental Biology* 222(2):392–404. doi: 10.1006/dbio.2000.9718.

Loppin, Benjamin, Raphaëlle Dubruille, and Béatrice Horard. 2015. “The Intimate Genetics of Drosophila Fertilization.” *Open Biology* 5(8):150076. doi: 10.1098/rsob.150076.

Loyola, Alejandra, Tiziana Bonaldi, Danièle Roche, Axel Imhof, and Geneviève Almouzni. 2006. “PTMs on H3 Variants before Chromatin Assembly Potentiate Their Final Epigenetic State.” *Molecular Cell* 24(2):309–16. doi: 10.1016/j.molcel.2006.08.019.

Luger, Karolin, Armin W. Mä Der, Robin K. Richmond, David F. Sargent, and Timothy J. Richmond. 1997. “Crystal Structure of the Nucleosome Core Particle at 2.8 A ˚ Resolution.” *Nature 389(6648):251-60. doi: 10.1038/38444.*

Luk, Ed, Ngoc Diep Vu, Kem Patteson, Gaku Mizuguchi, Wei Hua Wu, Anand Ranjan, Jonathon Backus, Subhojit Sen, Marc Lewis, Yawen Bai, and Carl Wu. 2007.

"Chz1, a Nuclear Chaperone for Histone H2AZ." *Molecular Cell* 25(3):357–68. doi: 10.1016/j.molcel.2006.12.015.

Ma, Tianlin, Brian A. Van Tine, Yue Wei, Michelle D. Garrett, David Nelson, Peter D. Adams, Jin Wang, Jun Qin, Louise T. Chow, and J. Wade Harper. 2000. "Cell Cycle-Regulated Phosphorylation of P220(NPAT) by Cyclin E/Cdk2 in Cajal Bodies Promotes Histone Gene Transcription." *Genes and Development* 14(18):2298–2313. doi: 10.1101/gad.829500.

Ma, Wubin, Shengsong Xie, Minjie Ni, Xingxu Huang, Shuanggang Hu, Qiang Liu, Aihua Liu, Jinsong Zhang, and Yonglian Zhang. 2012. "MicroRNA-29a Inhibited Epididymal Epithelial Cell Proliferation by Targeting Nuclear Autoantigenic Sperm Protein (NASP)." *Journal of Biological Chemistry* 287(13):10189–99. doi: 10.1074/jbc.M111.303636.

MacAlpine, Heather K., Raluca Gordân, Sara K. Powell, Alexander J. Hartemink, and David M. MacAlpine. 2010. "Drosophila ORC Localizes to Open Chromatin and Marks Sites of Cohesin Complex Loading." *Genome Research* 20(2):201–11. doi: 10.1101/gr.097873.109.

Maksimov, Vladimir, Miyuki Nakamura, Thomas Wildhaber, Paolo Nanni, Margareta Ramström, Jonas Bergquist, and Lars Hennig. 2016. "The H3 Chaperone Function of NASP Is Conserved in Arabidopsis." *Plant Journal* 88(3):425–36. doi: 10.1111/tpj.13263.

Mandel, C. R., Y. Bai, and L. Tong. 2008. "Protein Factors in Pre-MRNA 3′-End Processing." *Cellular and Molecular Life Sciences* 65(7-8):1099-122. doi: 10.1007/s00018-007-7474-3.

Mandel, Corey R., Syuzo Kaneko, Hailong Zhang, Damara Gebauer, Vasupradha Vethantham, James L. Manley, and Liang Tong. 2006. "Polyadenylation Factor CPSF-73 Is the Pre-mRNA 3′-End-Processing Endonuclease." *Nature* 444(7121):953–56. doi: 10.1038/nature05363.

Marzluff, William F., Preetam Gongidi, Keith R. Woods, Jianping Jin, and Lois J. Maltais. 2002. "The Human and Mouse Replication-Dependent Histone Genes." *Genomics* 80(5):487–98. doi: 10.1006/geno.2002.6850.

Marzluff, William F., Eric J. Wagner, and Robert J. Duronio. 2008. "Metabolism and Regulation of Canonical Histone MRNAs: Life without a Poly(A) Tail." *Nature Reviews Genetics* 9(11):843-54. doi: 10.1038/nrg2438.

Maślikowski, Bart M., Benjamin D. Néel, Ying Wu, Lizhen Wang, Natalie A. Rodrigues, Germain Gillet, and Pierre-André Bédard. 2010. "Cellular Processes of V-Src Transformation Revealed by Gene Profiling of Primary Cells-Implications for Human Cancer." *BMC Cancer* 10:41. doi: 10.1186/1471-2407-10-41.

McCleland, Mark L., Antony W. Shermoen, and Patrick H. O'Farrell. 2009. "DNA Replication Times the Cell Cycle and Contributes to the Mid-Blastula Transition in Drosophila Embryos." *Journal of Cell Biology* 187(1):7–14. doi: 10.1083/jcb.200906191.

Meeks-Wagner, Douglas, and Leland H. Hartwell. 1966. "Normal Stoichiometry of Histone Dimer Sets Is Necessary for High Fidelity of Mitotic Chromosome Transmission." *Cell* 44(1):43-52. doi: 10.1016/0092-8674(86)90483-6.

Von Moeller, Holger, Rachel Lerner, Adele Ricciardi, Claire Basquin, William F. Marzluff, and Elena Conti. 2013. "Structural and Biochemical Studies of SLIP1-SLBP Identify DBP5 and EIF3g as SLIP1-Binding Proteins." *Nucleic Acids Research* 41(16):7960–71. doi: 10.1093/nar/gkt558.

Moshkin, Yuri M., Jennifer A. Armstrong, Robert K. Maeda, John W. Tamkun, Peter Verrijzer, James A. Kennison, and Francois Karch. 2002. "Histone Chaperone ASF1 Cooperates with the Brahma Chromatin-Remodelling Machinery." *Genes and Development* 16(20):2621–26. doi: 10.1101/gad.231202.

Moss, Bernard, Alan Gershowitz, Lee A. Weber, and Corrado Baglioni. 1977. "Histone MRNAs Contain Blocked and Methylated 5' Terminal Sequences but Lack Methylated Nucleosides at Internal Positions." 113-20. doi: 10.1016/0092-8674(77)90145-3.

Munden, Alexander, Madison T. Wright, Dongsheng Han, Reyhaneh Tirgar, Lars Plate, and Jared T. Nordman. 2022. "Identification of Replication Fork-Associated Proteins in Drosophila Embryos and Cultured Cells Using iPOND Coupled to Quantitative Mass Spectrometry." *Scientific Reports* 12(1). doi: 10.1038/s41598-022-10821-9.

Nabeel-Shah, Syed, Kanwal Ashraf, Ronald E. Pearlman, and Jeffrey Fillingham. 2014. "Molecular Evolution of NASP and Conserved Histone H3/H4 Transport Pathway." *BMC Evolutionary Biology* 14(1). doi: 10.1186/1471-2148-14-139.

Nagatomo, Hiroaki, Nanami Kohri, Hiroki Akizawa, Yumi Hoshino, Nobuhiko Yamauchi, Tomohiro Kono, Masashi Takahashi, and Manabu Kawahara. 2016. "Requirement for Nuclear Autoantigenic Sperm Protein mRNA Expression in Bovine Preimplantation Development." *Animal Science Journal* 87(3):457–61. doi: 10.1111/asj.12538.

Namboodiri, Haridasan V. M., Shuchismita Dutta, IIdko V. Akey, James F. Head, and Christopher W. Akey. 2003. "The Crystal Structure of Drosophila NLP-Core Provides Insight into Pentamer Formation and Histone Binding." *Structure* 175–86. 11(2):175-86. doi: 10.1016/s0969-2126(03)00007-8.

Nashun, Buhe, Peter W. S. Hill, Sebastien A. Smallwood, Gopuraja Dharmalingam, Rachel Amouroux, Stephen J. Clark, Vineet Sharma, Elodie Ndjetehe, Pawel Pelczar, Richard J. Festenstein, Gavin Kelsey, and Petra Hajkova. 2015.

"Continuous Histone Replacement by Hira Is Essential for Normal Transcriptional Regulation and De Novo DNA Methylation during Mouse Oogenesis." *Molecular Cell* 60(4):611–25. doi: 10.1016/j.molcel.2015.10.010.

Natsume, Ryo, Masamitsu Eitoku, Yusuke Akai, Norihiko Sano, Masami Horikoshi, and Toshiya Senda. 2007. "Structure and Function of the Histone Chaperone CIA/ASF1 Complexed with Histones H3 and H4." *Nature* 446(7133):338–41. doi: 10.1038/nature05613.

Newport, John, and Marc Kirschner. 1982. "A Major Developmental Transition in Early Xenopus Embryos: I. Characterization and Timing of Cellular Changes at the Midblastula Stage." *Cell* 30(3):675-86. doi: 10.1016/0092-8674(82)90272-0.

Noll, Markus, and Roger D. Kornberg. 1977. "Action of Micrococcal Nuclease on Chromatin and the Location of Histone H1." *J. Mol. Biol* 109(3):393-404. doi: 10.1016/s0022-2836(77)80019-3.

Oliver, Denis, Daryl Granner, and Roger Chalkley. 1974. "Identification of a Distinction between Cytoplasmic Histone Synthesis and Subsequent Histone Deposition within the Nucleus." *Biochemistry* 13(4):746-9. doi: 10.1021/bi00701a017.

Osakabe, Akihisa, Hiroaki Tachiwana, Takaaki Matsunaga, Tatsuya Shiga, Ryu Suke Nozawa, Chikashi Obuse, and Hitoshi Kurumizaka. 2010. "Nucleosome Formation Activity of Human Somatic Nuclear Autoantigenic Sperm Protein (sNASP)." *Journal of Biological Chemistry* 285(16):11913–21. doi: 10.1074/jbc.M109.083238.

Osley, M. A. 1991. "The Regulation of Histone Synthesis in the Cell Cycle." *Annu Rev Biochem* 60:827-61. doi: 10.1146/annurev.bi.60.070191.004143.

O'Sullivan, Roderick J., Stefan Kubicek, Stuart L. Schreiber, and Jan Karlseder. 2010. "Reduced Histone Biosynthesis and Chromatin Changes Arising from a Damage Signal at Telomeres." *Nature Structural and Molecular Biology* 17(10):1218–25. doi: 10.1038/nsmb.1897.

Pardal, Alonso J., Filipe Fernandes-Duarte, and Andrew J. Bowman. 2019. "The Histone Chaperoning Pathway: From Ribosome to Nucleosome." *Essays in Biochemistry* 63(1):29-43. doi: 10.1042/EBC20180055.

Pardal, Alonso Javier, and Andrew James Bowman. 2022. "A Specific Role for Importin-5 and NASP in the Import and Nuclear Hand-off of Monomeric H3." *ELife* 11. doi: 10.7554/eLife.81755.

Perreault, Sally D., Robert A. Wolff, and Barry R. Zirkin. 1934. "The Role of Disulfide Bond Reduction during Mammalian Sperm Nuclear Decondensation in Vivo." *Developmental Biology* 101(1):160-7. doi: 10.1016/0012-1606(84)90126-x.

Perry, Michael, Gerald H. Thomsen, and Robert G. Roeder. 1985. "Genomic Organization and Nucleotide Sequence of Two Distinct Histone Gene Clusters from

Xenopus Laevis Identification of Novel Conserved Upstream Sequence Elements." 185(3):479-99. doi: 10.1016/0022-2836(85)90065-8.

Pettitt, Jonathan, Catriona Crombie, Daniel Schümperli, and Berndt Müller. 2002. "The *Caenorhabditis Elegans* Histone Hairpin-Binding Protein Is Required for Core Histone Gene Expression and Is Essential for Embryonic and Postembryonic Cell Division." 115(Pt 4):857-66. doi: 10.1242/jcs.115.4.857.

Philpott, Anna, and Gregory H. Lenot. 1992. "Nucleoplasmin Remodels Sperm Chromatin in Xenopus Egg Extracts." 69(5):759-67. doi: 10.1016/0092-8674(92)90288-n

Prioleau, Marie-Noqlle, Janine Huet, Andre Sentenac, and Marcel Mechali'. 1994. "Competition between Chromatin and Transcription Complex Assembly Regulates Gene Expression during Early Development." *Cell* 77(3):439-49. doi: 10.1016/0092-8674(94)90158-9.

Quinlan, Margot E. 2016. "Cytoplasmic Streaming in the Drosophila Oocyte." *Annual Review of Cell and Developmental Biology* 32:173-195. doi: 10.1146/annurev-cellbio-111315-125416.

Quivy, Jean-Pierre, Paola Grandi, and Genevieve Almouzni. 2001. "Dimerization of the Largest Subunit of Chromatin Assembly Factor 1: Importance in Vitro and during Xenopus Early Development." *The EMBO Journal* 20(8):2015-27. doi: 10.1093/emboj/20.8.2015.

Rabinowitz, Morris. 1941. "Studies on the Cytology and Early Embryology of the Egg of *Drosophila Melanogaster*." *Journal of Morphology* 69(1):1–49. doi: 10.1002/jmor.1050690102.

Ramos, Isbaal, Jaime Martín-Benito, Ron Finn, Laura Bretaña, Kerman Aloria, Jesú S. M. Arizmendi, Juan Ausió, Arturo Muga, José M. Valpuesta, and Adelina Prado. 2010. "Nucleoplasmin Binds Histone H2A-H2B Dimers through Its Distal Face." *Journal of Biological Chemistry* 285(44):33771–78. doi: 10.1074/jbc.M110.150664.

Ray-Gallet, Dominique, Jean-Pierre Quivy, Christine Scamps, Emmanuelle M-D Martini, Marc Lipinski, and Geneviè ve Almouzni. 2002. "HIRA Is Critical for a Nucleosome Assembly Pathway Independent of DNA Synthesis" *Molecular Cell*. 9(5):1091-100. doi: 10.1016/s1097-2765(02)00526-9.

Richardson, Richard T., Oleg M. Alekseev, Gail Grossman, Esther E. Widgren, Randy Thresher, Eric J. Wagner, Kelly D. Sullivan, William F. Marzluff, and Michael G. O'Rand. 2006. "Nuclear Autoantigenic Sperm Protein (NASP), a Linker Histone Chaperone That Is Required for Cell Proliferation." *Journal of Biological Chemistry* 281(30):21526–34. doi: 10.1074/jbc.M603816200.

Richardson, Richard T., Iglika N. Batova, Esther E. Widgren, Lian Xing Zheng, Michael Whitfield, William F. Marzluff, and Michael G. O'Rand. 2000. "Characterization of

the Histone H1-Binding Protein, NASP, as a Cell Cycle-Regulated Somatic Protein." *Journal of Biological Chemistry* 275(39):30378–86. doi: 10.1074/jbc.M003781200.

Rodrigues, João P. G. L. M., João M. C. Teixeira, Mikaël Trellet, and Alexandre M. J. J. Bonvin. 2018. "Pdb-Tools: A Swiss Army Knife for Molecular Structures." *F1000Research* 7. doi: 10.12688/f1000research.17456.1.

Rodriguez, Pedro, David Munroe, Dirk Prawitt, Lee Lee Chu, Eva Bric, Jungho Kim, Laura H. Reid, Chris Davies, Hitoshi Nakagama, Ralf Loebbert, Andreas Winterpacht, Mary-Jane Petruzzi, Michael J. Higgins, Norma Nowak, Glen Evans, Tom Shows, Bernard E. Weissman, Bernhard Zabel, David E. Housman, and Jerry Pelletier. 1997. "Functional Characterization of Human Nucleosome Assembly Protein-2 (NAP1L4) Suggests a Role as a Histone Chaperone." *Genomics* 44(3):253-65. doi: 10.1006/geno.1997.4868.

Romeo, Valentina, Esther Griesbach, and Daniel Schümperli. 2014. "CstF64: Cell Cycle Regulation and Functional Role in 3′ End Processing of Replication-Dependent Histone mRNAs." *Molecular and Cellular Biology* 34(23):4272–84. doi: 10.1128/mcb.00791-14.

Ruddell, Alanna, and Marcelo Jacobs-Lorenat. 1985. "Biphasic Pattern of Histone Gene Expression during Drosophila Oogenesis" *Proc Natl Acad Sci USA*82(10):3316-9. doi: 10.1073/pnas.82.10.3316.

Russell, Paul, and Paul Nurse. 1966. "Cdc25+ Functions as an Inducer in the Mitotic Control of Fission Yeast." *Cell* 45(1):145-53. doi: 10.1016/0092-8674(86)90546-5.

Ryan, Kevin, Olga Calvo, and James L. Manley. 2004. "Evidence That Polyadenylation Factor CPSF-73 Is the mRNA 3′ Processing Endonuclease." *RNA* 10(4):565–73. doi: 10.1261/rna.5214404.

Sànchez, Ricardo, and William F. Marzluff. 2002. "The Stem-Loop Binding Protein Is Required for Efficient Translation of Histone MRNA In Vivo and In Vitro." *Molecular and Cellular Biology* 22(20):7093–7104. doi: 10.1128/mcb.22.20.7093-7104.2002.

Sanematsu, Fumiyuki, Yaunari Takami, Hirak Kumar Barman, Ttsuo Fukagawa, Tatsuya Ono, Kei-Ichi Shibahara, and Tatsuo Nakayama. 2006. "Asf1 is required for viability and chromatin assembly during DNA replication in vertebrate cells". *Journal of Biological Chemistry* 281(19):13817-13827. doi: 10.1074/jbc.M511590200.

Schupbach, Trudi, Eric Wieschaus, and Rolf Nothiger. 1978. "A Study of the Female Germ Line in Mosaics of Drosophila." *Wilhelm Roux's Archives Dev Biol* 184(1):41-56. doi: 10.1007/BF00848668.

Shermoen, Antony W., Mark L. McCleland, and Patrick H. O'Farrell. 2010. "Developmental Control of Late Replication and S-Phase Length." *Current Biology* 20(23):2067–77. doi: 10.1016/j.cub.2010.10.021.

Shindo, Yuki, and Amanda A. Amodeo. 2019. “Dynamics of Free and Chromatin-Bound Histone H3 during Early Embryogenesis.” *Current Biology* 29(2):359-366.e4. doi: 10.1016/j.cub.2018.12.020.

Shindo, Yuki, and Amanda A. Amodeo. 2021. “Excess Histone H3 Is a Competitive Chk1 Inhibitor That Controls Cell-Cycle Remodeling in the Early Drosophila Embryo.” *Current Biology* 31(12):2633-2642.e6. doi: 10.1016/j.cub.2021.03.035.

Shindo, Yuki, Brown G. Brown, and Amanda A. Amodeo. 2022. “Versatile roles for histones in early development.” *Current Opinion in Cell Biology* 75:102069. doi: 10.1016/j.ceb.2022.02.003.

Sibon, C. M. Ody, A. Victoria Stevenson, and E. William Theurkauf. 1997. “DNA-Replication Checkpoint Control at the Drosophila Midblastula Transition.” *Letters to Nature* 388(6637):93-7. doi: 10.1038/40439.

Singh, Rakesh Kumar, Dun Liang, Ugander Reddy Gajjalaiahvari, Marie Helene Miquel Kabbaj, Johanna Paik, and Akash Gunjan. 2010. “Excess Histone Levels Mediate Cytotoxicity via Multiple Mechanisms.” *Cell Cycle* 9(20):4236–44. doi: 10.4161/cc.9.20.13636.

Smith, Rowena, Sue J. Pickering, Anna Kopakaki, K. J. Thong, Richard A. Anderson, and Chih Jen Lin. 2021. “HIRA Contributes to Zygote Formation in Mice and Is Implicated in Human 1PN Zygote Phenotype.” *Reproduction* 161(6):697–707. doi: 10.1530/REP-20-0636.

Song, Yanjun, Feng He, Gengqiang Xie, Xiaoyan Guo, Yanjuan Xu, Yixu Chen, Xuehong Liang, Igor Stagljar, Dieter Egli, Jun Ma, and Renjie Jiao. 2007. “CAF-1 Is Essential for Drosophila Development and Involved in the Maintenance of Epigenetic Memory.” *Developmental Biology* 311(1):213–22. doi: 10.1016/j.ydbio.2007.08.039.

Song, Yonghyun, Robert A. Marmion, Junyoung O. Park, Debopriyo Biswas, Joshua D. Rabinowitz, and Stanislav Y. Shvartsman. 2017. “Dynamic Control of DNTP Synthesis in Early Embryos.” *Developmental Cell* 42(3):301-308.e3. doi: 10.1016/j.devcel.2017.06.013.

Spradling, Allan C., and Anthony P. Mahowald. 1980. “Amplification of Genes for Chorion Proteins during Oogenesis in *Drosophila Melanogaster*.” *Proc. Natl. Acad. Sci. USA* 77(2):1096-100. doi: 10.1073/pnas.77.2.1096.

Straube, Korinna, Jeffrey S. Blackwell, and Lucy F. Pemberton. 2010. “Nap1 and Chz1 Have Separate Htz1 Nuclear Import and Assembly Functions.” *Traffic* 11(2):185–97. doi: 10.1111/j.1600-0854.2009.01010.x.

Strub, Katharina, Max L Birnstiel, and M L Birnstiel. 1986. “Genetic Complementation in the Xenopus Oocyte: Co-Expression of Sea Urchin Histone and U7 RNAs Restores

3’ Processing of H3 Pre-MRNA in the Oocyte”. *EMBO J.* 5(7):1675-82. doi: 10.1002/j.1460-2075.1986.tb04411.x

Sullivan, William, Patrick Fogarty, and William Theurkauf. 1993. “Mutations Affecting the Cytoskeletal Organization of Syncytial Drosophila Embryos.” *Development* 118(4):1245-54. doi: 10.1242/dev.118.4.1245.

Sun, Yu, Huai Li, Ying Liu, Mark P. Mattson, Mahendra S. Rao, and Ming Zhan. 2008. “Evolutionarily Conserved Transcriptional Co-Expression Guiding Embryonic Stem Cell Differentiation.” *PLoS ONE* 3(10). doi: 10.1371/journal.pone.0003406.

Sutovsky, Peter, and Gerald Schatten. 1997. “Depletion of Glutathione during Bovine Oocyte Maturation Reversibly Blocks the Decondensation of the Male Pronucleus and Pronuclear Apposition during Fertilization.” *Biol Reprod* 56(6):1503-12. doi: 10.1095/biolreprod56.6.1503.

Tagami Hideaki, Ray-Gallet Dominique, Almouzni Genevieve, and Nakatani Yoshihiro. 2004. “Histone H3.1 and H3.3 Complexes Mediate Nucleosome Assembly Pathways Dependent or Independent of DNA Synthesis.” *Cell* 116(1):51-61. doi: 10.1016/s0092-8674(03)01064-x.

Talbert, Paul B., and Steven Henikoff. 2017. “Histone Variants on the Move: Substrates for Chromatin Dynamics.” *Nature Reviews Molecular Cell Biology* 18(2): 115-126. doi: 10.1038/nrm.2016.148.

Torner, Helmut, Nasser Ghanem, Christina Ambros, Michael Hölker, Wolfgang Tomek, Chirawath Phatsara, Hannelore Alm, Marc André Sirard, Wilhelm Kanitz, Karl Schellander, and Dawit Tesfaye. 2008. “Molecular and Subcellular Characterisation of Oocytes Screened for Their Developmental Competence Based on Glucose-6-Phosphate Dehydrogenase Activity.” *Reproduction* 135(2):197–212. doi: 10.1530/REP-07-0348.

Tirgar, R., Davies, J. P., Plate, L., & Nordman, J. T. (2023). The histone chaperone NASP maintains H3-H4 reservoirs in the early Drosophila embryo. *PLoS Genetics*, 19(3). https://doi.org/10.1371/journal.pgen.1010682.

Trcek, T., Lionnet, T., Shroff, H., & Lehmann, R. (2017). mRNA quantification using single-molecule FISH in Drosophila embryos. Nature Protocols, 12(7), 1326–1347. https://doi.org/10.1038/nprot.2017.030.

Vastenhouw, Nadine L., Wen Xi Cao, and Howard D. Lipshitz. 2019. “The Maternal-to-Zygotic Transition Revisited.” *The Company of Biologists* 146(11). doi: 10.1242/DEV.161471.

Walker, Janis, and Mary Bownes. 1998. “The Expression of Histone Genes during Drosophila Melanogaster Oogenesis.” *Dev Genes Evol* 535-41. doi: 10.1007/s004270050144.

Wang, Huanyu, Scott T. R. Walsh, and Mark R. Parthun. 2008. “Expanded Binding Specificity of the Human Histone Chaperone NASP.” *Nucleic Acids Research* 36(18):5763–72. doi: 10.1093/nar/gkn574.

Wang, Zeng-Feng, Tatiana Krasikov, Mark R. Frey, Jean Wang, A. Gregory Matera, and William F. Marzluff. 1996. “Characterization of the Mouse Histone Gene Cluster on Chromosome 13:45 Histone Genes in Three Patches Spread over 1 Mb.” *Genome Res* 6(8):688-701. doi: 10.1101/gr.6.8.688.

Wang, Zeng-Feng, Rich Tisovec, Ron W. Debry, Mark R. Frey, A. Gregory Matera, and William F. Marzluff -3’. 1996. “Characterization of the 55-Kb Mouse Histone Gene Cluster on Chromosome 3.” *Genome Res* 6(8):702-14. doi: 10.1101/gr.6.8.702.

Welch, Jeffrey E., and Michael G. O’rand. 1990. “Characterization of a Sperm-Specific Nuclear Autoantigenic Protein. II. Expression and Localization in the Testis.” *Biology of Reproduction* 43(4):569-78. doi: 10.1095/biolreprod43.4.569.

Wells, Sandra E., Paul E. Hillner, Ronald D. Vale, and Alan B. Sachs. 1998. Circularization of MRNA by Eukaryotic Translation Initiation Factors. *Molecular Cell* 135-40. doi: 10.1016/s1097-2765(00)80122-7

Wessel, Sarah R., Kareem N. Mohni, Jessica W. Luzwick, Huzefa Dungrawala, and David Cortez. 2019. “Functional Analysis of the Replication Fork Proteome Identifies BET Proteins as PCNA Regulators.” *Cell Reports* 28(13):3497-3509.e4. doi: 10.1016/j.celrep.2019.08.051.

White, Anne E., Brandon D. Burch, Xiao Cui Yang, Pamela Y. Gasdaska, Zbigniew Dominski, William F. Marzluff, and Robert J. Duronio. 2011. “Drosophila Histone Locus Bodies Form by Hierarchical Recruitment of Components.” *Journal of Cell Biology* 193(4):677–94. doi: 10.1083/jcb.201012077.

Whitfield, Michael L., Handan Kaygun, Judith A. Erkmann, W. H. Davin Townley-Tilson, Zbigniew Dominski, and William F. Marzluff. 2004. “SLBP Is Associated with Histone MRNA on Polyribosomes as a Component of the Histone MRNP.” *Nucleic Acids Research* 32(16):4833–42. doi: 10.1093/nar/gkh798.

Wieschaus, Eric, and Janos Szabad. 1979. “The Development and Function of the Female Germ Line in Drosophila Melanogaster: A Cell Lineage Study.” *Developmental Biology* 29-46. doi: 10.1016/0012-1606(79)90241-0.

Woodland, H. R., and E. D. Adamson. 1977. “The Synthesis and Storage of Histones during the Oogenesis of Xenopus Laevis.” *Developmental Biology* 57(1):118-35. doi: 10.1016/0012-1606(77)90359-1.

Wu, Yu Chih, Sung Po Hsu, Meng Chun Hu, Yu Ting Lan, Edward T. H. Yeh, and Feng Ming Yang. 2022. “PEP-sNASP Peptide Alleviates LPS-Induced Acute Lung Injury Through the TLR4/TRAF6 Axis.” *Frontiers in Medicine* 9. doi: 10.3389/fmed.2022.832713.

Yang, Feng Ming, Yong Zuo, Wei Zhou, Chuan Xia, Bumsuk Hahm, Mark Sullivan, Jinke Cheng, Hui Ming Chang, and Edward T. H. Yeh. 2018. “sNASP Inhibits TLR Signaling to Regulate Immune Response in Sepsis.” *Journal of Clinical Investigation* 128(6):2459–72. doi: 10.1172/JCI95720.

Yang, Feng-Ming, Hui-Ming Chang, Edward T. H Yeh, Winthrop P. Rockefeller, and Edited by Jenny P-Y Ting. 2021. “Regulation of TLR4 Signaling through the TRAF6/SNASP Axis by Reversible Phosphorylation Mediated by CK2 and PP4.” *PNAS*. 118(47):e2107044118. doi: 10.1073/pnas.2107044118.

Yang, Xiao-Cui, Ivan Sabath, Jan Dębski, Magdalena Kaus-Drobek, Michał Dadlez, William F. Marzluff, and Zbigniew Dominski. 2013. “A Complex Containing the CPSF73 Endonuclease and Other Polyadenylation Factors Associates with U7 SnRNP and Is Recruited to Histone Pre-MRNA for 3′-End Processing.” *Molecular and Cellular Biology* 33(1):28–37. doi: 10.1128/mcb.00653-12.

Yocum, Anastasia K., Theresa E. Gratsch, Nancy Leff, John R. Strahler, Christie L. Hunter, Angela K. Walker, George Michailidis, Gilbert S. Omenn, K. Sue O’Shea, and Philip C. Andrews. 2008. “Coupled Global and Targeted Proteomics of Human Embryonic Stem Cells during Induced Differentiation.” *Molecular and Cellular Proteomics* 7(4):750–67. doi: 10.1074/mcp.M700399-MCP200.

Yu, Beiqin, Xuehua Chen, Jianfang Li, Qinlong Gu, Zhenggang Zhu, Chen Li, Liping Su, and Bingya Liu. 2017. “MicroRNA-29c Inhibits Cell Proliferation by Targeting NASP in Human Gastric Cancer.” *BMC Cancer* 17(1). doi: 10.1186/s12885-017-3096-9.

Yuan, Kai, Jeffrey A. Farrell, and Patrick H. O’Farrell. 2012. “Different Cyclin Types Collaborate to Reverse the S-Phase Checkpoint and Permit Prompt Mitosis.” *Journal of Cell Biology* 198(6):973–80. doi: 10.1083/jcb.201205007.

Yuan, Kai, Charles A. Seller, Antony W. Shermoen, and Patrick H. O’Farrell. 2016. “Timing the Drosophila Mid-Blastula Transition: A Cell Cycle-Centered View.” *Trends in Genetics* 32(8):496–507. doi: 10.1016/j.tig.2016.05.006.

Yuan, Kai, Antony W. Shermoen, and Patrick H. O’Farrell. 2014. “Illuminating DNA Replication during Drosophila Development Using TALE-Lights.” *Current Biology* 24(4). doi: 10.1016/j.cub.2014.01.023.

Zalokar, Marko. 1976. “Autoradiographic Study of Protein and RNA Formation during Early Development of Drosophila Eggs.” *Developmental Biology* 49:425–37. doi: 10.1016/0012-1606(76)90185-8.

Zhang, Mengying, Hejun Liu, Yongxiang Gao, Zhongliang Zhu, Zijun Chen, Peiyi Zheng, Lu Xue, Jixi Li, Maikun Teng, and Liwen Niu. 2016. “Structural Insights into the Association of Hif1 with Histones H2A-H2B Dimer and H3-H4 Tetramer.” *Structure* 24(10):1810–20. doi: 10.1016/j.str.2016.08.001.

Zhang, Sipeng, Jie Yang, Dandan Ji, Xinyi Meng, Chonggui Zhu, Gang Zheng, Joseph Glessner, Hui Qi Qu, Yuechen Cui, Yichuan Liu, Wei Wang, Xiumei Li, Hao Zhang, Zhanjie Xiu, Yan Sun, Ling Sun, Jie Li, Hakon Hakonarson, Jin Li, and Qianghua Xia. 2024. “NASP Gene Contributes to Autism by Epigenetic Dysregulation of Neural and Immune Pathways.” *Journal of Medical Genetics*. doi: 10.1136/jmg-2023-109385.

Zhang, Zijing, Amber R. Krauchunas, Stephanie Huang, and Mariana F. Wolfner. 2018. “Maternal Proteins That Are Phosphoregulated upon Egg Activation Include Crucial Factors for Oogenesis, Egg Activation and Embryogenesis in *Drosophila Melanogaster*.” *G3: Genes, Genomes, Genetics* 8(9):3005–18. doi: 10.1534/g3.118.200578.

Zhao, Jiyong, Brian Dynlacht, Takashi Imai, Tada-Aki Hori, and Ed Harlow. 1998. “Expression of NPAT, a Novel Substrate of Cyclin E-CDK2, Promotes S-Phase Entry.” *Genes Dev 12(4): 456–461*.doi: 10.1101/gad.12.4.456.

Zhao, Jiyong, Brian K. Kennedy, Brandon D. Lawrence, David A. Barbie, A. Gregory Matera, Jonathan A. Fletcher, and Ed Harlow. 2000. “NPAT Links Cyclin E-Cdk2 to the Regulation of Replication-Dependent Histone Gene Transcription.” *Genes and Development* 14(18):2283–97. doi: 10.1101/gad.827700.

Zhao, Ruixue, Zhiwen Zhu, Ruxu Geng, Xuguang Jiang, Wei Li, and Guangshuo Ou. 2022. “Inhibition of Histone H3-H4 Chaperone Pathways Rescues C. Elegans Sterility by H2B Loss.” *PLoS Genetics* 18(6). doi: 10.1371/journal.pgen.1010223.

Zheng, Lianxing, Zbigniew Dominski, Xiao-Cui Yang, Phillip Elms, Christy S. Raska, Christoph H. Borchers, and William F. Marzluff. 2003. “Phosphorylation of Stem-Loop Binding Protein (SLBP) on Two Threonines Triggers Degradation of SLBP, the Sole Cell Cycle-Regulated Factor Required for Regulation of Histone MRNA Processing, at the End of S Phase.” *Molecular and Cellular Biology* 23(5):1590–1601. doi: 10.1128/mcb.23.5.1590-1601.2003.

Zhu, Yungang, Baoguo Li, Guoping Xu, Changrui Han, and Gang Xing. 2021. “Knockdown of Long Noncoding RNA Colorectal Neoplasia Differentially Expressed Inhibits Hepatocellular Carcinoma Progression by Mediating the Expression of Nuclear Autoantigenic Sperm Protein.” *Oncology Reports* 46(6). doi: 10.3892/or.2021.8203.

Zlatanova, Jordanka, Corrine Seebart, and Miroslav Tomschik. 2007. “Nap1: Taking a Closer Look at a Juggler Protein of Extraordinary Skills.” *The FASEB Journal* 21(7):1294–1310. doi: 10.1096/fj.06-7199rev.